

South Dakota State University

Open PRAIRIE: Open Public Research Access Institutional Repository and Information Exchange

Electronic Theses and Dissertations

1976

Venezuelan Equine Encephalomyelitis Virus Induced Mammalian and Mosquito Cell Volume Changes as Detected with the Coulter Counter

Richard H. Fulker

Follow this and additional works at: <https://openprairie.sdstate.edu/etd>

Recommended Citation

Fulker, Richard H., "Venezuelan Equine Encephalomyelitis Virus Induced Mammalian and Mosquito Cell Volume Changes as Detected with the Coulter Counter" (1976). *Electronic Theses and Dissertations*. 4939.

<https://openprairie.sdstate.edu/etd/4939>

This Thesis - Open Access is brought to you for free and open access by Open PRAIRIE: Open Public Research Access Institutional Repository and Information Exchange. It has been accepted for inclusion in Electronic Theses and Dissertations by an authorized administrator of Open PRAIRIE: Open Public Research Access Institutional Repository and Information Exchange. For more information, please contact michael.biondo@sdstate.edu.

VENEZUELAN EQUINE ENCEPHALOMYELITIS VIRUS INDUCED MAMMALIAN AND MOSQUITO
CELL VOLUME CHANGES AS DETECTED WITH THE COULTER COUNTER

BY

RICHARD H. FULKER

A thesis submitted
in partial fulfillment of the requirements for the
degree Master of Science, Major in
Microbiology, South Dakota
State University
1976

SOUTH DAKOTA STATE UNIVERSITY LIBRARY

VENEZUELAN EQUINE ENCEPHALOMYELITIS VIRUS INDUCED MAMMALIAN AND MOSQUITO
 CELL VOLUME CHANGES AS DETECTED WITH THE COULTER COUNTER

This thesis is approved as a creditable and independent investigation by a candidate for the degree, Master of Science, and is acceptable as meeting the thesis requirements for this degree, but without implying that the conclusions reached by the candidate are necessarily the conclusions of the major department.

Thesis Advisor

1 Date/

Head
Microbiology Department

Date _____

ACKNOWLEDGEMENTS

I sincerely thank Dr. Gokaldas C. Parikh, my major advisor, for his assistance in this investigation and thesis effort. Though his acceptance of the Directorship of the Allied Health Science Graduate Programs at Quinnipiac College took him to Hamden, Connecticut, late in this investigation, he is still providing valuable advice and counsel.

I would like to thank Dr. T. R. Wilkinson for consulting with me in the absence of my major advisor and for reviewing this thesis.

I am grateful to Dr. Paul R. Middaugh for his critical review of the published sections of this thesis and for his proof reading of this thesis.

I am indebted to Dr. David Reed for reviewing this thesis. I extend my gratitude to Mr. Wilber Reitzel for his mechanical maintenance of equipment and for his technical assistance.

The computer expertise of Mr. Landon Nusz and Mr. John Kappenman is appreciated. They offered invaluable assistance in developing and maintaining the computer programs used for data analysis in this thesis.

The Vero cell line came from Mr. John McAdaragh and Ms. Pam Leslie of the Veterinary Science Diagnostic Laboratory at S. D. S. U. and the Aedes albopictus mosquito cell line was gratefully received from Dr. Sonja M. Buckley of Yale University School of Medicine.

Acknowledgement goes to Mr. Norman Meeks of the Office of Naval Research Resident Representative, University of Minnesota and Mr. Roy Holloway of the Naval Weapons Laboratory, Dahlgreen, Virginia, for granting permission for the extended use of the Coulter Counter Model F after contract termination through September 30, 1976.

I thank Chris Knutson for typing and correcting this thesis.

Finally, I wish special recognition to go to my wife, Chris, for her patient understanding, Zin Wilderness for his encouraging optimism, and Art and Dorothy for their concentrated thoughtfulness.

R. H. F.

LIST OF ABBREVIATIONS

A	Angstrom
Aa1	<u>Aedes albopictus</u> mosquito cell culture
arbovirus	Arthropod-borne virus
BHK 21	Baby hamster kidney cells
BSS	Balanced salt solution
cAMP	Cyclic Adenine monophosphate
CHO	Chinese hamster cells
con A	Concanavalin A
CPE	Cytopathic effect
DNA	Deoxyribonucleic acid
EEE	Eastern equine encephalomyelitis
FBS	Fetal bovine serum
iFBS	Inactivated fetal bovine serum
G ₁ , G ₂	Phases of cell growth
GKN	Glucose, potassium, and sodium chloride solution (Calcium and magnesium-free saline)
HBSS	Hank's balanced salt solution
HeLa	Cervical carcenoma cell line
HI	Hemagglutination inhibition
IC	VEE virus infected Vero cell cultures
I cent.	Centroids of VEE virus infected Vero cell volume profiles
LD ₅₀	Fifty percent lethal dose

LIST OF ABBREVIATIONS (Con't.)

L cells	Lymphoid cells
M	Mitosis phase of cell cycle
MCM	Mosquito culture medium
MEM	Minimum essential medium
ml	Mililiters
p.f.u.	Plaque forming units
RNA	Ribonucleic acid
S	Phase of cell growth
SFV	Semliki forest virus
u	Micron
UC	Uninfected Vero cell cultures
U cent.	Centroids of uninfected Vero cell volume profiles
VEE	Venezuelan equine encephalomyelitis
Vero	African green monkey kidney cells
WEE	Western equine encephalomyelitis

TABLE OF CONTENTS

	Page
INTRODUCTION.	1
LITERATURE REVIEW	6
Venezuelan Equine Encephalomyelitis Virus.	6
Vero Cell Line	11
<u>Aedes Albopictus</u> Cell Culture Development and Viral Infectivity.	13
Cell Volume Analysis with Coulter Counter.	18
Cell Growth and Division Simulation.	21
Concanavalin A	25
MATERIALS AND METHODS	35
Tissue Culture Materials and Procedures.	35
Materials and Procedures for Subculturing Vero Cells .	36
Materials and Procedures for Subculturing <u>Aedes</u> <u>Albopictus</u> Cells	40
Optical Micrometer Measurement Materials and Procedures	41
Coulter Counter Volume Profile Analysis Materials and Procedures	45
Computer Simulation of Cell Cycle Volume Dynamics Materials and Procedures	56
Coulter Counter Detection of Inactivated VEE Virus Treated Vero Cell Cultures Materials and Procedures. .	63
Coulter Counter Concanavalin A Cell Agglutination Materials and Procedures	64

TABLE OF CONTENTS (Con't.)

	Page
RESULTS AND DISCUSSION.	68
Latex Particle Control Measurements.	68
Interference Count Control	85
Vero Cell Volume Analysis Control.	87
Uninfected and VEE Virus Infected Vero Cell Volume Analysis	96
Computer Simulation of Uninfected and VEE Virus Infected Vero Cell Growth and Division.	110
Coulter Counter Measurement of Inactivated VEE Virus Treated Vero Cell Cultures	126
Coulter Counter Measurement of Concanavalin A Agglutination of Uninfected and VEE Virus Infected Aal Cell Cultures.	128
CONCLUSIONS	139
APPENDIX.	143
Table I. Optical Micrometer Histogram and Statistics Computer Program.	144
Table II. Coulter Counter Computer Program.	146
Table III. Computer Cell Model Program	151
Table IV. Data Smoothing Computer Program	154
Table V. Interpolation and Graphing Computer Program	155
LITERATURE CITED.	160

LIST OF TABLES

Table		Page
1.	Partial List of Viruses Infective and Noninfective to Vero Cells.	14
2.	Example of Optical Micrometer Computer Program Data List.	44
3.	Example of Coulter Counter Program Data List . . .	55
4.	Optical Micrometer Calibration using Stage Micrometer	70
5.	Volume Range for All Attenuation and Aperture Sensitivity Settings	72
6.	Coulter Counter Resolution (Cubic u/channel) at All Attenuation and Aperture Sensitivity Settings.	74
7.	Optical Micrometer and Coulter Counter Percent and Cumulative Percent of 6- to 14-Micron Diameter Latex Particles (Coulter Counter using Vero Cell Sensitivity Settings).	76
8.	Optical Micrometer and Coulter Counter Percent and Cumulative Percent of 6- to 14-Micron Diameter Latex Particles (Coulter Counter using Aal Cell Sensitivity Settings).	77
9.	Isoton Interference Counts for Coulter Counter Attenuation and Aperture Sensitivity Settings. . .	88
10.	Optical Micrometer Measurement of Vero Cells . . .	90
11.	Percent Relative Frequency of Vero Cells Measured with the Optical Micrometer.	91
12.	Percent Relative Frequency of Vero Cells Measured with the Coulter Counter	95
13.	Channels 7 to 30 Centroid Analysis of 0-, 4-, 12-, and 24-Hour Uninfected and Virus Infected Vero Cell Volume Profiles.	104

LIST OF TABLES (Con't.)

Table		Page
14.	Channels 7 to 40 Centroid Analysis of 0-, 4-, 8-, 12-, and 16-Hour Uninfected and Virus Infected Vero Cell Volume Profile.	108
15.	Rate of Growth Determination of Uninfected and Virus Infected Cells	112
16.	Example of Smoothed Data List of an Uninfected Vero Cell Volume Profile	120
17.	Percent and Cumulative Percent of Aal Cells Measured with the Optical Micrometer and the Coulter Counter.	133
18.	Centroid Analysis of Concanavalin A Agglutinated <u>Aedes albopictus</u> Cell Volume Profiles.	136

LIST OF FIGURES

Figure		Page
1.	Schematic Representation of Thesis Research. . . .	4
2.	Morphogenesis of Venezuelan Equine Encephalomyelitis Virus.	10
3.	VEE Virus Production in L Cells.	12
4.	Cell Growth and Division Simulation Designs. . . .	22
5.	Structure of Concanavalin A and Binding Sugar. . .	28
6.	Example of Optical Micrometer Computer Program Statistics, Histogram, and "Cell" Statistics . . .	46
7.	Functional Operation of Coulter Counter Model F. .	49
8.	Vero Cell Volume Analysis Experimental Design. . .	50
9.	Conceptual Diagram of Coulter Counter Computer Pro- gram which Defines the Function Keys	52
10.	Conceptual Cell Model with Half-Volume Channels Equal to 1	58
11.	The Possible Channels into which Post-Division Cells Enter, Assuming Half-Volume Channel is 18, Volume Variation is 1 Channel and Probabilities of All Events are Equal	60
12.	The Approximate Relationship of Cellular Rate Versus Cellular Volume.	60
13.	Experimental Design of Clinical Application of Coulter Counter Virus Detection System	65
14.	Aal Cell Agglutination Analysis Experimental Design	67
15.	Statistics and Histogram of Latex Particles. . . .	71

LIST OF FIGURES (Con't.)

Figure		Page
16.	Percent Frequency of 6- to 14-Micron Diameter Latex Particles Measured with the Optical Micrometer and the Coulter Counter (Coulter Counter using the Vero Cell Sensitivity Settings	79
17.	Cumulative Percent Relative Frequency of 6- to 14-Micron Diameter Latex Particles Measured with the Optical Micrometer and the Coulter Counter (Coulter Counter using the Vero Cell Sensitivity Settings).	81
18.	Percent Frequency of 6- to 14-Micron Diameter Latex Particles Measured with the Optical Micrometer and the Coulter Counter (Coulter Counter using the Aal Cell Sensitivity Settings)	82
19.	Cumulative Percent Relative Frequency of 6- to 14-Micron Diameter Latex Particles Measured with the Optical Micrometer and the Coulter Counter (Coulter Counter using the Aal Cell Sensitivity Settings) .	84
20.	Coulter Counter Control Measurements of 2.02-Micron Diameter Latex Particles	86
21.	Example of a Vero Cell Volume Profile.	94
22.	Cumulative Percent Relative Frequency of a Vero Cell Population Measured with the Optical Micrometer and the Coulter Counter.	97
23.	Cell Population Volume Profiles of 0-Hour Uninfected, 4-Hour Uninfected, and 4-Hour VEE Virus Infected Vero Cells	99
24.	Cell Population Volume Profiles of 4-Hour Uninfected and 4-Hour VEE Virus Infected Vero Cells	100
25.	Centroid Analysis of a Vero Cell Volume Profile. .	101
26.	Centroid Analysis of 0-Hour Uninfected, 4-Hour Uninfected, and 4-Hour VEE Virus Infected Vero Cell Volume Profiles.	103

LIST OF FIGURES (Con't.)

Figure		Page
27.	Centroids of Uninfected and Virus Infected Vero Cell Volume Profiles Versus Time (Centroids for 0-, 4-, 12-, and 24-Hour Uninfected and VEE Virus Infected Vero Cell Volume Profiles).	106
28.	Centroids of Uninfected and Virus Infected Vero Cell Volume Profiles Versus Time (Centroids for 0-, 4-, 8-, 12-, and 16-Hour Uninfected and VEE Infected Vero Cell Volume Profiles).	109
29.	Computer Cell Model Test with 2000 Cells in Channel 18	113
30.	Computer Cell Model Test with 2000 Cells in Channel 18 at 10-Hour Intervals.	116
31.	Computer Cell Model Test with 2000 Cells in Channel 18 at 18-Hour Intervals.	117
32.	Example of 7 Point Smoothing of an Uninfected Vero Cell Volume Profile.	119
33.	Example of Computer Cell Model Simulation of Uninfected Vero Cell Cycle Dynamics.	121
34.	Experimental Smoothed and Computer Simulated 4-Hour Uninfected Vero Cell Volume Profiles.	122
35.	Example of Computer Cell Model Simulation of VEE Virus Infected Vero Cell Cycle Dynamics.	124
36.	Experimental Smoothed and Computer Simulated 4-Hour VEE Virus Infected Vero Cell Volume Profiles.	125
37.	Uninfected, VEE Plus Antiserum Treated, and VEE Virus Infected Vero Cell Volume Profiles	127
38.	Statistics, Histogram and "Cell" Statistics of Aal Cells Measured with the Optical Micrometer	131

LIST OF FIGURES (Con't.)

Figure		Page
39.	Uninfected Aal Cell Volume Profile	132
40.	Cumulative Percent Relative Frequency of Uninfected Aal Cells Measured with the Optical Micrometer and the Coulter Counter	135
41.	Centroid Analysis of Uninfected and VEE Virus Infected Aal Cell Volume Profiles. Centroid Versus Increasing Con A Concentrations.	137

INTRODUCTION

Traditional confirmation of togavirus infected cases may take from 7 to 12 days, and the togavirus assay results from shipping serum samples to the few equipped laboratories in the United States. This laboratory staff is concerned with the development of a more rapid and economical method to detect these viruses because irrigation water from the Oahe Reservoir may soon provide increased mosquito breeding grounds in Northern South Dakota and implement extended togavirus activity.

Dr. Neil Levit of the U.S. Army Medical Research Institute at Ft. Detrick, Maryland stated that there is an urgent need for more rapid and economical methods of arbovirus detection. He said that elimination of the need for animal assay and certain tedious biological procedures would greatly facilitate the detection and identification process (66).

Togaviruses grow to high titer in fibroblasts, BHK 21, or Vero cells and display a latent period of three hours. Virions are produced by budding from the plasma membrane and reach a maximum after 7 hours. "Cloudy swelling" occurs and extensive proliferation of cytoplasmic vacuoles which may have a function in the viral envelope production, viral RNA replication, or protein synthesis are produced.

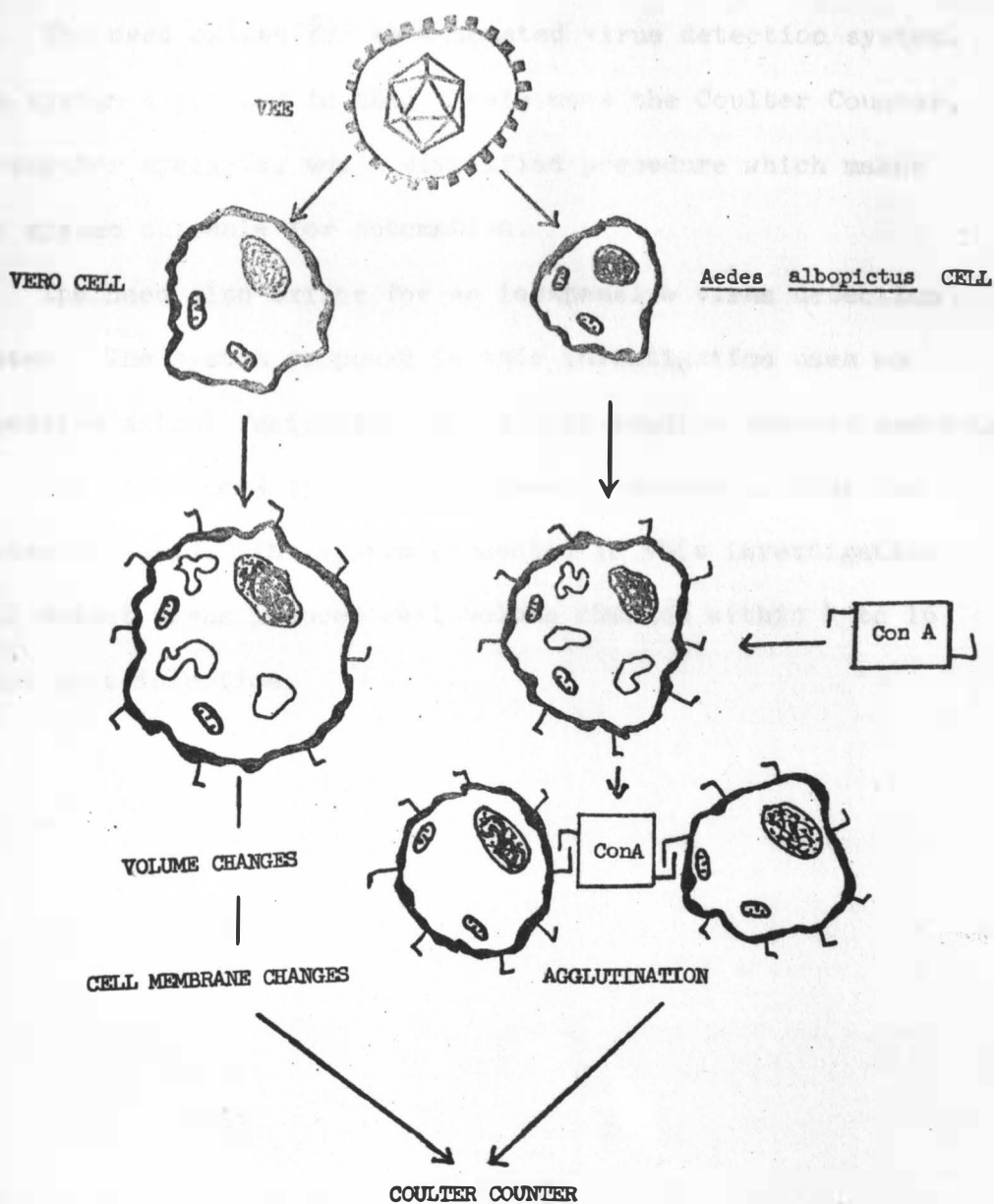
It has been hypothesized that cell cultures infected with togaviruses will display different volumes than the uninfected

virus production systems. Analysis of this cell line to detect volume differences between uninfected and Venezuelan equine encephalomyelitis (VEE) virus infected Aal cells has been previously done in this laboratory (74). The results were somewhat difficult to interpret. Further investigation of the Aal cell line using con A agglutination will aid in the understanding of virus production in this recently established cell line and demonstrate more significant differences between the VEE virus infected and the uninfected Aal cells.

The schematic representation of this thesis investigation is given in Figure 1. The VEE virus is used to infect both the Vero and the Aal cell cultures. The virus infection in both cell lines results in volume changes and virus-specific cell membrane binding site development. The Vero cells are measured with the Coulter Counter for volume changes before CPE. The Aal cells are treated with con A and measured with the Coulter Counter for agglutination. This results in differences between uninfected and infected cell culture volume profiles.

The need exists for the development of a universal virus detection system. The system proposed in this investigation may be adapted to use any host cell cultures that show cytotoxic or noncytotoxic effects. This system may also be used to detect a variety of viruses such as the "unconventional slow viruses", some of the RNA tumor viruses, vaccinia viruses,

Figure 1. Schematic Representation of Thesis Research.



herpes viruses, reoviruses, rabiesviruses, measles, polio, and other togaviruses.

The need exists for a detection system which is specific in its diagnosis of viruses. The system presented in this investigation uses antiserum treated virus infected cell cultures to establish specificity.

The need exists for an automated virus detection system. The system described in this thesis uses the Coulter Counter, a computer analysis, and a simplified procedure which makes the system suitable for automation.

The need also exists for an inexpensive virus detection system. The system proposed in this investigation uses no expensive animal facilities and it will require reduced man-hours.

The final need of a virus detection system is that the system be rapid. The system presented in this investigation will detect virus induced cell volume changes within 4 to 16 hours post-infection.

LITERATURE REVIEW

Venezuelan Equine Encephalomyelitis Virus

The initial isolation of Venezuelan equine encephalomyelitis virus (VEE) occurred in 1938 with the sampling of the brains of dead horses killed in the severe horse encephalitis epizootic in Venezuela (5, 61). Symptoms were similar to eastern equine encephalomyelitis, but virus concentration determined in guinea pig studies was from ten to one hundred times greater. Later studies of infected horses by Kissling (57) demonstrated that VEE produced the encephalitis form of disease with additional clinical signs, such as fever or generalized infection.

In Columbia not less than seventy human cases of mild to short febrile disease, commonly called "pesta loca," were reported between March and June in 1952. This epidemic was the first determined to be of VEE viral etiology (94). Human epidemics of VEE etiology were suspected as early as 1933, however, no virus could be isolated. In 1962-1963 another epidemic occurred. This Venezuelan epidemic resulted in more than thirty thousand human cases with one thousand two hundred cases of nervous involvement and one hundred and ninety deaths (99). Symptoms of VEE infection in humans included sudden onset of malaise, chills and fever, nausea or vomiting, headache, and muscle and bone pains (94).

Several accidental laboratory infections with VEE, such as the Trinidad incident in 1943, have occurred in humans (114). Kissling noted that while the laboratory workers in his study were infected via the respiratory tract, the only agent of transmission in horse cases was the mosquito (57).

Before the 1960's VEE was considered a virus which was limited to the tropical Americas. Then in 1960 evidence of the first United States human infection was documented in the Florida Seminole Indians. Up to 58 percent of the members of some of the tribes tested possessed VEE antibodies. Admittedly these tribes could have been exposed to a related virus, but indications were strongly in favor of VEE, since the virus was isolated from mosquitos, mice, rats, and white-tailed deer in the area (16, 122).

In an opposite environment, that of the Utah desert, VEE was isolated in the 1960's in squirrels, rabbits, and foxes. Evidence of this isolation was never published, however. Gillette (32) speculated that the Utah isolation of VEE may have been accelerated by the storage of VEE in Utah by the government for use as a biological weapon.

Though the United States strain of VEE caused the first human case in Florida in 1968, it was unable to multiply in horse blood (29, 42).

A more virulent strain of VEE which originated in the South American Amazon basin began spreading into Central America and Northern

Mexico in the late 1960's. The equine fatalities of the strain of VEE were 80 to 90 percent. Only the well prepared United States containment effort held the epidemic to a few Southern Texas counties (32).

The VEE virus is classified by the International Committee on Nomenclature of Viruses (ICNV) as a togavirus (formerly termed arbovirus denoting the arthropod-borne or mosquito-transmitted characteristic).

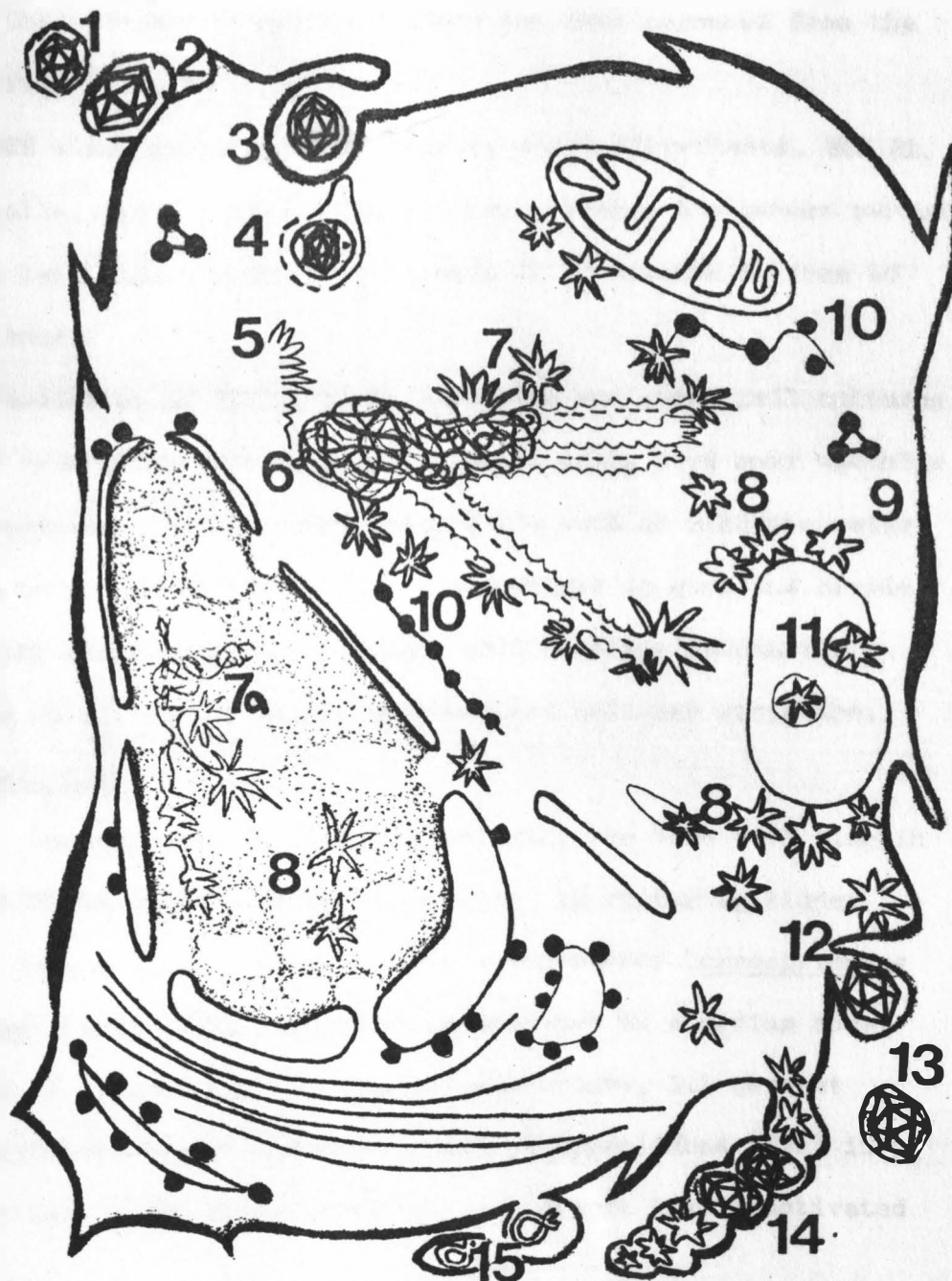
Casals and Brown (13) and Casals (14) divided the more than two hundred togaviruses into twenty-one antigenic categories with major groups based on cross reactions in one or more serologic tests. The VEE virus is assigned to the alphavirus genus (formerly called group A arbovirus) under the family togavirus. The alphaviruses include such exotic viruses as: chickungunya, eastern equine encephalomyelitis (EEE), pixuna, Semliki Forest virus (SFV), sindbis, western equine encephalomyelitis (WEE), and twelve other less well known viruses. Walder further characterized VEE using virulence-markers for strains of VEE categorizing them as A, B, C, ... O types (119).

VEE viruses are filterable through Berkefeld V, N candles, EK Seitz pads, and bacteria retaining Millipore filters. They are inactivated by heat, formalin, and beta-propiolactone. VEE contains a single-stranded ribonucleic acid (RNA) genome with a molecular weight of 2.6×10^6 daltons and possesses 15 genes (15).

Electron microscope studies of the VEE virus by Mussgay and Weibel in 1961 have shown it to be a spherical particle, 40 to 45 milimicrons in diameter (73). VEE contains a lipoprotein envelope which makes the entire virion from 60 to 70 milimicrons in diameter (59). The total lipid content of VEE is 24.3 percent though initial results were somewhat higher because of different purification methods (43). Ribonucleic acid makes up 6.2 percent and the total protein content is 69.5 percent of the VEE virus (118). Pedersen separated three protein components from VEE by discontinuous polyacrylamide gel electrophoresis. All proteins stimulated precipitating antibody in rabbits, while only the largest protein, which is contained in the envelope, stimulated neutralizing and hemagglutination inhibition (HI) antibody against the intact virion (81).

Assembly of the VEE virions takes place near the cell membrane. Bykovsky et al. (12) described the morphogenesis of VEE viruses as illustrated in Figure 2. The extracellular virions (Fig. 2-1) attach to the cell (Fig. 2-2) and enter the cell via pinocytosis (Fig. 2-3, 4). The viral ribonucleoprotein or nucleic acid is released (Fig. 2-5) and virus controlled synthesis occurs. Virus-specific structures appear in the cytoplasm (Fig. 2-6, 7) and in the nucleus (Fig. 2-7a). The virus production areas are the sites of synthesis of viral ribonucleic acid, protein, and nucleoids of virions (Figure 2-8, 8a). The viral

Figure 2. Morphogenesis of Venezuelan Equine Encephalomyelitis Virus.



nucleoids localize around the cytoplasmic vacuoles (Fig. 2-9), near polyribosomal accumulations, or near the mitochondria (Fig. 2-10). Construction of virions occurs with the participation of the vacuole membrane (Fig. 2-11) or the cell membrane (Fig. 2-12). Complete and anomalous virions are then released from the cell (Fig. 2-14, 15).

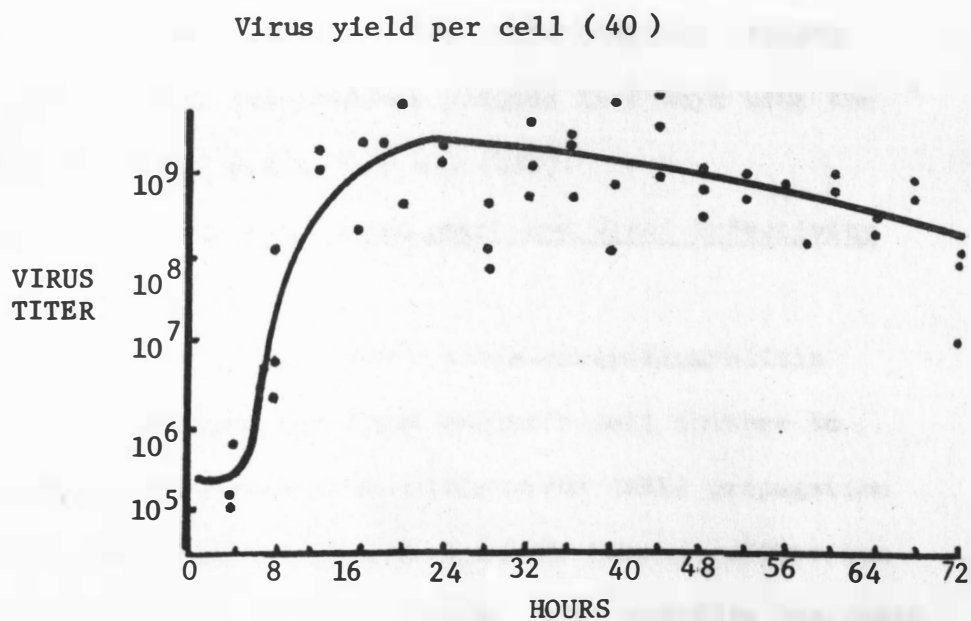
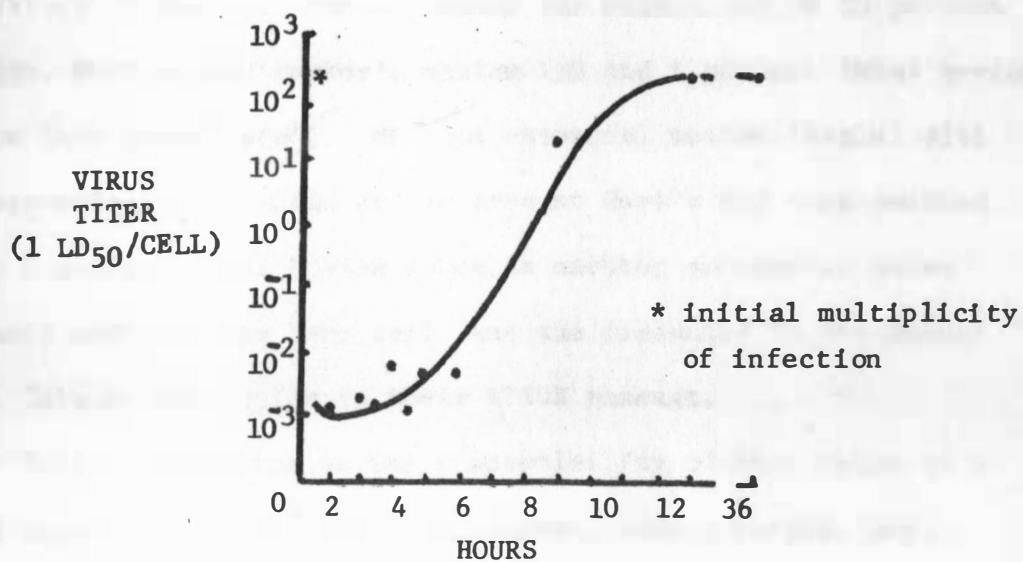
VEE virus grows to high titer on chick fibroblasts, BHK 21, Vero cells, and L cells. Figure 3 demonstrates the latent period can be less than 4 hours with maximum titer reached in from 10 to 12 hours.

Production of VEE virus in mammalian and avian cell cultures causes cytopathic effects (CPE) in which cells form many vacuoles and degenerate (38). Invertebrate cells such as mosquito cells showed no cytotoxic effect (52) and continue to grow and divide with only minor changes in volume, cell membrane saccharide binding sites, and in as yet undetermined cellular structure.

Vero Cell Line

Y. Yasumura and Y. Kawakita initiated the Vero cell line in 1962 at Chiba University in Chiba Japan, by culturing kidney tissue from a normal, adult African green monkey (cercopithecus aethiops) (123). The cells were established in a medium consisting of 0.5 percent lactalbumin hydrolysate, 0.1 percent yeast extract, and 0.1 percent polyvinyl pyrrolidone (PVP) in 98 percent Earl's BSS supplemented with 2 percent heat inactivated

Figure 3. VEE Virus Production in L Cells.



Virus growth (39)

calf serum. Improved cell growth resulted from increasing the calf serum to 5 percent. Dr. B. Simizu delivered the Vero cell line in their 97th passage to the Laboratory of Tropical Virology, National Institute of Health and Infectious Diseases, National Institute of Health. Their passage was maintained on 95 percent Morgan, Morton, and Parker's medium 199 and 5 percent fetal bovine serum (not inactivated). Minimum essential medium (Eagle) with nonessential amino acids and 96 percent Earl's BSS supplemented with 5 percent fetal bovine serum is another successful maintenance medium. The Vero cell line was presented to the Animal Cell Culture Collection in their 113th passage.

Table 1 demonstrates the susceptibility of Vero cells to a wide range of viruses including polyoma, adeno, herpes, pox, picorna, toga, orthomyxo, paramyxo, corona, arena, bunyamwera, and reovirus groups and families. VEE virus displays typical cytopathic effect (CPE) and produces plaques in 2 days with the high titer of $9.4 \log_{10}$ p.f.u./0.2 ml. (110).

Aedes albopictus Cell Culture Development and Viral Infectivity Properties

In 1938, prompted by the 1930's horse-encephalomyelitis epidemic, Trager developed the first mosquito cell culture to examine western equine encephalomyelitis virus (WEE) propagation (116). For the next twenty-five years insect tissue culture was disadvantaged by the use of the expensive media additive hemolymph

Table 1. Partial List of Viruses Infective and Noninfective to Vero Cells.

FAMILY OR GENUS	INFECTIVE COMMON NAME	NONINFECTIVE COMMON NAME	REFERENCES
Polyoma	SV5		55,89,90
	SV40		124
	SV41		51
Adeno	Types 3,12,18		49
Herpes	Infective group		49
Pox	Infective group		49
Picorna	Polio		49
		Cocksackie	49
Toga	Alphavirus (18 tested)		110
	VEE		45
	Chickungunya		67
	Ross river		113
	Flavavirus (38 tested)		110
		Several Flava	110
		Japanese encephalitis	49
	Rubella		50,90
Orthomyxo		Influenza A2 & B	49
Paramyxo	Measles		18,54
		Parainfluenza type 4	49
Corona	Avian infect. bronchitis		23
Arena	Tacaribe complex		110
Bunyamvera	Infective group		110
REO	Infective group		49

and aggravated by the growth stagnation properties exhibited by most insect cell cultures. The challenging problems seemed to animate interest rather than deter the investigators in this field (97).

In 1966 Grace established the continuous cell line of Aedes aegypti from axenually grown larva about to pupate. Hemolymph from the Antheraea eucalysti moth was still, however, necessary in the medium. Several attempts to adapt the cells to bovine albumin, calf serum, or the hemolymph from a more abundant moth species, Antheraea pernyi, proved unsuccessful. The large number of morphologically distinct cells which initially existed evolved after three months into a few most common cell types. The most common cells were spindle shaped, 40 to 50 microns long, 8 to 10 microns wide, and grew in clumps attached to the vessel wall. The second most common cell type was 20 microns in diameter and floated in the medium. The progenitor tissue of these cells could not be determined (35).

Converse and Nagel (20) replaced the moth hemolymph with fetal calf serum to grow moth cells and Aedes aegypti cells in 1967.

Other investigators soon established such continuous mosquito cell lines as Aedes aegypti and Aedes albopictus (Aal) by Singh (104), Aedes aegypti by Peleg (82, 83), Anopheles stephensi by Schneider (98), Aedes aegypti (L.) by Varma and Pudney (117),

Culiseta inornata and Aedes vexans by Sweet and McHale (112), and Culex salinarius by Lite and Wallis (68).

In 1967 Singh promoted Aedes albopictus (Aal) cell growth with the leaf hopper medium of Mitsuhashi and Maramousch (71). The cells averaged 10 to 15 microns in diameter, grew to monolayer within a few days, and displayed no contact inhibition. The cells therefore formed large multi-layered masses of cells.

From Poona, India, Virus Research Center, Dr. Singh delivered the Aal cell culture to Dr. Sonja M. Buckley at Yale Arbovirus Research Unit where storage under liquid nitrogen provides a supply of low-passage-number cells to other investigators.

Singh and Paul (105) examined viral infectivity of Aal cells and found that growth occurred in alpha and flava viruses of the togavirus family. The tests included the following viruses: chickungunya and sindbis viruses of the alphaviruses; and dengue type 1 through 4, Japanese encephalitis, Kyasanur Forest disease, and West Nile viruses of the flavaviruses. The flavaviruses were the only group of viruses to show CPE.

In 1969 Paul and Singh (106) and Paul et al. (80) demonstrated that Aal cells were sensitive to flavaviruses and described CPE from the alphavirus chickungunya. No CPE was observed, however, when Yunker and Cory (125) infected Aal cell cultures with Japanese B encephalitis, Saint Louis and West Nile viruses.

In an investigation by Buckley (11), Aal cell cultures were

assayed to determine the ability of twenty-three various arboviruses to produce CPE or to infect the cells. Thirteen viruses failed to produce CPE or multiply in the Aal cells. These included two flavaviruses with unknown vectors, Cowbone Ridge and Modoc; Sicilian and Naple sandfly fever viruses; and the tick-borne agents of Lanfat (flavavirus), Farallon, Silverwater, Chenuda, Johnston Atoll, Qalyub, Bandia, C5581, and URB-TMA 1381. Chickungunya, eastern equine encephalomyelitis, Semiliki Forest virus, Venezuelan equine encephalomyelitis, Saint Louis encephalomyelitis, and Colorado tick fever viruses infected Aal cell cultures and only the West Nile virus produced CPE.

Isolation of dengue virus type 2 using Singh's Aal cells was demonstrated in the early 1970's to be more effective than mice inoculation (17, 24, 102). The Aal cells are left undamaged by the dengue viruses.

Davey et al. (24) in 1973 studied the Kunjin and Semliki Forest virus infection kinetics in Aal cells, two other mosquito cell lines, and one mammalian cell line. Adsorption characteristics and percentage of cells infected were examined in detail. The results found similar latent periods, growth rates, and virus yield in each cell line. The VEE virus used in this study replicates in Aal and other cell lines (52), but does not produce CPE (11).

Generally, togaviruses have been found to produce devastating cytopathic effect on mammal cell cultures as their viral production cycles continue, but mosquito cells only display vacuolization and continue to function with possible volume and cell membrane changes as presently detectable alterations.

Cell Volume Analysis with Coulter Counter

The Coulter Counter principle of electronic microscopic particle counting and volumetric sizing was initiated by W. H. Coulter in 1953 (22). He designed a particle or cell counting instrument which was further modified in subsequent models to measure volume. Limitations and adaptibilities of the Coulter Counter were then tested by other investigators. Wales et al. (120) and Princen et al. (86) examined the Coulter Counter and developed new mathematical treatments of the theory of coincidence.

Medical investigators, citing hematologic errors and errors in blood counts made in a hemacytometer, were quick to demonstrate in clinical tests that the Coulter Counter gave a three-fold saving in time and a three and one half-fold increase in accuracy when counting red blood cells (8, 70). Continuous research from 1957 to the present to improve the utilization of the Coulter Counter in hematology has progressed with the introduction of each new model of the Coulter Counter (9, 21, 36, 91).

Kubitscheck (62) modified the Coulter Counter by replacing the 100 micron diameter aperture with a 10 micron diameter aperture to count and size E. coli and Bacillus megaterium. He also

predicted the extended application in biology, medicine, and industry for which the Coulter Counter has become known (63).

Early use of the Coulter Counter by Landinsky (65) in 1964 in rapid detection of uterine cancer offered a method of prescreening large numbers of females with the advantage of eliminating the false negative tests obtained with the conventional cytologic methods. The transformed cells were larger than the untransformed cells, therefore the Coulter Counter sizing could augment but not eliminate the Papanicolaou smear.

Lymphoma cells volumetrically sized by Haughten (41) in 1965 were also found to be larger than normal untransformed lymphoid cells. Cell volume analysis using the Coulter Counter has also been used to determine diploid and tetraploid nucleated rat spleen cells (95).

Theoretical expressions relating the current change caused by the passage of mammalian cells through a Coulter Counter aperture to their volume was developed by Gregg and Steidley in 1965 (37). Further work with Chinese hamster (CHO) cells, HeLa S3, and murine lymphoma cells by Anderson and Petersen (2) gave proof that volume distribution spectrums from mammalian cells could be precisely determined with the Coulter Counter. Simons (101) entered Coulter Counter volume data of mammalian cells into an IBM computer in 1970 to establish the importance of statistical treatment such as the mean, standard deviation,

skewness, and kurtosis of such data.

Other Coulter Counter applications in microbiology include the assay of pure and mixed bacterial cultures (72, 26), the influence of bacteriophage on bacteria pairing (76), and the measurement of immunological reactions such as cold agglutinins (84).

The Coulter Counter has recently been used in agglutination studies of trypsin treated BHK 21 cells (28); and an English celloscope model 401 which is similar to the Coulter Counter measured neuraminidase treated rat dermal fibroblasts (69), and inhibition of agglutination of rabbit peritoneal exudate (64).

The use of the Coulter Counter by this laboratory to detect noncytotoxic virus infected cell volume changes was undertaken previously (74), however as the concanavalin A literature review in this paper indicates, concanavalin A will provide a more encouraging procedure to assay for the cellular changes of these virus infected Aal cell cultures with the Coulter Counter.

The efficiency of the Coulter Counter demonstrated in this laboratory (74, 78, 79, 108) and the selective agglutinating ability of concanavalin A will be merged into the development of a rapid detection system of virus infected mosquito cells.

The measurement of early volume changes in Vero cells with the Coulter Counter will be executed to demonstrate the ability of the Coulter Counter to detect cellular volume changes before

CPE and mammalian cell death occurs.

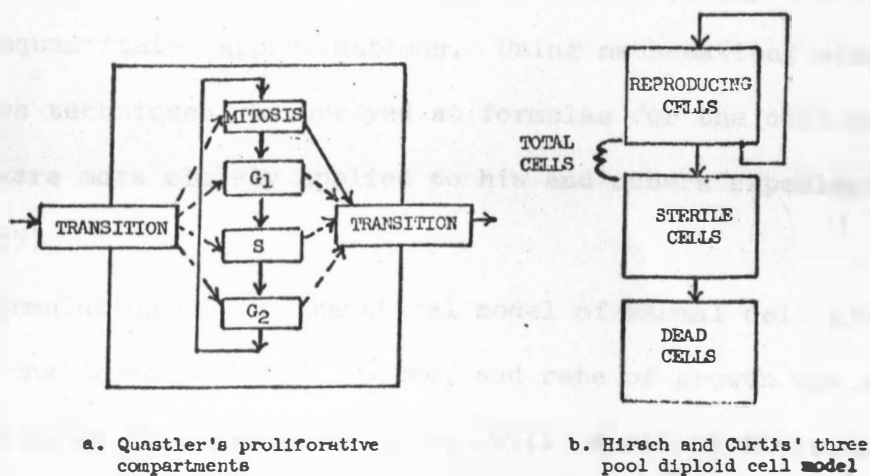
Cell Growth and Division Simulation

A mathematical treatment of the dynamic cell was attempted as early as 1932 when Kelly and Rahm developed theories of generation time for bacterial cells (60). They postulated that a cell divides when all of the independent reactions are completed. Kendal similarly pointed out in 1948 that division occurs when a number of successive steps have been completed (6). He agreed with Kelly and Rahm that the generation times of cells were independent of one another. Kelly and Rahm's theories were statistically refined later by Finney and Martin (60).

Theoretical cell renewal systems were described by Quastler in 1960 in which cell populations were compartmentalized into a basic flow diagram shown in Figure 4a. The cells pass from a transition "box" through mitosis into G_1 , S, and G_2 phases and back into the transition "box" (87).

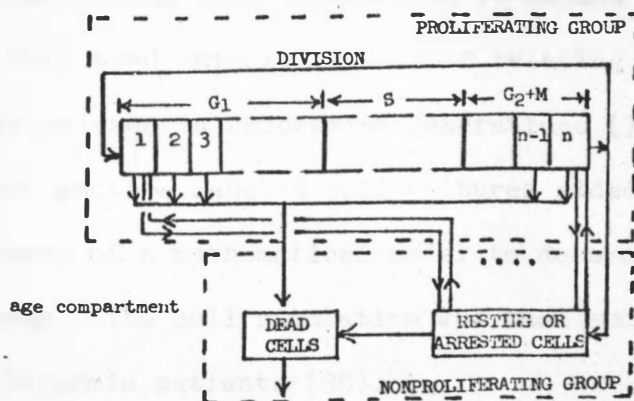
Koch and Schaechter in 1961 proposed a statistical model of cell division using enteric bacteria. They stated that 1.) cell growth is deterministic, 2.) control of cell division is cellular and environmental, 3.) the distribution of sizes of cells at cell division has a small coefficient of variation and is independent of the size at previous divisions, and 4.) cells divide into approximately equal halves. These theories demand cell division at what is called a critical volume and that generation

Figure 4. Cell Growth and Division Simulation Designs.



a. Quastler's proliferative compartments

b. Hirsch and Curtis' three pool diploid cell model



c. Kim et al. cell cycle kinetics model

times are not independent of one another (60).

In 1962 Rigas attempted quantitation of time periods of the events of cell growth and division using radioactive labeling procedures and developed equations of mean generation time, mean life span, and distribution functions of each of these cell properties (92).

Koch and Schaechter's hypothesis was further analyzed in 1964 by Powell who vindicated many of the previously unjustifiable and nonquantitated approximations. Using mathematical simplification techniques, he arrived at formulas for the cell model which were more closely applied to his and others experimental data (85).

Formulation of a mathematical model of mammal cell growth which considered cell age, volume, and rate of growth was accomplished by Bell and Anderson in 1967. A cell's division probability was determined by the cell's age and Coulter Counter determined volume (6). Continuing to expand this previous cell model, Bell used integral equations relating the distribution of birth volumes in successive generations (7).

Radioisotope labeled cell cultures aided Fried in the development of a mathematical model to determine median generation time. The cell simulation was then successfully applied in two leukemia patients (30).

Sinclair and Ross compared the Coulter Counter volume

profile data of Chinese hamster lung cells to a mathematical model of cell volume increases (103). They found no definite distinction between linear and exponential modes of volume increase in the initial generation of cells. Also, they proposed use of only segments of a cell population through electronic separation to overcome the disadvantages of unsynchronized cell cultures.

Later Ross and Mel developed a procedure to apportion volume to the nucleus, the cytoplasm, and the mitochondria. They accomplished this by using the electron microscope and the Coulter Counter to develop a more intricate cell simulation (93).

A careful consideration of sterile and dead cells was included in the 1973 mammalian diploid cell model of Hirsh and Curtis (44). Their set of differential equations was based on the diagram in Figure 4b.

Kim, Bahrami, and Woo (56) described a cell model of Ehrlich ascites tumor cells and included a consideration of cell division, cell death, the resting cell, and the dead cell in the modeling. Each progressive phase of growth G_1 , S, G_2 , and cell division M, are shown in the schematic diagram in Figure 4c.

Computer modeling of the VEE virus infected cell can complement the experimental analysis of these cells, aid in the gathering of basic knowledge of virus-cell interaction, and point to areas in the present understanding of the virus infected cell which must be further resolved.

Concanavalin A

Lectins are proteins which possess many interesting and useful biological and chemical properties. They agglutinate a wide variety of organic material such as erythrocytes, protozoa (27), and viruses (48, 75). They may stimulate cell division or have mitogenic properties, they may activate lymphocytes (115), and they may even protect certain cells from viral invasion. Plant lectins are termed phytohemagglutinins and are found associated with many of the legume plant seeds, roots, leaves, and bark. Vertebrates as fish produce it, and a hepatic protein from a rabbit has been the first reported mammalian lectin (111). Examples of the more notable lectins other than concanavalin A (con A) from jack bean include: soy bean agglutinin and wheat germ agglutinin.

Recent studies using lectins have shown that tumor cell membranes differ from normal untransformed cell membranes. Sella, Inbar, and Sachs (46) used polyoma virus transformed rat cells to show that some lectins selectively agglutinate transformed cells. The transformed cells were aggregated into giant complexes while the normal rat cells were mostly monomers, dimers, trimers, and tetramers. These studies have encouraged virologists for further research efforts into the properties of lectins and virus-cell membrane interaction in hopes of a new understanding of viral disorders. Since concanavalin A

and other lectins have only recently come to the attention of virologists, it is important to realize: 1.) the historical roots, 2.) the structure and properties, and 3.) the present uses of lectins and con A in the areas of cell-virus interaction and virus effect on the cell membrane.

Stillmark first described hemagglutination with a plant lectin in 1888. He noted that castor beans contained ricin, a toxic protein capable of agglutinating red blood cells of humans and animals. Soon another lectin called abrin from jequirity beans was discovered.

In 1908 Landsteiner and Raubitschek compared hemagglutinating powers of various lectins with different animals and contrasted their specificity with that of antibodies in animal serum.

Crude extracts of lectins from plants had been used prior to the 1919 crystalization of concanavalin A from jack bean by Sumner. This meant more precise chemical and physical properties could be determined. Wheat germ agglutinin was not purified until Burger and Goldberg accomplished the technique in the early 1960's.

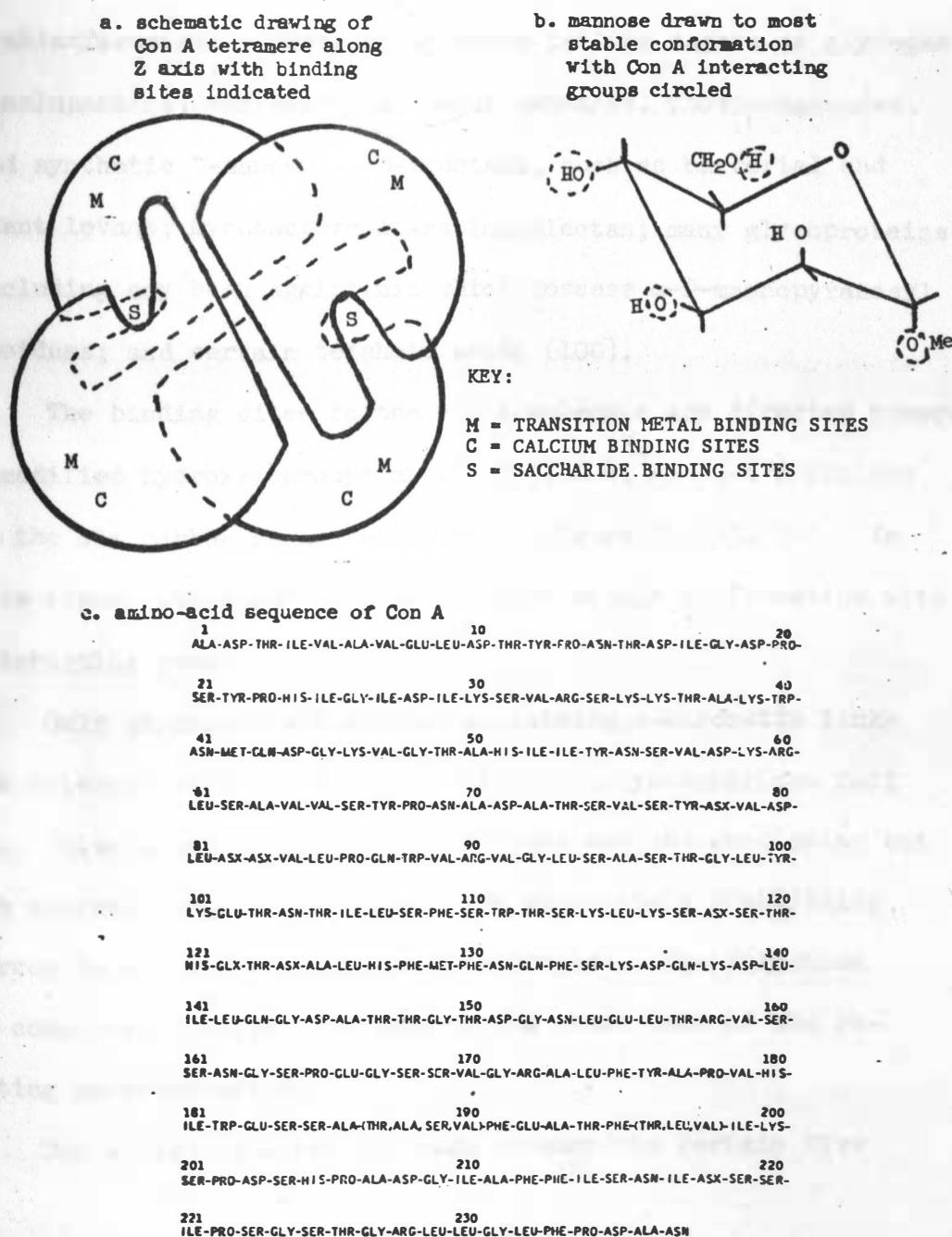
Boyd and Reguera discovered that lectins possess specific agglutinating powers for some human blood group antigens. This late 1940's discovery found, for example, lima bean is specific for the A antigen and tufted vetch acts more strongly on A than on B or O antigens. Later in 1952, Watkins and Morgan showed

that sugars have a role as determinants of blood group specificity (100).

Of all the eight hundred or more lectins, the physiochemical properties and structure of con A has been studied in the most detail because concanavalin A is relatively abundant, is easy to prepare, and is able to interact with a wide variety of high and low molecular weight saccharides which are themselves readily available. Con A has been called a metaloprotein and occurs as a dimer with the molecular weight of 54,000 at a pH below 6. Above pH 6 tetramers form (4, 10, 96). Each con A subunit called a protomer has a molecular weight of 27,000 and forms an elliptical dome with a base of approximately 46 by 26A and a height of 42A, as show in figure 5a with metal ions, calcium, and saccharide binding sites indicated by M, C, and S. Though the amino acid sequence is only tentatively known (Figure 5c), a depression on the surface of the con A molecule may be involved in the binding and agglutinating activities of the lectin (100).

The saccharide specific binding sites that exist on con A are dependent on divalent metal ions. Two metal ion binding sites exist per monomer. Site one (S 1) is the transition metal ion binding site with binds N^{2+} , CU^{2+} , Co^{2+} , $2N^{2+}$, Fe^{2+} , and Mn^{2+} but not Ca^{2+} , or Mg^{2+} . Site two (S 2) is selective for Ca^{2+} only after previous binding of N^{2+} or Mg^{2+}

Figure 5. Structure of Concanavalin A and Binding Sugar.



in site one. Occupancy of both sites is necessary for saccharide binding to occur (10), and carboxyl groups may be present in or near the con A binding site.

Con A precipitates with α -D-mannopyranosyl or its 2-acetamino derivatives, α -D-mannopyranosyl, B-D-fructofuranosyl, and α -D-arabinofuranosyl. Examples of these include sugars as glycogen, monolopectins, and dextrans; yeast mannanes, phosphomannanes, and synthetic D-mannanes; D-fructans, such as bacterial and plant levans; mycobacterial arabinogalactan; many glycoproteins including soy bean agglutinin which possess α -D-mannopyranosyl residues; and certain teichoic acids (100).

The binding sites on the con A molecule are directed toward unmodified hydroxyl groups at the C-3, C-4, and C-6 positions on the six carbon sugars as shown in Figure 5b (33, 34). In this figure the sugar is drawn in most stable conformation with the interacting groups circled.

Only glycogans and mannans containing α -glycoside linkage interact with con A, while β -linked polysaccharides fail to. Polar interaction, such as H bonds and charge-dipolar but not charge-charge interactions, are predominate stabilizing forces in a con A - polysaccharide complex. The formation of complexes involves the nonreducing chain ends of the reacting polysaccharides.

Con A binding sites can also accommodate certain five

membered rings such as β -D-fructofuranosides and D-arabinofuranosides. These are much weaker than con A glycopyranoside reactions (109). Furanoid sugar binding to con A has been explained on the basis of common configuration features with sugars possessing the pyranoid ring. Evidence from L. L. So and I. J. Goldstein (107) exists that con A may possess more extended binding sites than the single saccharide originally postulated. They suggested the possibility of two or more con A molecules being associated with extended sequences of α -(1-2)-D-mannopyranosyl residues.

Con A is used as a reagent in analytical and preparative biochemistry. It, for example, helps purify the antihemophilic factor (factor VIII) from the blood (53), determines the presence of a new group related to the A B O blood group, and extracts the structural specificities of rabbit gamma globulin (100). This lectin also helps isolate immunoglobulins and blood group substances (25), purifies glycoprotein enzymes such as glucose oxidase and peroxidase (3), and partially purifies receptors from lymphocyte plasma membranes (1). The use of con A has even been suggested in class demonstrations of antigen-antibody reactions where antigen and antiserum are not available (100).

The use of lectins by virologists has been growing explosively since the mid 1960's. In 1963 Aub and co-workers using

wheat germ lipase which was later found to be contaminated with a lectin agglutinated tumor cells more readily than normal cells. Then in 1969 Inbar and Sachs demonstrated that con A in concentrations of 250 ug/ml. agglutinated leukemic cells and tissue culture cells that had been transformed by polyoma virus, simian virus 40, chemical carcinogens, and irradiation with X-rays. Agglutination was thought to occur because a higher number of exposed sites for the binding were present in transformed and trypsin treated cells. Con A did not agglutinate normal cells under the same conditions (46).

In 1971 Semliki Forest virus (SFV) was agglutinated with only 40 ug/ml. of con A by Oram et al. (75). SFV is an alpha-virus in the togavirus family and it contains an envelope which is like many cell membranes possessing the specific saccharide receptor sites for con A. Double diffusion studies showed con A forms a precipitate line with the envelope component of the virion but not the virus core. More recently Japanese encephalitis virus, a flavavirus group in the togavirus family, was agglutinated with con A (124).

Animal viruses released by budding from the cell membrane, such as togaviruses, rhabdoviruses, myxoviruses, and RNA tumor viruses, which possess con A specific receptor sites similar to those on the cell membrane from which they were released, can also be agglutinated by con A. Inhibition of binding by

α -methyl-D-glycopyranoside or α -methyl-D-mannopranoside infers that mannose is the determinant sugar in con A virus envelope binding, and these sugars are located on glycoprotein spikes on the virus envelope. A hidden layer of glycolipid is exposed when the glycoprotein spikes are stripped off so addition of con A causes flocculation (88).

Con A was found to inactivate herpes simplex by Ito and Barron (48), while phytohemagglutinin, wheat germ agglutinin and poke weed mitogen had no affect. In these 1974 studies viral aggregation was determined not to be the cause of inactivation by filtration procedures. The con A inactivation was interestingly compared to neutralization by antiserum, with the con A action being more rapid and less temperature dependent than the antiserum. Con A binding sites on the virion envelope must be essential for the binding process. Addition of con A blocks these sites inactivating the virus. Approximately 0.2 to 1 percent of the virions remain infective due to possible possession of receptor sites which do not interact with con A. The con A blocked virions absorb to the test cells but are reactivated by release of con A inhibitors at the cell surface. Klenk et al. (58) demonstrated using polyacrylamide gel electrophoresis that con A treated influenza virus infected cells synthesize virions, however, the virion synthesis is blocked at the late stage of release. Ozanne further studies con A

resistant viruses (77). Similar inactivation by con A treatment was observed in rhabdovirus but no inactivation occurred with poxvirus, adenovirus, or picornavirus. The phenomenon must be related to enveloped viruses (75). This was earlier mentioned in this review in the double diffusion studies by Oram (75).

Radioactive ^{125}I labeled concanavalin A has raised new questions about the saccharide binding properties of lectins. Experiments showed there is not a direct correlation between the amount of lectin bound and the agglutinability of cells (19, 47, 109). Often normal and transformed cells as well as cells which have undergone proteolysis bind more or less the same amount of lectin. These findings postulate that agglutination by lectins depend on the relative distribution of sugar receptors on the surface of the cell. In normal cells the receptors are dispersed, whereas after proteolysis or malignant transformation a redistribution of sites occurs which results in their clustering into an arrangement favorable for cell agglutination. Conclusions of the arrangement of these transformed sites are based on new electron microscope methods developed by Ben-Basset, Inbar, and Sachs for studying the specific localization of antigens and saccharides on cell membrane surfaces. It is possible that only a small percentage of the lectin molecules bound to the cell are involved in

agglutination; whereas the bulk is bound to sites that contain appropriate saccharide receptors in which the binding to those receptors does not lead to agglutination. This "unproductive" binding could mask any small but real differences in the number of "productive" binding sites (100).

In 1974 Willingham and Pastan (121) devised a method of measuring con A agglutination in transformed mouse fibroblast cells with a particle counter from Particle Data Inc., England. Here the low cyclic adenosine monophosphate (cAMP) levels were correlated to high agglutinability. An agglutination index representing the percentage increase of counts at a volume range double the monomer volume range was created as a standard. They found lower levels of cAMP in transformed cells as compared to the parent cells caused cell alterations in adhesiveness, morphology, motility, and cell surface properties. Higher agglutinability of many cells at mitosis can then be explained since cAMP levels are low in this cell phase. The significance of the Willingham and Pastan work to this investigation is the development of electronic particle counter measurement of agglutination of cell cultures treated with concanavalin A.

MATERIALS AND METHODS

Tissue Culture Materials and Procedures

Mammalian and mosquito continuous cell lines are utilized in this investigation. The mammalian cell line is the Vero cell culture (African green monkey kidney cells) which is obtained from the Veterinary Science Diagnostic and Research Laboratory, South Dakota State University, Brookings, S.D. 57006. The Vero cells are between passage numbers 129 to 171. These cells are used as the host for a detection system of virus infection based on cellular volume changes as detected with the Coulter Counter (Coulter Electronics Inc., Hialeah, Florida). The mosquito cell line which is used to detect increased agglutination when the cells are treated with the plant chemical concanavalin A (con A) is the Aedes albopictus (Aal) cell culture. These cells are obtained from Dr. Sonja Buckley, M. D., Yale Arbovirus Research Unit, Department of Epidemiology and Public Health, New Haven, Conn. 06510. The Aal cell culture is between passage numbers 29 to 45 in this investigation.

The volume measurement procedures described here are similar to those discussed by Naeve (74) and Parikh et al. (78, 79). Modification and updating of these methods has been done. Also, several new analysis procedures have been introduced. The con A agglutination procedure is an adaptation of a method used previously in this laboratory (79) for work with latex particles.

This procedure has been redesigned to analyze cell culture agglutination.

Materials and Procedures for Subculturing Vero Cells

A. The materials required for the propagation of Vero cells included the following:

1. Minimum Essential Medium, Eagles (MEM). This medium is purchased commercially from Grand Island Biological Company (GIBCO), Grand Island, New York, in a dehydrated form. MEM is rehydrated, supplemented with 10 percent inactivated fetal bovine serum and L-glutamine, and filtered (0.22 u Millipore filter) before it is used.
2. Fetal Bovine Serum (FBS). This is purchased from GIBCO in a dehydrated form. Rehydration procedures specify addition of 100 ml. of sterile distilled water and inactivation to remove viral inhibitors that may be present. Inactivation is accomplished by placing the rehydrated serum in a 56°C water bath for 30 minutes.
3. Calcium and Magnesium Free Saline (GKN). A ten-fold concentration of the solution is composed of the following:

NaCl	80.0 gm.
KCl	4.0 gm.
Glucose	10.0 gm.
Distilled water	1000.0 ml.

The solution is sterilized by autoclaving at 121°C for fifteen minutes and is diluted 1:10 in sterile distilled water.

4. Trypsin - Versene Solution. A ten-fold solution is prepared containing the following:

Trypsin	5.0 gm.
Versine	2.0 gm.
(ethylenediaminetetraacetic acid disodium salt)	
Doubled distilled water	900.0 ml.
Phenol Red (0.5 percent)	4.0 ml.
Penicillin	1.0 gm.
Streptomycin	1.0 gm.
Kanamycin	0.5 gm.
NaCl	80.0 gm.
KCl	4.0 gm.
NaHCO ₃	3.5 gm.
Glucose	1.0 gm.

The solution is filtered (0.22 u Millipore filter) and stored in 1 ml. aliquotes at 20°C. The trypsin solution is thawed rapidly and diluted 1:10 in sterile distilled water before it is used.

5. Hank's Balanced Salt Solution. A 1000 ml. solution is composed of the following:

Hank's	9.90 gm.
Double distilled water	1000.00 ml.
NaHCO ₃	0.53 gm.

The solution is filtered (0.22 u Millipore filter) and refrigerated.

6. Carbon Dioxide Incubator at 37°C. A National incubator is used to keep a 5 percent carbon dioxide atmosphere.
7. Falcon Plastic 25 cm² Tissue Culture Flasks. These flasks arrive presterilized and pretreated for cell cultures. They may be purchased from Falcon Plastics,

Oxnard, California; GIBCO; or from Scientific Products, Sioux Falls, S.D.

8. Prescription Bottles (20 ounce, glass). These pre-sterilized bottles are purchased from any local drug stores.
9. Pasteur Pipettes. These are purchased from any biological supply house, and then sterilized by autoclaving.
10. Pipetting Dispenser (Kontes Glass Company).
11. VEE Virus. The VEE virus used in this investigation is the tissue culture vaccine strain entitled VEE/TC-283. The stock virus titer is 5.0×10^8 LD₅₀/0.2 ml. or 2.5×10^9 LD₅₀/ml., while the 1:100 dilution in HBSS is 2.5×10^7 LD₅₀/ml.

B. The procedure for subculturing Vero cells is as follows:

A flask containing Vero cells which have been allowed to grow for at least 4 days is removed from the 37°C incubator, and the old medium is poured off into a waste flask that is covered with foil which has several small holes punched in it. Three to 5 ml. of GKN which has been diluted 1:10 is added to the cell culture flask. After a 1 ml. aliquot of trypsin is thawed rapidly, it is diluted 1:10 in 9 ml. of sterile water which has been previously prepared. The GKN is then poured off of the cell culture, and the trypsin (1 to 2 ml.) is added. When the trypsin has covered the cell culture for about a minute,

the flask is inverted and incubated at 37°C for 2 to 5 minutes. After this incubation the trypsin is poured out of the cell culture flask; MEM which has been previously supplemented with 10 percent inactivated fetal bovine serum (iFBS) is added.

One to 3 ml. of MEM is added for each subculture to be made.

Note: usually four to eight subcultures are the maximum allowable number of subcultures which may be made from a single flask.

After the cells have been agitated or suspended by gentle pipetting, they are dispensed at the desired volume into labeled subculture flasks. The Vero cells are incubated at 37°C with a 5 percent carbon dioxide atmosphere for 4 to 6 days. By turning the flask caps down after the first day, carbon dioxide is conserved.

C. The procedure for infecting Vero Cell cultures with VEE is as follows:

The cell culture flasks are removed from the incubator and placed in a laminar flow hood (Specialaire Cabinet made by Torit Manufact. Co., St. Paul, Minn.) which has been disinfected with 70 percent alcohol. After discarding the old MEM, 1 ml. of HBSS is added to one half of the cell culture flasks, while 1 ml. of HBSS with VEE virus (0.4 ml.) is added to the remaining flasks. Incubation is carried out at 37°C for 30 minutes to allow virus adsorption. Then the HBSS and the HBSS with VEE virus are poured off of the cell cultures. The cells are rinsed three times with HBSS, and 2 to 3 ml. of fresh MEM which is

supplemented with 10 percent iFBS is added. The uninfected and the virus infected cell culture flasks are incubated for specified periods of time at 37°C before the Coulter Counter volume sizing is done.

Materials and Procedures for Subculturing Aedes Albopictus Cells

A. The following materials are used in growth and maintenance of Aedes albopictus (Aal) cell cultures:

1. Mosquito Culture Medium (MCM). This medium is purchased from GIBCO and must be supplemented with 20 percent iFBS for the growth medium and 5 percent iFBS for the maintenance medium. MCM arrives as a liquid in sterile glass bottles.
2. Fetal Bovine Serum (FBS). This serum and the inactivation of it are described in the materials section of the Vero cells.
3. Falcon Plastic Flasks. These flasks have been described previously in the Vero cell materials section.
4. Trypsin - Versine Solution. A ten-fold concentration of this is prepared as discussed in the Vero cell materials section.
5. Pasteur Pipettes and a Pipetting Dispenser. These have also been described in the Vero cell materials section of this paper.

6. Incubator. A Precision Scientific Company incubator at 27°C is used for the Aal cell cultures.
- B. The procedure for subculturing Aedes albopictus cells is similar to the subculturing procedure for Vero cells except that no GKN is used to wash the cells, MCM is used instead of MEM, the cells must be transferred every 4 to 6 days, and the Aal cells may be subcultured 1:20 or more. These Aal cells were also periodically frozen by adding growth medium plus 10 percent glycerol, wrapping in cotton, and freezing slowly at -70°C.
- C. The procedure for infecting the Aal cells with VEE virus is the same procedure as that described for the Vero cells.

Optical Micrometer Measurement Materials and Procedures

- A. The materials for the optical micrometer measurement of latex particles, Vero cells, and Aal cells include:
1. Optical Micrometer (American Optical Co., Buffalo, N.Y.).
 2. Bausch and Lomb Graduated Slide.
 3. Spencer AO Microscope.
 4. Hand-held Counter (Veeder-Root Inc., Hartford Conn.).
 5. Hewlett Packard 9830A Programmable Calculator (Hewlett Packard, Palo Alto, California). This mini-computer is the data analysis system used in this investigation. It uses Basic language programs and stores data and programs on magnetic cassette tapes.

B. The procedure for the optical micrometer measurement is as follows:

The 6 to 14 micron diameter latex particles are diluted 1:400 with Isoton; the Vero cells and the Aal cells which are harvested with trypsin are diluted 1:10 with Isoton. A drop of the latex particles or the cell cultures is suspended on a slide. The cover slip is gently lowered to the slide surface and placed over the suspended particles or cells. Two hundred consecutive particles or cells are counted at a total magnification of 1000 X on the Spencer AO microscope with the American Optical micrometer which has been previously calibrated. The optical micrometer data is then entered into the Hewlett Packard programmable calculator for statistical analysis and for plotting of the data.

The optical micrometer computer program (Appendix I) is similar to the math pack histogram program developed by Hewlett Packard. Modification of the math pack program was necessary, however, so that it may accept optical micrometer data. This software is stored on the special function keys and is accessed by the commands "Load Key 3 Execute" from the cassette storage tape Fulker I.

The program is initiated by pressing "Run" and special function key " f_0 ". The special function key f_0 is the initialization which asks the computer operator which area of tape storage

space is to be utilized.

The first special function key is the data initialization key. This key is pressed only when using a new file before data has been entered. Pressing f_1 assigns zeros to all data storage spaces so that the entire data file may be loaded or stored.

The second special function key loads a data file which has been previously entered.

Special function key three is the data entry key. Pressing f_3 allows up to 200 optical micrometer data points to be entered.

The fourth special function key is the data storage key which stores the entered data.

The fifth special function key is the data print key. When f_5 is pressed the optical micrometer data such as the particle or cell diameter in microns, and the particle or cell volume in cubic microns is printed. An example of a data list of special function key five is shown in Table 2.

Special function key six is the basic statistics key. When this key is pressed, values for the offset (location of the histogram "X") and the cell width (the range of width of the volume into which the entered data will be grouped) must be entered. Note that it may be useful to set the offset value equal to one half of the cell width value. After the offset and the cell width values are entered into the mini-computer, a series of statistical calculations are listed as described in

Table 2. Example of Optical Micrometer Computer Program Data List.

INPUT CELL DIAMETER	DIAMETER (MICRONS)	CELL VOLUME (CUBIC MICRONS)
11.00	20.48	4500.43
8.50	15.83	2076.50
9.00	16.76	2464.92
8.75	16.29	2265.17
10.00	18.62	3381.24
9.00	16.76	2464.92
9.75	18.16	3133.93
9.75	18.16	3133.93
8.00	14.90	1731.19
8.00	14.90	1731.19
8.00	14.90	1731.19
8.75	16.29	2265.17
7.00	13.04	1159.76
10.25	19.09	3641.22
11.00	20.48	4500.43
8.00	14.90	1731.19
12.00	22.35	5842.78
9.75	18.16	3133.93
5.00	9.31	422.65
6.00	11.17	730.35
8.50	15.83	2076.50
9.25	17.23	2676.09
5.00	9.31	422.65
8.00	14.90	1731.19
7.75	14.43	1573.91
8.00	14.90	1731.19
10.00	18.62	3381.24
9.00	16.76	2464.92
8.00	14.90	1731.19
8.50	15.83	2076.50
13.00	24.21	7428.58
9.00	16.76	2464.92
7.00	13.04	1159.76
8.25	15.36	1898.62

Figure 6. These statistics include the number of points entered, the mean, the standard deviation, the skewness, the kurtosis, the minimum and maximum values of the data points entered, and the range of the data points entered.

The seventh special function key is the key which prints a bar graph of the data with a best fit curve when it is pressed. The graph is incremented according to the cell width given; the "X" symbols are printed at the point which is indicated by the offset value. In Figure 6 the offset is 250, and the cell width is 500.

The eighth special function key is the statistics key. When f8 is pressed a list is made of the number of objects which have been grouped in each "cell" or what is better termed volume range. Also the percentage relative frequency of the objects in each volume range is calculated and listed. These statistics are listed in Figure 6.

Coulter Counter Volume Profile Analysis Materials and Procedures

A. The materials for Vero cell volume profile analysis include:

1. Model F Coulter Counter (Coulter Electronics Inc., Hialeah, Florida).
2. Isoton (Coulter Electronics Inc.). Isoton is a saline solution with a sodium azide preservative added to it.
3. Hemacycometer (C. A. Hausser and Son, Philadelphia, Penn.).
4. Spencer AO Microscope.

Figure 6. Example of Optical Micrometer Computer Program Statistics, Histogram, and "Cell" Statistics.

N = 200
 MEAN = 2072.9254
 STD. DEV = 1232.8891
 SKEWNESS = 1.5519
 KURTOSIS = 6.5045
 XMIN = 91.2934
 XMAX = 7428.5803
 RANGE = 7337.2869

EACH X= 0.58 PERCENT



CELL#	LOWER LIMIT	NO. OF CBS	%RELATIVE FREQ
1	0.0000	9	4.50000
2	500.0000	19	9.50000
3	1000.0000	39	19.50000
4	1500.0000	46	23.00000
5	2000.2000	38	19.00000
6	2500.0000	13	6.50000
7	3000.0000	18	9.00000
8	3500.0000	4	2.00000
9	4000.0000	1	0.50000
10	4500.0000	6	3.00000
11	5000.0000	1	0.50000
12	5500.0000	4	2.00000
13	6000.0000	0	0.00000
14	6500.0000	0	0.00000
15	7000.0000	2	1.00000

5. Hand-held Counter (Veeder-Root Inc., Hartford, Conn.).

6. Hewlett Packard 9830A Programmable Calculator. This mini-computer has been previously described in the optical micrometer materials section.

B. The Methods for the Coulter Counter Vero cell volume profile analysis are as follows:

A single Vero cell culture from Veterinary Science Diagnostic and Research laboratory is subcultured 1:12 and grown to monolayer in 3 to 6 days. When a monolayer of cell growth is reached, 1 ml. of HBSS is added to eight flasks, while 1 ml. of HBSS with 0.4 ml. of 2.5×10^7 LD₅₀/ml. titrated stock of VEE virus is added to the remaining four flasks. The twelve flasks are incubated at 37°C for 30 minutes. The HBSS and the HBSS plus the virus is poured off; the flasks are rinsed three times with HBSS. Two milliliters of fresh MEM which has been supplemented with 20 percent iFBS is then added to each flask. Four flasks of the uninfected cell cultures and four flasks of the VEE virus infected cell cultures are incubated 4 to 24 hours (depending on the experimental design). Four of the other flasks are immediately harvested into 3 ml. of Isoton per flask. Two milliliters of this cell suspension is taken for a hemacytometer count. The remaining 10 ml. of cell suspension is diluted in 90 ml. of Isoton (1:10) and counted in the Coulter Counter model F.

The Coulter Counter passes particles or cells, which are suspended in the electrolytic fluid Isoton, through a tiny aperture. The cells displace their volume of electrolytic fluid which causes a change in conductivity that is picked up by platinum electrodes located on inner and outer sides of the aperture. Electronic pulses proportional in height to the cell volume and proportional in number to the total cell number are displayed on an oscilloscope screen. Adjustment of the threshold dial on the Coulter Counter selectively blocks out all pulses below a desired height. Counts which are called threshold counts may be taken at each successive threshold dial calibration. The difference between successive threshold counts equals the channel count e.g. threshold 1 count minus threshold 2 count equals channel 1 count. Channel counts are the number of cells which are found in a certain volume range and may be plotted and graphed. A channel can be set from approximately 0.01 cubic microns to over 360 cubic microns wide. Over 100 channels can be utilized which makes this instrument useful over a wide range of particle sizes (0.01 cubic microns to 36,000 cubic microns). Figure 7 is a description of the functional operation of the Coulter Counter, and Figure 8 is a presentation of the Vero cell volume analysis experimental design.

The Coulter Counter threshold counts are stored on magnetic tape and analyzed by the Basic language programs on the Hewlett

Figure 7. Functional Operation of the Coulter Counter Model F.

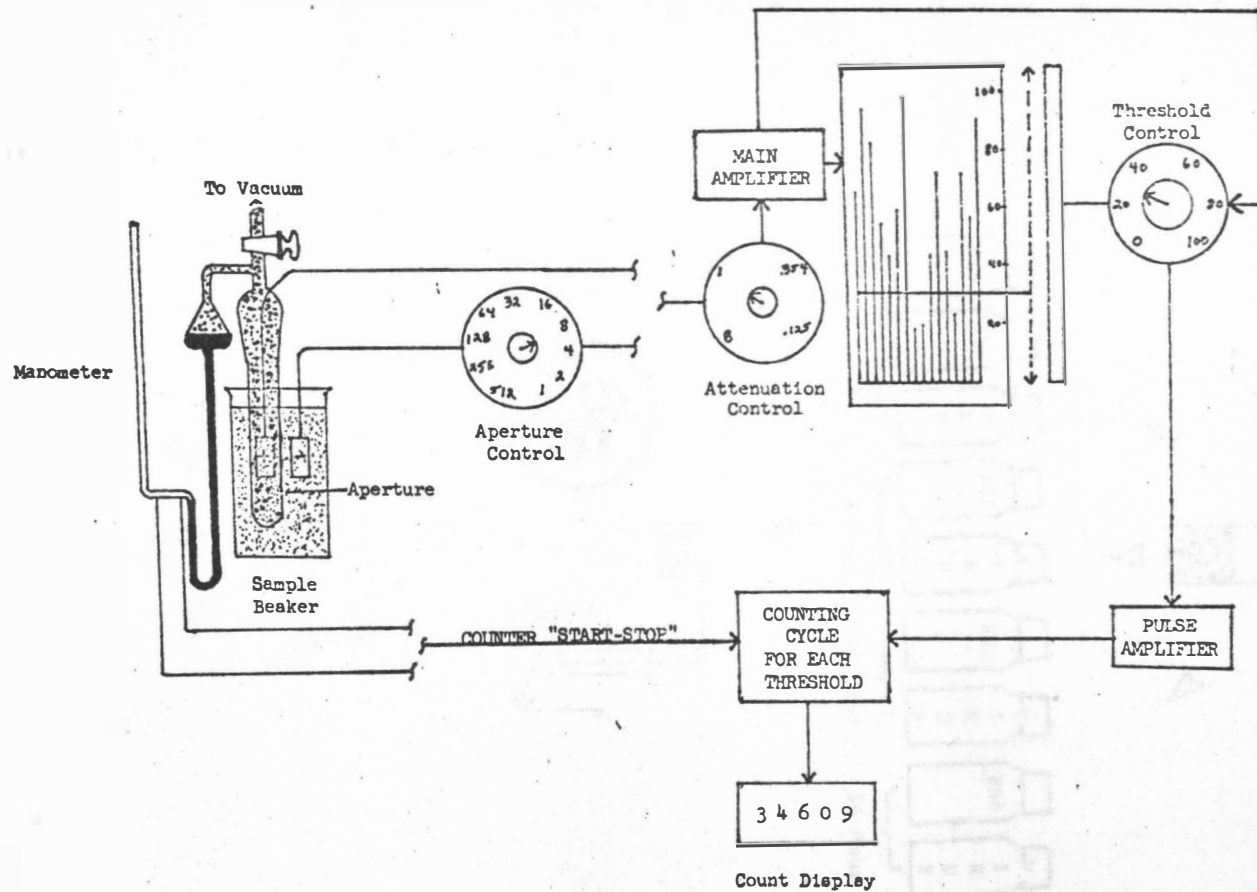


Figure 8. Vero Cell Volume Analysis Experimental Design.

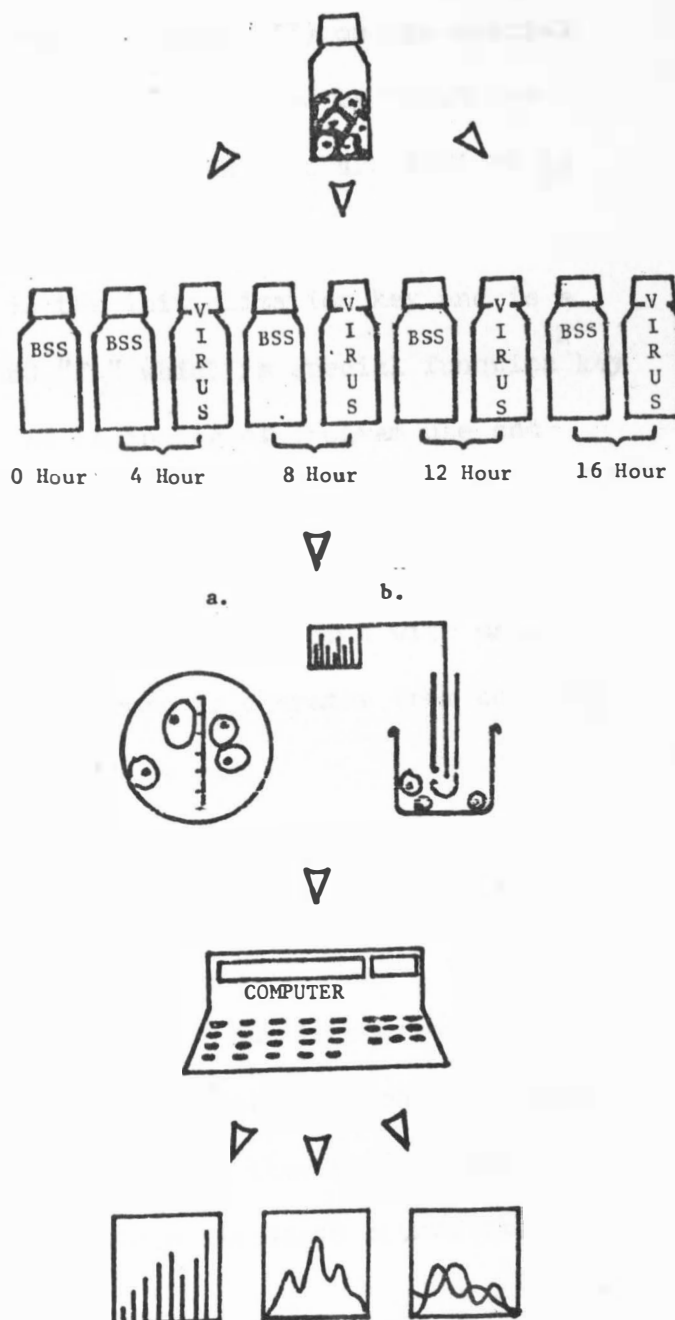
1. CELLS TRANSFERRED 1:9

2. CELLS TREATED WITH
BSS OR BSS+VIRUS

3. CELLS VOLUMETRICALLY SIZED
AT SPECIFIC POST INFECTION
TIME WITH COULTER COUNTER (b.)
AND CONTROL MEASUREMENTS MADE
WITH OPTICAL MICROMETER (a.)

4. DATA ANALYSIS WITH
HEWLET PACKARD
MODEL 9830 A
PROGRAMMABLE CALCULATOR

5. COMPUTER OUTPUT:
GRAPHING AND
STATISTICAL
ANALYSIS



Packard 9830A programmable calculator. Although limited initial data analysis in this research was done with the existing programs of this laboratory, an innovative set of interlocking programs was developed as a core program to which future adjustments can easily be made. These programs are stored on the General Tape 3 called the Coulter Counter Tape (Appendix II) on the special function keys of the mini-computer and accessed by "Load Key 0 Execute" commands. The special function keys are defined in a conceptual diagram in Figure 9.

Special function key 0 is the initialization key and is accessed by pressing "Run" and "f₀" which is special function key 0. This is pressed only at the beginning of program use and it prepares file storage space for data entry.

The first special function key is the data entry key. The threshold counts for each threshold may be entered with many engineered measures to protect the computer operator from entering invalid and nonsense data.

The third special function key lists the newly entered data. It may also list data from files on tape storage, however, only the mean threshold counts and the channel counts will be listed because only the mean threshold count is stored on tape to conserve memory space. The data list of newly entered data, not stored data, includes the three input threshold counts for up to one hundred thresholds, the mean threshold count, the

Figure 9. Conceptual Diagram of Coulter Counter Computer Program which Defines the Function Keys.

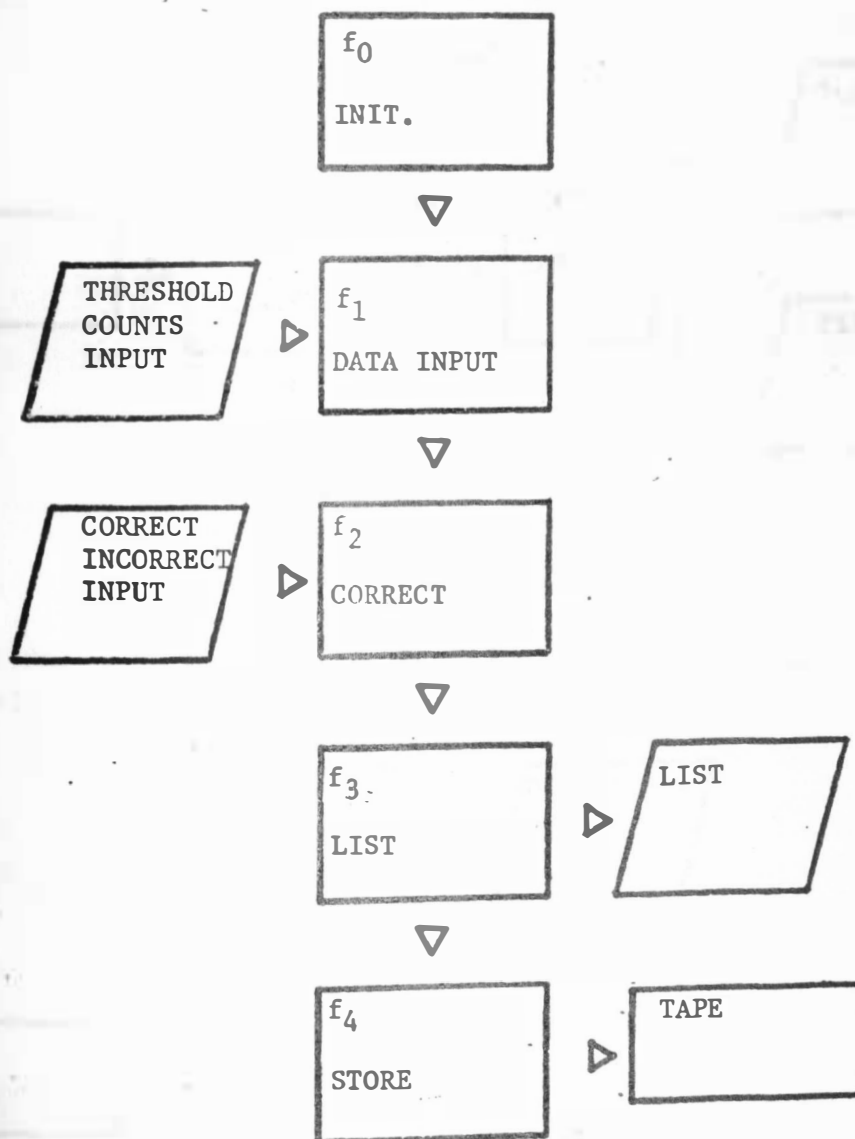
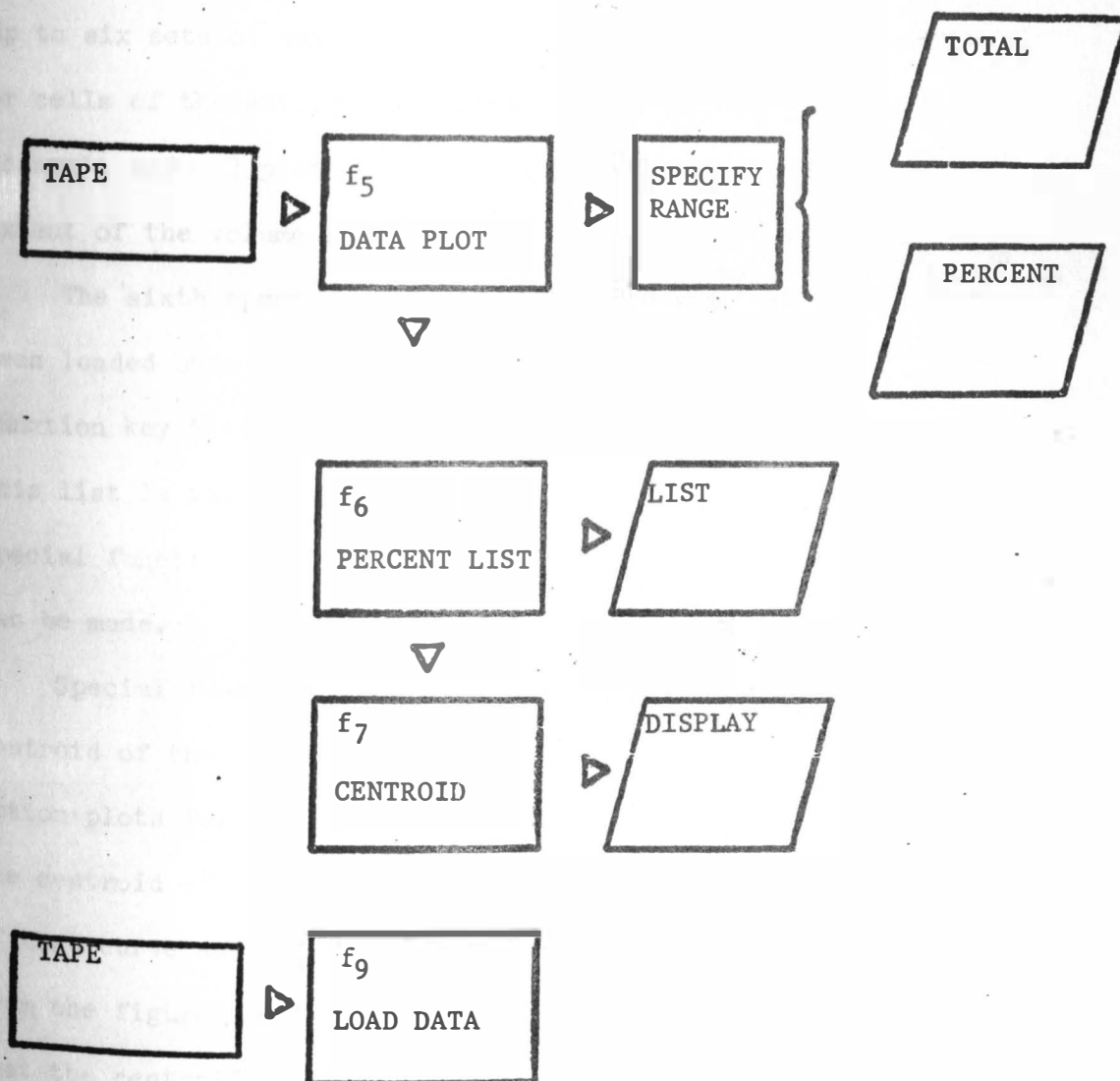


Figure 9. (Con't.)



percent standard deviation of the threshold counts, and the channel counts as shown in Table 3.

Special function key 4 merely stores the mean threshold count calculated from the three input threshold counts.

The fifth special function key loads the cassette tape data files and has the option of 1.) plotting the channel counts for up to six sets of data, 2.) plotting the percentage of particles or cells of the entire population which are located in each channel, and 3.) plotting the first two options with any specified extent of the volume range.

The sixth special function key can be used after data has been loaded onto computer memory or directly after use of special function key 5 to list the plotted data in tabular form. This list is valuable when plotting the percentage option at special function key 5. A listing of up to 6 plotted curves can be made.

Special function key 7 calculates the centroid of the channel count or percentage option plots for any specified volume range. The centroid of a curve is the center of mass of that curve and is given in channel units. From the figure on the right it can be noted that the centroid of this theoretical curve is at about volume unit 7. Since centroid

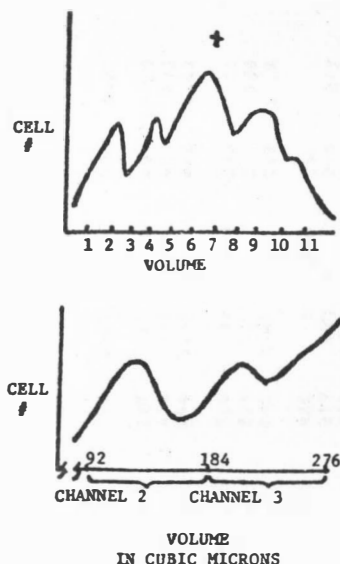


Table 3. Example of Coulter Counter Computer Program Data List.

COULTER COUNTER DATA LIST 2/11/76 OHR UNINFECTED VERO CELL

EXP# 12.10

ATTENUATION SETTING = 4

APERTURE SETTING = 256

THRESHOLD NUMBER
THRESHOLD COUNTS
MEAN THRESHOLD COUNT
CHANNEL COUNT
PERCENT STANDARD DEVIATION

7	4215	213	8	3920	38	9	3850	54	10	3856	165	11	3638	74	12	3541	48
	4030	4137		3935	3924		3906	3836		3843	3832		3691	3667		3592	3593
	4166	3.3%		3916	0.4%		3933	1.1%		3796	1.2%		3672	1.0%		364	2.1%
13	3564	190	14	3302	104	15	3232	135	16	3084	77	17	3173	171	18	2892	113
	3501	3545		3399	3355		3297	3251		3090	3116		3035	3039		2832	2868
	3569	1.5%		3364	2.1%		3204	2.3%		3175	2.3%		2908	6.2%		2881	1.6%
19	2752	212	20	2565	29	21	2532	318	22	2229	75	23	2121	195	24	1914	70
	2716	2755		2502	2543		2529	2514		2179	2196		2080	2121		1932	1926
	2716	2.1%		2555	1.7%		2432	1.3%		2181	1.8%		2162	2.7%		1932	0.8%
25	1664	190	26	1653	84	27	1553	60	28	1522	109	29	1373	119	30	1331	56
	1236	1856		1622	1666		1592	1582		1569	1522		1459	1413		1282	1294
	1867	1.3%		1662	1.3%		1600	2.2%		1476	4.3%		1407	4.3%		1262	4.3%
31	1242	114	32	1120	76	33	1039	102	34	935	75	35	900	43	36	813	54
	1202	1238		1146	1124		1050	1046		975	946		862	871		822	828
	1264	3.7%		1107	2.5%		1056	1.2%		929	3.7%		851	4.2%		849	3.2%
37	745	42	38	756	35	39	692	60	40	637	23	41	615	91	42	510	30
	770	774		714	732		697	697		647	637		610	614		545	523
	806	5.6%		726	4.2%		695	0.3%		627	2.2%		617	0.8%		513	5.2%
43	512	20	44	497	39	45	412	20	46	429	43	47	378	19	48	349	17
	473	493		457	473		456	434		415	414		365	371		346	352
	494	5.6%		464	6.4%		435	7.2%		398	5.3%		369	2.5%		360	3.0%
49	325	27	50	313	11	51	306	30	52	278	19	53	258	19	54	237	4
	335	335		315	308		301	277		266	267		244	248		229	229
	345	4.2%		295	5.1%		284	5.5%		236	14.2%		243	4.8%		222	4.0%
55	230	8	56	221													
	217	225		216	217												
	228	4.4%		214	2.3%												

units are given in channels the centroid in the example would be near channel 7. Recall that channels are volume ranges as indicated by the lower figure on the preceding page. Channel two in this example extends from 92 cubic microns to 184 cubic microns; channel three extends from 184 cubic microns to 276 cubic microns. From this information it can be noted that the centroid of the upper figure is located at about channel 7.

The centroid value is determined by the following set of relationships:

$$\text{mass} = (\text{channel } n) (\text{channel } n \text{ count})$$

$$\text{moment } 2 = (\text{channel } n^2) (\text{channel } n \text{ count})$$

$$\text{moment } 3 = (\text{channel } n^3) (\text{channel } n \text{ count})$$

$$\text{centroid} = \frac{\sum \text{moments}}{\sum \text{masses}}$$

The \sum of the mass of particles or cells in any range of channels may be calculated, the moment at the various degrees of bias may be determined, and then the centroid can be calculated from the \sum masses and the \sum the moments.

Computer Simulation of Cell Cycle Volume Dynamics Materials and Procedures

- A. Materials required for the computer simulation of cell cycle dynamics include the Hewlett Packard 9830A programmable calculator and cassette storage tapes.
- B. The method of computer simulation of cell cycle volume dynamics

is as follows:

As cells grow, they increase in volume to a specific level and divide, forming two new cells, each with approximately one half the dividing volume. Each new cell then starts growing, increasing its volume until reaching the division volume, and again splits, as the cycle is repeated. This cell growth process can be represented in terms of Coulter Counter data by showing cells "moving" from one channel to another. This implies there is a rate of cell population "flow" between channels. Generally, this process can be described as shown in Figure 10.

The computer, in effect, scans the channel data from low to high numbered channels, and calculates the new population level of each channel by adding the cells coming in and subtracting the cells going out. The general equation describing this process is:

$$C_i \text{ (new)} = C_i \text{ (old)} = R_{i-1}C_{i-1} - R_iC_i$$

Cells
Cells

coming in
going out

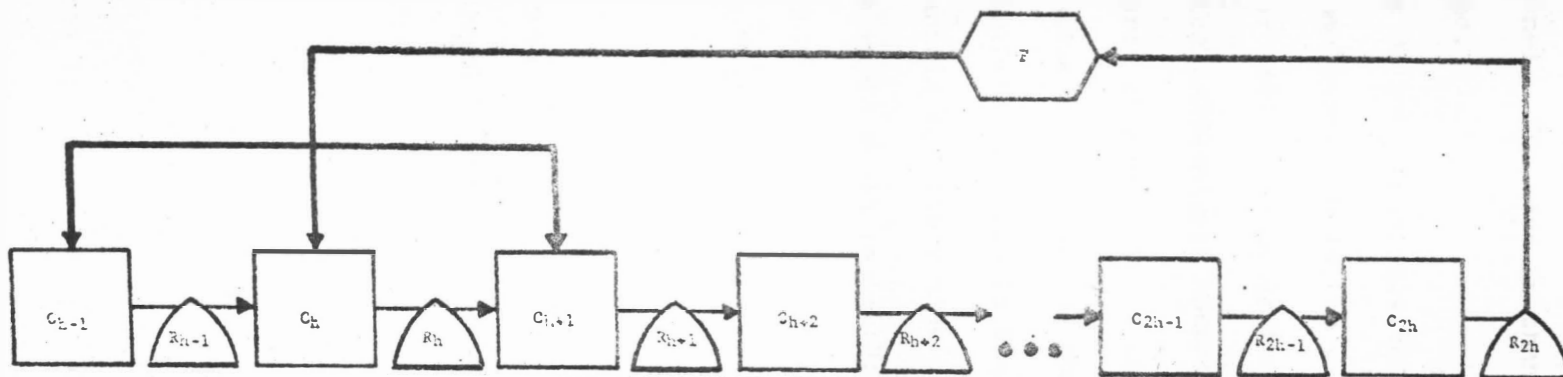
Where i = channel no.

C_i = cell population in channel i

R_i = rate of cell flow between channels i and $i + 1$

At the end of a scan, the cells moving out of the last channel are multiplied by a factor less than one, based on death and sterility rates, (non-multiplying cells), to account for the cells that are eliminated naturally. The remaining cells are multiplied by two to simulate cell division and returned to the

Figure 10. Conceptual Cell Model with Half-Volume Channels Equal to 1.



KEY

C=channel, subscript denotes channel no.

R=rate

h=half-volume channel no.

F=division, death, & sterility factor

half-volume channel. The scan is then repeated for the next increment of time.

Since cells do not always divide into two equal volumes, there must be some variation in the particular channel they "return" to. For example, suppose the variation is 1 channel on either side of the half-volume channel. This means, that there is a range of three channels that a daughter cell can return to. Listing the possible combination as shown in Figure 11, makes evident the distribution. This is the ratio 1:2:1. If the variation is two channels on either side of the half-volume channel, the distribution ratio would be 1:1:2:1:1. The pattern is the same for any number of channel variations; the half-volume channel gets two "returned" cells for every cell the variation channels get.

The only undetermined quantities left to make the model complete and workable are the rates. This poses an interesting problem, since there is really no rate of cell "flow" between channels. The channels in reality are divisions along a continuous line of volume. As the cells grow in volume, they move along the line gradually shifting from one channel to the next as arbitrarily measured by the Coulter Counter. For modeling purposes, it can be assumed that the entire cell population of a particular channel is located at the mean volume of that channel. Then when a cell has stayed in the channel for a length of time

Figure 11. The Possible Channels into which Post-Division Cells Enter, Assuming Half-Volume Channel is 18, Volume Variation is 1 Channel and Probabilities of All Events are Equal.

Possibilities are two:

1. Equal volume division - both cells "return" to channel 18.
2. Unequal volume division - one cell goes to channel 17, the other to channel 19.

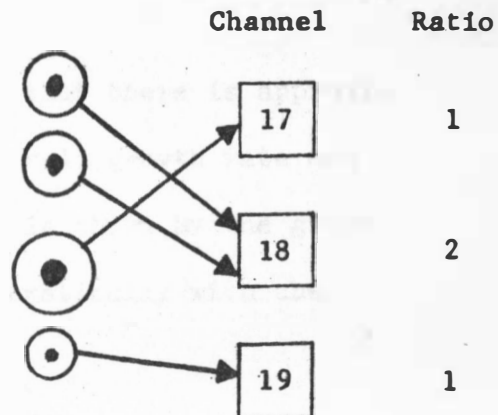
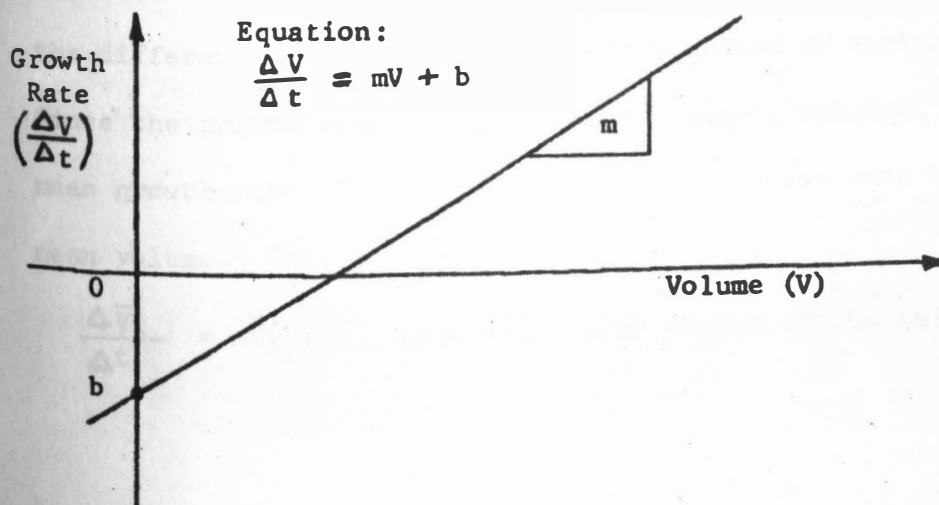


Figure 12. The Approximate Relationship of Cellular Rate Versus Cellular Volume.



corresponding to the time it would take for the cell to grow to the channel limit, the cell suddenly "jumps" to the mean volume of the next channel. There the cell stays for a time, until it has grown enough to "jump" to the next higher channel. Now there is an equivalent cell flow between channel means which can be described in terms of rate.

Sinclair and Ross (103) established that there is approximately a linear relationship between the cell growth rate and the volume of a cell. This relationship is shown by the graph in Figure 12 and can be represented mathematically with the equation:

$$\frac{\Delta V}{\Delta t} = mV + b, \text{ where}$$

t	= time
V	= cell volume
m	= slope
b	= y intercept

The growth rate can be found, given the cell volume, because m and b can be experimentally determined. But it is the rate of cell flow between channels that is required for the model. This rate of flow between channels can be computed by finding the differences between the mean growth rates of each channel. Since the growth rate and volume are linearly related, the mean growth rate of a channel will be the growth rate at the mean volume. This is expressed by:

$$\frac{\Delta \bar{V}_i}{\Delta t} = m\bar{V}_i + b, \text{ where } \bar{V}_i = \text{mean volume of channel } i.$$

The rate between channels, R , would be:

$$R_i = \frac{V_{i+1}}{t} - \frac{V_i}{t} = (m\bar{V}_{i+1} + b) - (m\bar{V}_i + b)$$

Simplifying:

$$R_i = m(\bar{V}_{i+1} - \bar{V}_i)$$

The quantity $(V_{i+1} - V_i)$ is the difference between channel means. This is nothing more than the range of one channel. Since the units of output are expressed in channels, $V_{i+1} - V_i = 1$ channel, the rate difference equation becomes:

$$R_i = m$$

It would seem unusual that the growth rate difference between channels is the same for all channels, since the actual rate is increasing as the channel number (volume) increases. This is due to the fact that the growth rate increase is linear and that the channels are equally spaced. Thus, the growth rate is increasing the same amount for each successive channel. Therefore, the difference is constant and has been shown to be the slope m . If the channels were not equally spaced, or the rate increase non-linear, the growth rate difference between channels would be a function of the channel.

The cell model (Appendix III) is accessed by the commands "Load 2 Execute" from the Coulter Counter tape. The data required for the model simulation includes the file number from which the initial cell volume profile will be taken, the first

cell volume which is the mean cell volume given in cubic microns, the cell variation which is the deviation in cell volume after division given in cubic microns, the rate of volume increase given in channels, the interval of time at which the computer will calculate the volume changes, the initial and final time of the simulation, and the output time at which the computer will store the simulated cell volume profile in internal memory to be printed out later.

Coulter Counter Detection of Inactivated VEE Virus Treated Vero Cell Cultures Materials and Procedures

- A. The materials for the clinical application of the Coulter Counter virus detection system are similar to those described in the Vero cell subculturing materials section and the Coulter Counter volume profile materials section except for the antiserum.
1. Convalescent Horse Immune Serum (Anti-VEE). This antiserum is obtained from the Department of H. E. W., P. H. S. N. C. D. C. Biological Reagents Section, Atlanta, Ga.
- B. The procedure for detection of inactivated VEE virus treated Vero cell cultures is as follows:
- A single flask of Vero cells is subcultured 1:15 and allowed to grow to a monolayer. One milliliter of HBSS is added to four flasks; 1 ml. of HBSS plus VEE virus (0.4 ml.) is added to four

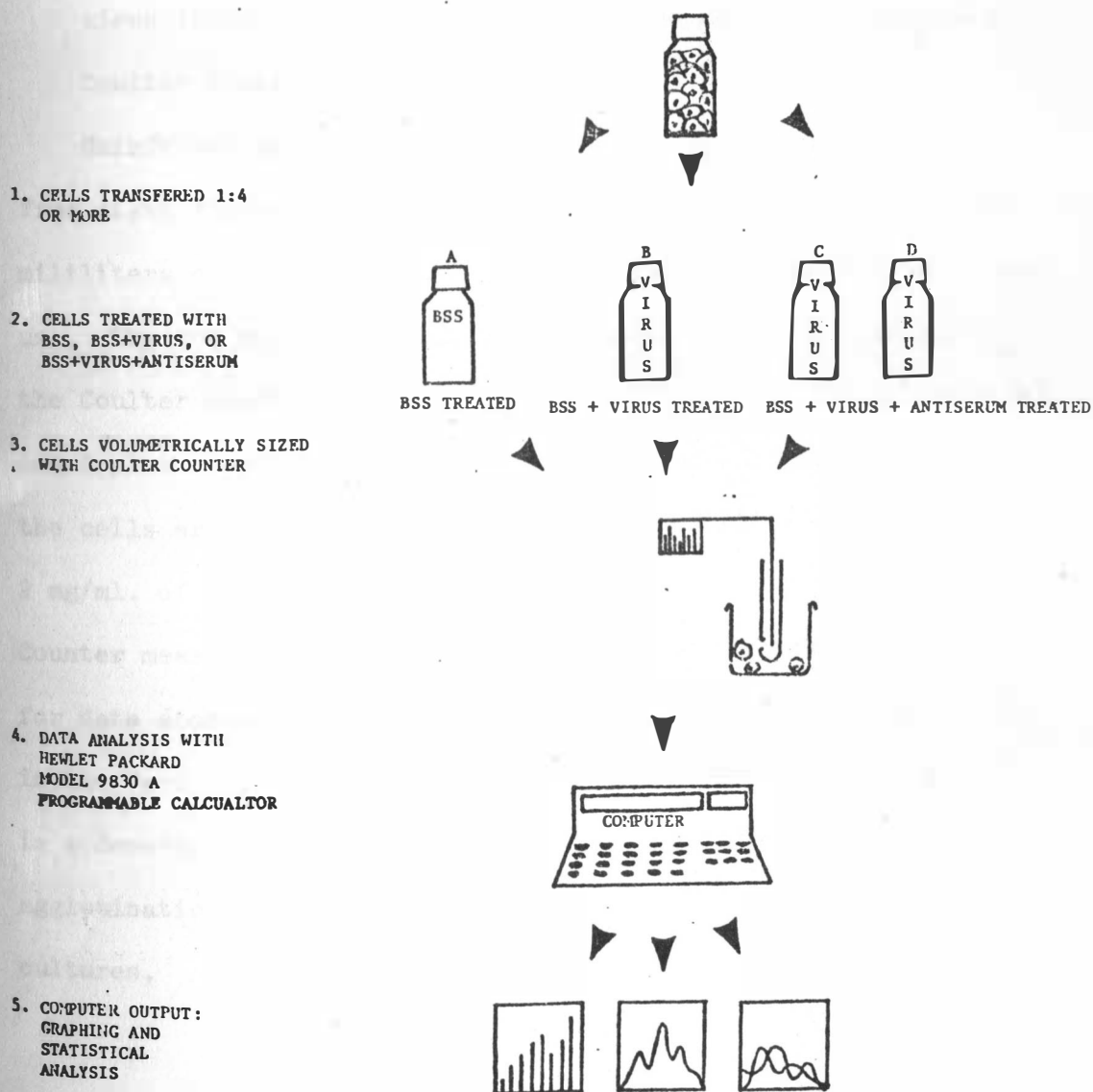
more flasks; 1 ml. of HBSS plus VEE virus (0.4 ml.) which was previously mixed for 30 minutes with excess antiserum is added to the remaining flasks. Note: 0.2 ml. of VEE virus plus 1.8 ml. of reconstituted antiserum are mixed for 30 minutes. All flasks of cells are rinsed three times and 2 ml. of fresh MEM which is supplemented with 10 percent iFBS is added. The cell cultures are incubated 4 to 24 hours (depending on the experimental design), and harvested with 3 ml. of Isoton per flask. A 2 ml. suspension is taken for a hemacytometer count, while the remaining 10 ml. is diluted in 90 ml. of Isoton (1:10) and counted in the Coulter Counter model F. Figure 13 describes the clinical application of the Coulter Counter to rapid detection of viruses.

Coulter Counter Concanavalin A Aedes Albopictus Cell Agglutination

Materials and Procedures

- A. The materials for the concanavalin A agglutination of Aal cell cultures are as follows:
1. Coulter Counter, Isoton, Hemacytometer, Microscope, Hand-held Counter, and Hewlett Packard Programmable Calculator (as described in the Coulter Counter volume analysis materials section).
 2. Concanavalin A (con A). This is purchased in a freeze-dried form from Pharmica Fine Chemicals, Uppsala, Sweden. Con A was prepared from 100 mg/10 ml. frozen stock

Figure 13. Experimental Design of Clinical Application of Coulter Counter Virus Detection System.



solutions. One milliliter contains 10 mg. con A, therefore 8 ml. of 10 mg/ml. con A is diluted 1:5 in 32 ml. of Isoton to produce 40 ml. of 2 mg/ml. con A.

- B. The procedure for con A agglutination of uninfected and VEE virus infected Aal cell cultures to be measured with the Coulter Counter is as follows:

Uninfected and VEE virus infected Aal cells are harvested from eight flasks and diluted 1:10 in 250 ml. of Isoton. Fifty milliliters of the Isoton and cell suspension is removed for later use. The 200 ml. suspension of Isoton and cells is counted in the Coulter Counter model F. After addition of 1 ml. of 10 mg/ml. con A plus 1 ml. of the cells from the 50 ml. of stock suspension, the cells are again counted. Successive addition of 2 ml. of 2 mg/ml. of con A plus 2 ml. of cells are made, and Coulter Counter measurements are taken. Use of the computer programs for data storage and data analysis is similar to that described in the Vero cell volume analysis procedures section. Figure 14 is a description of the Coulter Counter procedures for con A agglutination of uninfected and VEE virus infected Aal cell cultures.

Figure 14. Aal Cell Agglutination Analysis Experimental Design.

1. CELLS TRANSFERED 1:9

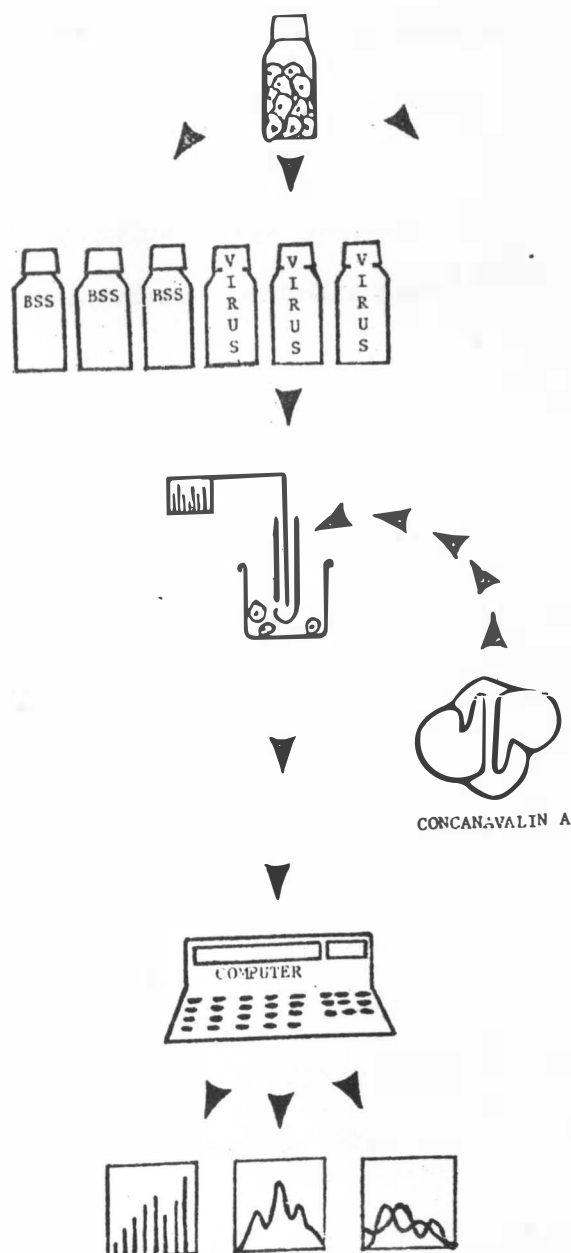
2. CELLS TREATED WITH
BSS OR BSS+VIRUS

3. CELLS VOLUMETRICALLY SIZED
WITH COULTER COUNTER

4. CELLS TREATED WITH INCREASING
CONCENTRATIONS OF CON A AND
SUCCESSIVE COULTER COUNTER
MEASUREMENTS TAKEN

5. DATA ANALYSIS WITH
HEWLETT PACKARD
MODEL 9830 A
PROGRAMMABLE CALCULATOR

6. COMPUTER OUTPUT:
GRAPHING AND
STATISTICAL
ANALYSIS



RESULTS AND DISCUSSION

Latex Particle Control Measurements

The development of a rapid system for virus detection, which utilizes the physical property of volume change in animal cell cultures as the criterion of virus infection, demands an accurate instrument which gives reproducible results. The Coulter Counter, as described in the literature review, has been shown to possess many desirable volume measurement capabilities. However, human or mechanical error may distort the Coulter Counter data, therefore, extensive measurement controls must accompany any series of Coulter Counter experiments.

Control measurements of 6 to 14 micron diameter latex particles and of Vero and Aedes albopictus cell cultures were taken with an optical micrometer and with the Coulter Counter. The optical micrometer measured the particle diameter which was converted to volume with the assistance of a Hewlett Packard computer program. The Coulter Counter measured volume as described in the materials and methods section. These control measurements were done so that comparisons could be made between the two types of measurements, and they were done to demonstrate the accuracy of the Coulter Counter. Coulter Counter measurements were also taken of 2.02 ± 0.0135 micron diameter latex particles for further verification of the Coulter Counter accuracy.

Optical means were initially employed to measure the particle or cell volumes. The calibration of the American optical micrometer is documented in Table 4. In this calibration twelve optical measurements were taken of fifty graduations of a Bousch and Lomb stage micrometer. One optical micrometer graduation was determined to equal 1.86 microns. This factor was subsequently used in the optical micrometer computer program for determining particle and cell volume profiles.

Two hundred latex particles were measured with the optical micrometer and were found to range from 40 to 2303 cubic microns in volume and displayed a mean volume of 363.4 cubic microns. Figure 15 is an illustration of the number of latex particles which were found at the specified volume ranges. Knowledge of the range and volume of the majority of latex particles insures that correct Coulter Counter sensitivity settings will be chosen. As illustrated in Table 5, the Coulter Counter attenuation settings extend for ten values from 0.125 through 8.000. The aperture settings extend for ten values, however, they range from 1.000 to 512.000.

Two groups of sensitivity settings were chosen for the Coulter Counter measurements of the 6 to 14 micron diameter latex particles as displayed in Table 5 and 6. An attenuation of 4 and an aperture of 256 with a range extending from 92 to 9227 cubic microns were chosen to match the desirable range

Table 4. Optical Micrometer Calibration Using Stage Micrometer.

<u>OPTICAL MICROMETER GRADUATIONS</u>	<u>STAGE MICROMETER UNITS (MICRONS)</u>
26.8	50
26.8	50
26.6	50
26.8	50
26.8	50
27.0	50
26.8	50
26.8	50
27.0	50
27.0	50
26.8	50
26.8	50

TOTAL	<u>322.2</u>
-------	--------------

MEAN	26.85 = 50 microns
------	--------------------

∴ 1 OPTICAL MICROMETER GRADUATION EQUALS 1.8622 MICRONS

An American Optical Micrometer is placed on a Spencer microscope using a magnification of 1000 X.

Figure 15. Statistics and Histogram of Latex Particles.

N = 200
 MEAN = 363.3973
 STD. DEV = 336.2162
 SKGWNNESS = 2.7823
 KURTOSIS = 13.3048
 XMIN = 38.5144
 XMAX = 2265.1634
 RANGE = 2226.6510

EACH X= 0.68 PERCENT

```

    0.0000 .          *
            .XXXXXXXXXX*XXXXXXXXXXXX
    92.1000 .          *
            .XXXXXXXXXXXXXXXX*XXXXXXXXX
   184.2000 .          *
            .XXXXXXXXXXXXXXXX*XXXXXXXXXXXXXXXXXXXXXXXXXXXX
   276.3000 .          *
            .XXXXXXXXXXXXX          *
   368.4000 .          *
            .XXXXXXXXXXXXXXXXXXXXX *
   460.5000 .          *
            .XXXXXXXXXX          *
   552.6000 .          *
            .XXXXXXXXXXXXXXXXX *
   644.7000 .          *
            .XXXXX          *
   736.8000 .          *
            .XXX          *
   828.9000 .          *
            .          *
   921.0000 .          *
            .XX          *
  1013.1000 .          *
            .X          *
  1105.2000 .          *
            .          *
  1197.3000 .          *
  
```

Table 5. Volume Range for All Attenuation and Aperture Sensitivity Settings.

Ap. ¹	Attn. ²	Vol. Range ³	Ap. ¹	Attn. ²	Vol. Range ³
1	0.125	0 - 1	8	0.125	0 - 9
	0.177	0 - 1		0.177	0 - 12
	0.250	0 - 2		0.250	2 - 18
	0.354	0 - 3		0.354	8 - 25
	0.500	0 - 4		0.500	5 - 36
	0.707	3 - 6		0.707	22 - 51
	1.0	0 - 9		1.0	5 - 75
	2.0	2 - 18		2.0	10 - 140
2	4.0	4 - 36	16	4.0	20 - 290
	8.0	18 - 72		8.0	23 - 570
	0.125	0 - 2		0.125	2 - 18
	0.177	0 - 3		0.177	0 - 26
	0.250	0 - 4		0.250	4 - 36
	0.354	0 - 6		0.354	16 - 51
	0.500	5 - 9		0.500	5 - 72
	0.707	6 - 12		0.707	43 - 100
4	1.0	2 - 18	32	1.0	9 - 150
	2.0	4 - 36		2.0	17 - 290
	4.0	5 - 72		4.0	23 - 580
	8.0	23 - 99		8.0	23 - 1159
	0.125	0 - 4		0.125	4 - 37
	0.177	0 - 6		0.177	0 - 52
	0.250	0 - 9		0.250	5 - 73
	0.354	4 - 12		0.354	32 - 100
	0.707	11 - 25		0.500	20 - 140
	1.0	4 - 37		1.0	3 - 300
	2.0	5 - 73		2.0	17 - 580
	4.0	10 - 140		4.0	23 - 1156
	8.0	26 - 280		8.0	23 - 2302

Table 5. (Con't.)

Ap. ¹	Attn. ²	Vol. Range ³	Ap. ¹	Attn. ²	Vol. Range ³
64	0.125	7 - 73	256	0.125	5 - 290
	0.177	0 - 100		0.177	4 - 410
	0.250	10 - 140		0.250	17 - 580
	0.354	33 - 200		0.354	33 - 820
	0.500	20 - 290		0.500	23 - 1152
	0.707	45 - 400		0.707	24 - 1625
	1.0	6 - 600		1.0	49 - 2307
	2.0	23 - 1153		2.0	24 - 4625
128	4.0	23 - 2300	512	4.0	92 - 9227
	8.0	46 - 4600		8.0	530 - 18400
	0.125	12 - 140		0.125	17 - 580
	0.177	2 - 200		0.177	8 - 820
	0.250	20 - 290		0.250	23 - 1161
	0.354	33 - 410		0.354	33 - 1625
	0.500	23 - 580		0.500	23 - 2300
	0.707	57 - 790		0.707	65 - 3250
256	1.0	12 - 1153	1024	1.0	44 - 4636
	2.0	23 - 2307		2.0	93 - 9258
	4.0	46 - 4625		4.0	370 - 18500
	8.0	92 - 9200		8.0	370 - 37000

¹ Aperture² Attenuation³ Volume Range in Cubic Microns

Table 6. Coulter Counter Resolution (Cubic u/ Channel) at All Attenuation and Aperture Sensitivity Settings.

ATTENUATION

APERTURE

	1	2	4	8	16
0.125	0.0113	0.0225	0.0450	0.0900	0.1800
0.177	0.0159	0.0319	0.0637	0.1274	0.2549
0.250	0.0225	0.0450	0.0900	0.1800	0.3600
0.354	0.0319	0.0637	0.1274	0.2549	0.5098
0.500	0.0450	0.0900	0.1800	0.3600	0.7200
0.707	0.0636	0.1273	0.2545	0.5090	1.0181
1.000	0.0900	0.1800	0.3600	0.7200	1.4400
2.000	0.1800	0.3600	0.7200	1.4400	2.8800
4.000	0.3600	0.7200	1.4400	2.8800	5.7600
8.000	0.7200	1.4400	2.8800	5.7600	11.5200

ATTENUATION

APERTURE

	32	64	128	256	512
0.125	0.3600	0.7200	1.4400	2.8800	5.7600
0.177	0.5098	1.0195	2.0390	4.0781	8.1562
0.250	0.7200	1.4400	2.8800	5.7600	11.5200
0.354	1.0195	2.0390	4.0781	8.1562	16.3123
0.500	1.4400	2.8800	5.7600	11.5200	23.0400
0.707	2.0362	4.0723	8.1446	16.2893	32.5786
1.000	2.8800	5.7600	11.5200	23.0400	46.0800
2.000	5.7600	11.5200	23.0400	46.0800	92.1600
4.000	11.5200	23.0400	46.0800	92.1600	184.3200
8.000	23.0400	46.0800	92.1600	184.3200	368.6400

and sensitivity settings used to measure Vero cells. The determination of these sensitivity settings will be described later in these results.

The second group of sensitivity settings was chosen to match the desirable range and sensitivity settings used to measure Aal cells. This attenuation was 0.354, the aperture was 512, and the range extended from 33 to 1625 cubic microns.

A comparison of measurements taken with the optical micrometer and with the Coulter Counter is made in Table 7 and 8, and in interpolation graphs in Figures 16, 17, 18, and 19. Table 7 is a list in the percentage and cumulative percentage of latex particles with the volume ranges given in the Coulter Counter sensitivity settings for Vero cells, while Table 8 is a list of the same statistics, but it uses the sensitivity settings of the Aal cells.

An interpolation plot of the percentage relative frequency of latex particles measured with the optical micrometer and with the Coulter Counter using the Vero cell sensitivity settings is given in Figure 16. Every fourth plotted point is a data point. The optical micrometer curve has six distinct peaks or particle populations. The largest population is located at 230 cubic microns. The Coulter Counter curve has approximately four of five particle populations, some of which match the optical micrometer particle populations. The largest

Table 7. Optical Micrometer and Coulter Counter Percent and Cumulative Percent of 6 to 14 Micron Diameter Latex Particles (Coulter Counter using Vero Cell Sensitivity Settings).

Volume (cubic microns)	OPTICAL MICROMETER		COULTER COUNTER	
	Percent	Cumulative Percent	Percent	Cumulative Percent
46.1	14.5	14.5		
138.2	15.0	29.5		
228.3	27.0	56.5		
322.3	8.0	64.5	28.37	28.37
414.7	10.5	75.0	24.29	53.35
506.9	5.5	80.5	12.70	66.05
599.1	8.5	89.0	10.73	76.78
691.2	3.0	92.0	4.89	81.67
783.4	2.5	94.5	5.88	87.55
875.5	0.0	94.5	3.34	90.86
967.7	1.5	96.0	2.42	93.13
1059.9	1.0	97.0	2.00	95.13
1152.0	0.5	97.5	1.26	96.39
1244.2	0.0	97.5	1.12	97.60
1336.3	0.0	97.5	0.51	98.11
1428.3	0.0	97.5	0.59	98.70
1520.7	0.0	97.5	0.42	99.12
1612.8	0.0	97.5	0.29	99.41
1750.0	1.5	99.0*	0.22	99.63
1797.0			0.19	99.82*

* 1 Percent of Optical Micrometer Measured Latex Particles Were Found Larger than 1749 but Smaller than 2303 Cubic Microns.

* Coulter Counter Measured Latex Particles Showed 0.18 Percent Error Due to Rounding.

Table 8. Optical Micrometer and Coulter Counter Percent and Cumulative Percent of 6 to 14 Micron Diameter Latex Particles (Coulter Counter using Aal Cell Sensitivity Settings).

Volume (cubic microns)	OPTICAL MICROMETER		COULTER COUNTER	
	Percent	Cumulative Percent	Percent	Cumulative Percent
8.2	0.0	0.0		
24.5	0.0	0.0		
40.8	2.0	2.0		
57.1	2.5	4.5		
73.4	1.0	5.5		
89.8	9.0	14.5	3.23	3.23
106.1	0.0	14.5	4.02	7.25
122.4	7.0	18.0	3.06	10.31
138.7	4.5	22.5	5.60	15.91
155.0	0.0	22.5	5.65	21.56
171.3	7.0	29.5	3.39	24.95
187.6	0.0	29.5	3.72	28.67
203.9	0.0	29.5	5.42	34.09
220.2	20.0	49.5	2.81	36.90
236.5	0.0	49.5	6.19	43.09
252.8	7.0	56.5	5.63	48.72
269.1	0.0	56.5	4.97	53.69
285.4	0.0	56.5	2.18	55.87
301.7	5.5	62.0	2.19	58.06
318.0	0.0	62.0	3.85	61.91
334.3	0.0	62.0	4.08	66.99
350.6	0.0	62.0	2.25	68.24
366.9	2.5	64.5	2.43	70.67
383.2	0.0	64.5	1.76	72.43
399.5	0.0	64.5	1.53	73.96
415.8	10.5	75.0	2.75	76.71
432.1	0.0	75.0	1.37	78.08
448.4	0.0	75.0	2.59	80.67
465.0	0.0	75.0	1.45	82.12
481.3	0.0	75.0	1.15	83.27
497.6	5.5	80.5	1.51	84.78
513.9	0.0	80.5	0.73	85.51
530.2	0.0	80.5	1.48	86.99

Table 8. (Cont.)

Volume (cubic microns)	OPTICAL MICROMETER		COULTER COUNTER	
	Percent	Cumulative Percent	Percent	Cumulative Percent
546.6	0.0	80.6	0.97	87.96
562.8	5.5	86.0	2.31	90.27
579.1	0.0	86.0	0.99	91.26
595.4	0.0	86.0	0.26	91.52
611.7	0.0	86.0	0.26	91.78
628.0	0.0	86.0	0.52	92.30
644.3	3.0	89.0	1.37	93.67
660.6	0.0	89.0	0.00	93.67
676.9	0.0	89.0	1.20	94.87
693.2	0.0	89.0	0.60	95.47
709.5	0.0	89.0	0.38	95.85
725.8	3.0	92.0	0.52	96.37
742.1	0.0	92.0	0.90	97.27
758.4	0.0	92.0	0.31	97.58
774.7	0.0	92.0	0.32	97.90
791.0	0.0	92.0	0.43	98.33
807.3	0.0	92.0	0.84	99.17
823.6	0.0	92.0	0.20	99.37
839.9	0.0	92.0	0.26	99.63
856.2	0.0	92.0	0.06	99.69
872.5	0.0	92.0*	0.35	100.40*

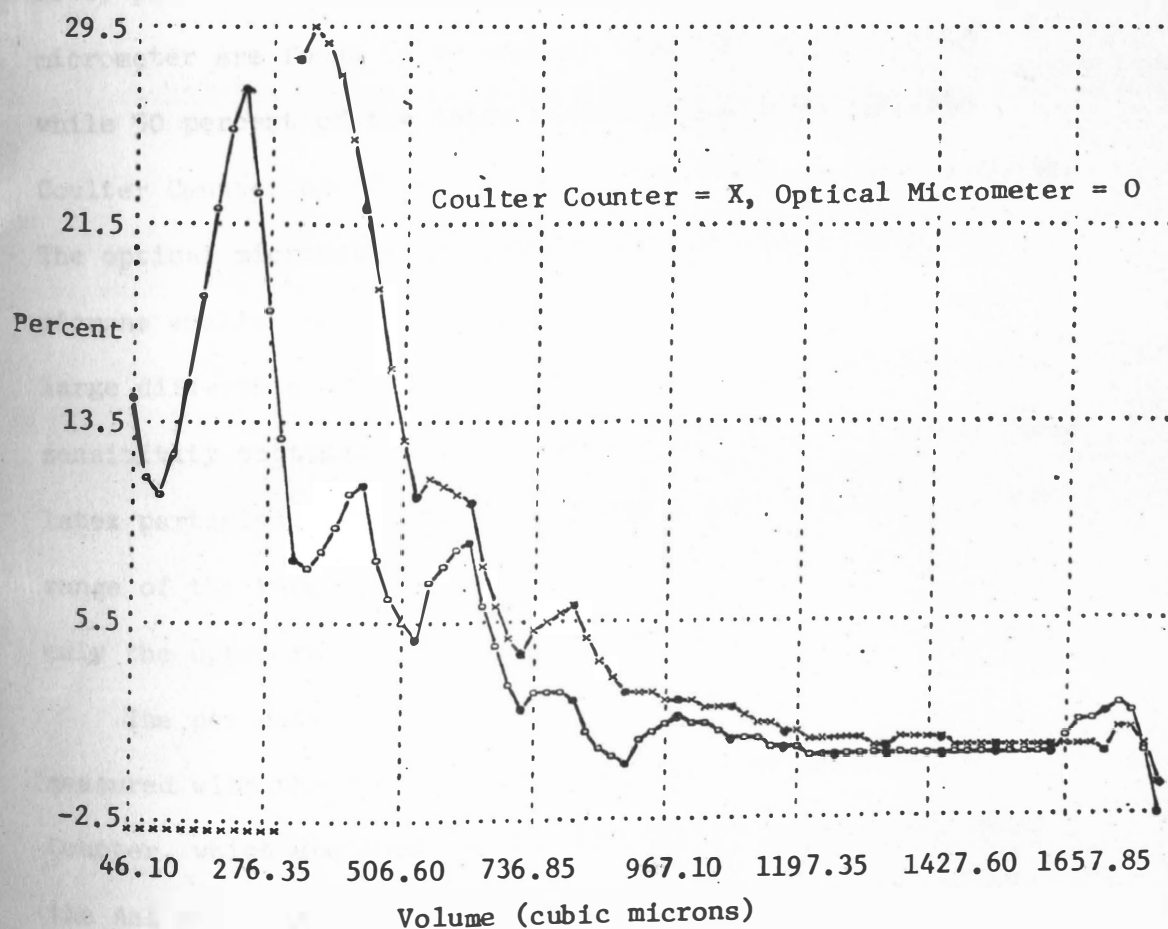
* Eight Percent of Optical Micrometer Measured Latex Particles Were Found Larger than 872.5 Cubic Microns.

* Coulter Counter Measured Latex Particles Showed 0.4 Percent Error Due to Rounding.

Table 8a. Example of Given and Interpolated Data Points for the Plot of Percent Frequency of 6 to 14 Micron Diameter Latex Particles Measured with the Optical Micrometer in Figure 16.

OPTICAL MICROMETER			
=== INTERPOLATED ===		===== GIVEN =====	
X	Y	X	Y
46.100	14.4999	46.100	14.5000
69.130	11.1975		
92.160	10.6267		
115.190	12.1183		
138.220	15.0030	138.200	15.0000
161.250	18.6115		
184.280	22.2745		
207.310	25.3226		
230.340	27.0867	228.300	27.0000
253.370	22.8836		
276.400	17.9311		
299.430	12.6898		
322.460	7.9687	322.300	8.0000
345.490	7.7829		
368.520	8.4211		
391.550	9.4718		
414.580	10.4956		
437.610	11.0534	414.700	10.5000
460.640	7.9770		
483.670	6.6143		
506.700	5.5075		
529.730	4.8975	506.900	5.5000
552.760	7.0250		
575.790	7.8973		
598.820	8.4985		
621.850	8.5711	599.100	8.5000
644.880	5.9846		
667.910	4.4503		
690.940	3.0150		
713.970	1.8893	691.200	3.0000
737.000	2.5633		
760.030	2.5397		
783.060	2.5020		
806.090	2.3405	783.400	2.5000
829.120	1.1349		
852.150	0.4930		
875.180	0.0057		
898.210	-0.2333	875.500	0.0000
921.240	0.6169		

Figure 16. Percent Frequency of 6 to 14 Micron Diameter Latex Particles Measured with the Optical Micrometer and the Coulter Counter (Coulter Counter using the Vero Cell Sensitivity Settings).



percentage of latex particles measured with the Coulter Counter is at 345 cubic microns. From these peak particle populations, the optical micrometer measurement of the latex particles is shown to be over 100 cubic microns smaller than the Coulter Counter measurement of these similarly sized particles.

The cumulative percentage of latex particles measured with the optical micrometer and with the Coulter Counter using the Vero cell sensitivity settings is plotted in Figure 17. Fifty percent of the latex particles measured with the optical micrometer are found to be smaller than 210 cubic microns, while 50 percent of the latex particles measured with the Coulter Counter are found to be smaller than 390 cubic microns. The optical micrometer measurement is once again 100 cubic microns smaller than the Coulter Counter measurement. This large difference may be caused by the imposition of Vero cell sensitivity settings on the Coulter Counter for measuring these latex particles. The latex particles are at the lower volume range of the Vero cells, and the Coulter Counter is measuring only the upper range of the latex particles.

The percentage relative frequency of latex particles measured with the optical micrometer and with the Coulter Counter, which are found at the specified volume ranges using the Aal cell sensitivity settings, are plotted in Figure 18. The use of the Aal sensitivity settings allows for a fine

Figure 17. Cumulative Percent Relative Frequency of 6 to 14 Micron Diameter Latex Particles Measured with the Optical Micrometer and the Coulter Counter (Counter Counter using the Vero Cell Sensitivity Settings).

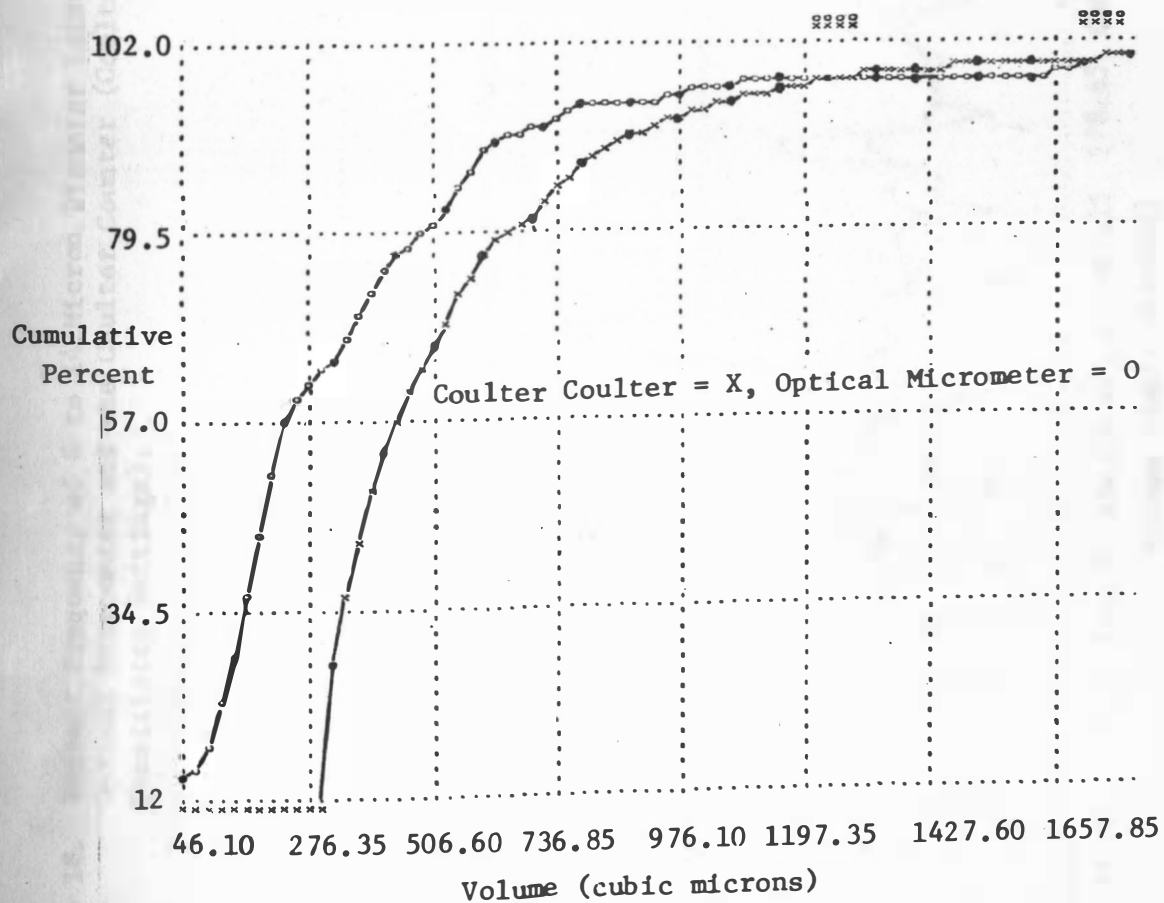
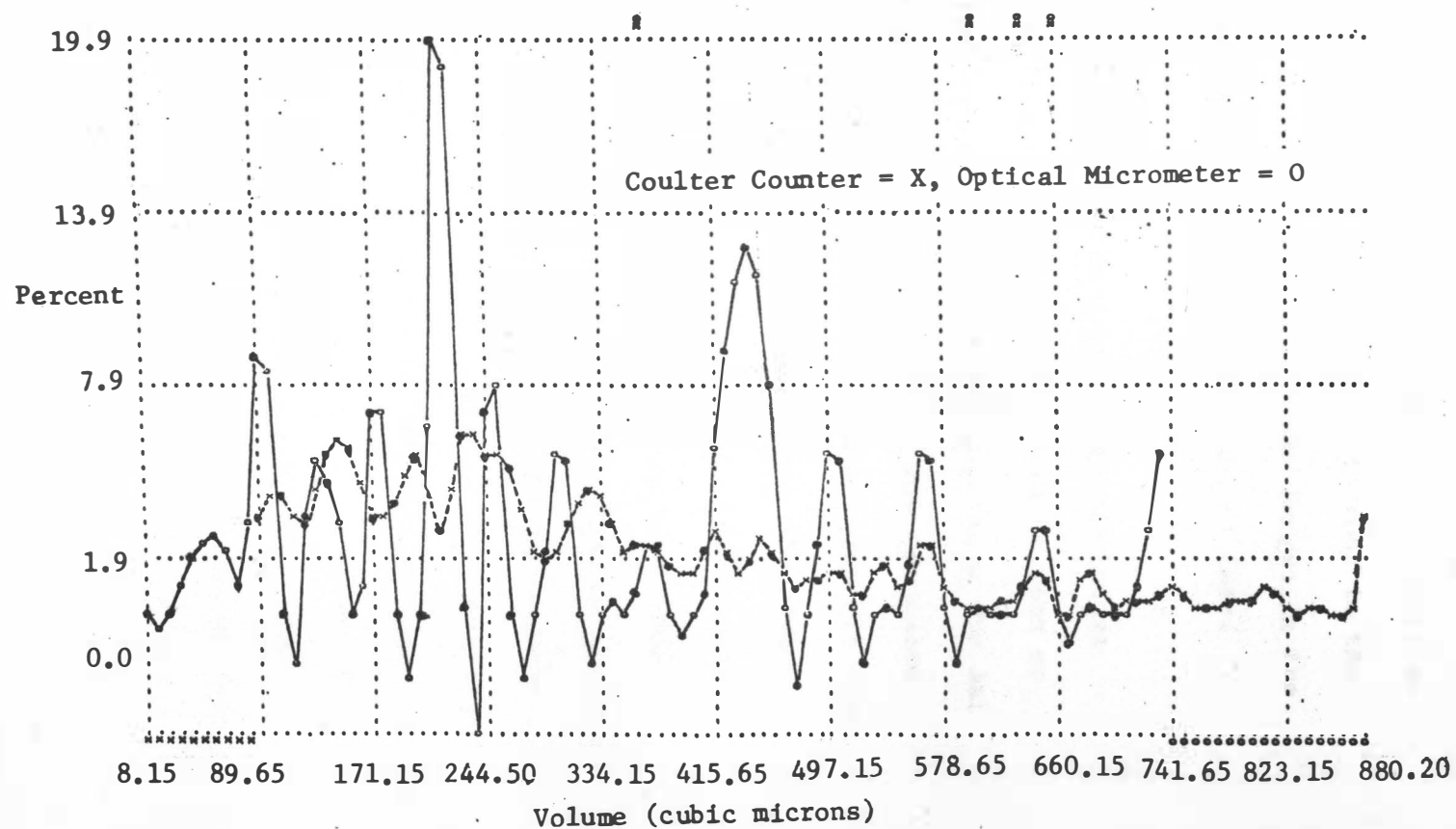


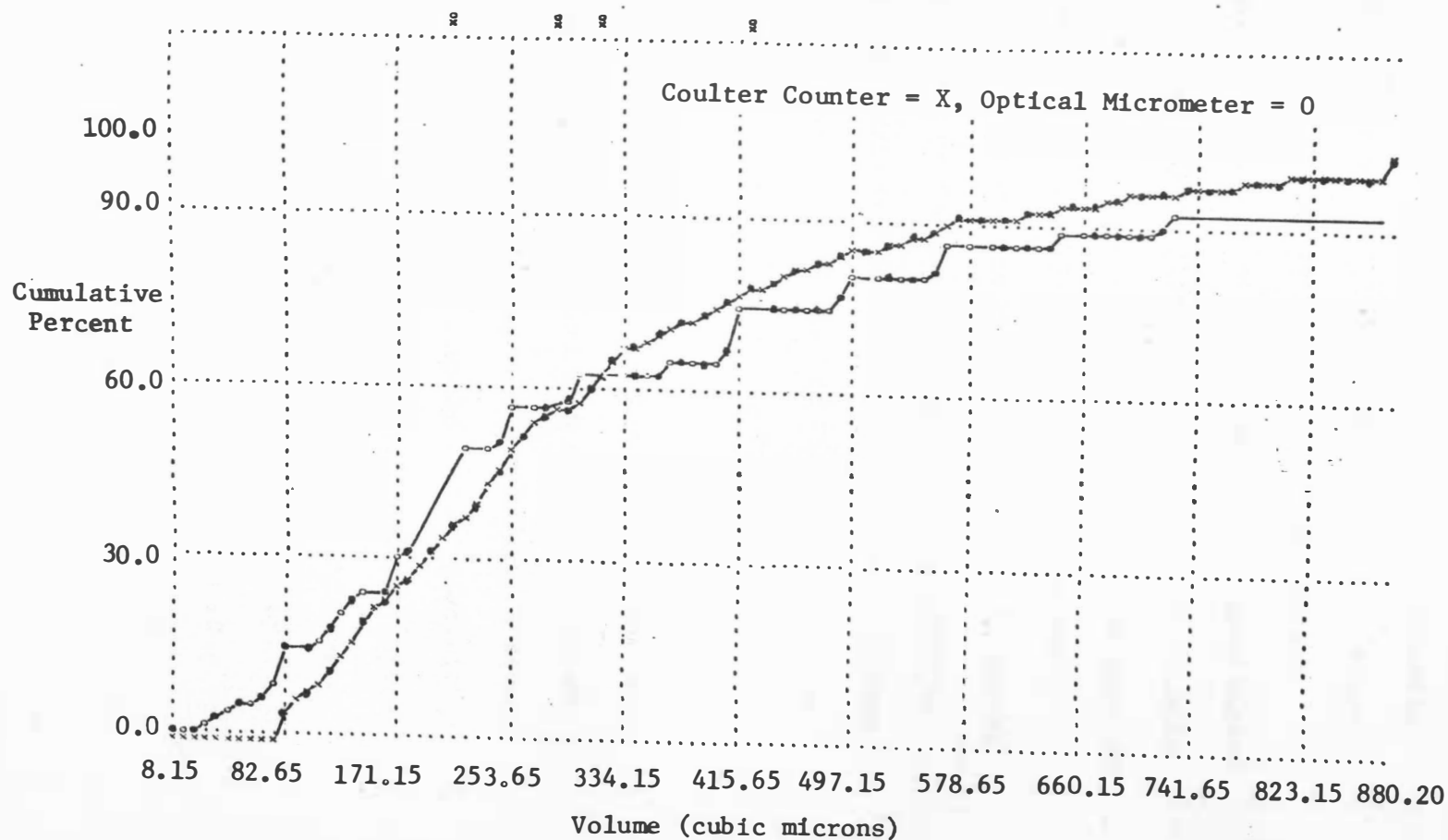
Figure 18. Percent Frequency of 6 to 14 Micron Diameter Latex Particles Measured with the Optical Micrometer and the Coulter Counter (Coulter Counter Using the Aal Cell Sensitivity Settings).



resolution of the latex particles by the Coulter Counter and, therefore, the channel range is small. In this interpretation plot every other point is a data point. Major latex populations can be found at 90, 230, and 460 cubic microns in the optical micrometer curve, while several volume ranges in the Coulter Counter curve share similar populations of latex particles.

Figure 19 is an interpolation plot of the cumulative percentage relative frequency of latex particles at each of the specified volume ranges. It is incremented using the Aal sensitivity settings. Fifty percent of the latex particles measured with the optical micrometer are smaller than 245 cubic microns, while 50 percent of the latex particles measured with the Coulter Counter are smaller than 260 cubic microns. The optical micrometer cumulative percentage curve is only 15 cubic microns smaller than the Coulter Counter curve by using the format of comparing the volume at which the cumulative percentage equals 50 percent. The Aal sensitivity settings allow a fine particle resolution; the Aal cells are smaller than the Vero cells which makes the Aal cells closer to the latex volume range. These optical micrometer and Coulter Counter cumulative percentage curves, which are incremented using the Aal sensitivity settings, more closely parallel each other than do the cumulative percentage curves, which are incremented using

Figure 19. Cumulative Percent Relative Frequency of 6 to 14 Micron Diameter Latex Particles Measured with the Optical Micrometer and the Coulter Counter (Coulter Counter using the Aal Cell Sensitivity Settings).



the Vero cell sensitivity settings.

Control measurements were taken of 2.02 micron diameter (4.32 cubic microns in volume) latex particles as a further demonstration of the volume sizing ability of the Coulter Counter. Figure 20 is a plot of the percentage of latex particles found at the specified volume ranges when Coulter Counter measurements are taken with an attenuation of 0.177, an aperture of 32, and a resolution of 0.509 cubic microns. The small box in the figure represents the volume at which a 2.02 micron diameter particle can be found. The Coulter Counter detects the latex particles between 2 and 9.7 cubic microns in volume. The largest populations of particles are located in channels 7, 9, 11, and 12 which extend from 3.6 to 7.6 cubic microns.

Interference Count Control

Another control experiment was performed to document the inherent interference counts obtained when recording Coulter Counter data. Interference or background counts are caused by electronic interference from proximally located electric motors or incident small dust particles from the air. Interference counts were taken by recording the Coulter Counter counts of Isoton on a day with normal activity at midday. Ten counts were taken at threshold 5 and at threshold 10 for five different groups of sensitivity settings proposed to be used in this investigation.

Figure 20. Coulter Counter Control Measurements of 2.02 Micron Diameter Latex Particles.

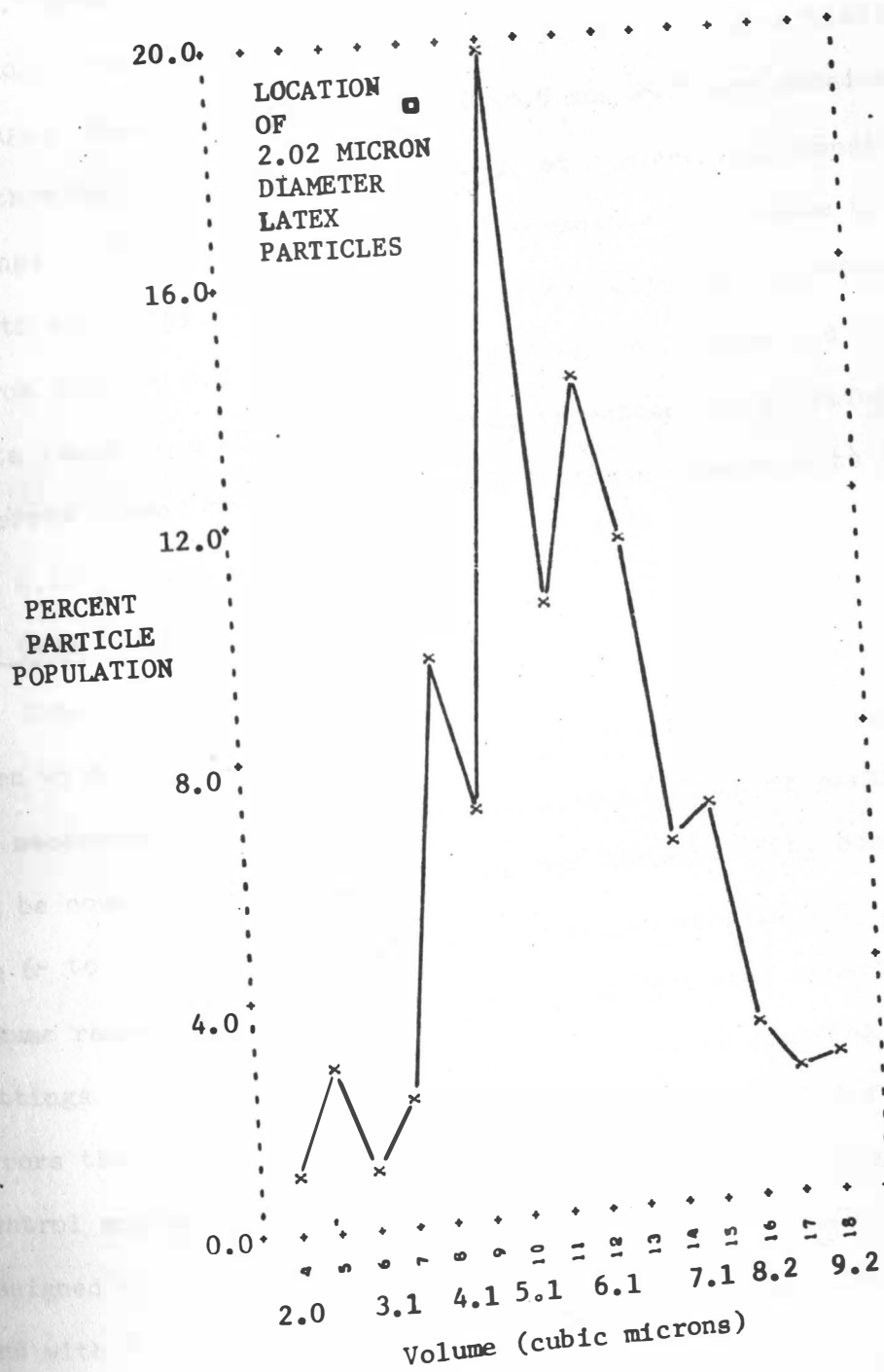


Table 9 is a list of the counts and the mean of the counts of interference for each of the sensitivity settings. There are 19.9 mean threshold counts at threshold 5 and 8.4 mean threshold counts at threshold 10 for the Vero cell sensitivity settings. Mean threshold counts of 48.5 and 24.1 are obtained from threshold 5 and 10, respectively, at the Aal cell sensitivity settings. Since typical Vero cell threshold counts range from 4000 to 40,000 at threshold 10, the error caused by interference is from 0.23 to 0.02 percent. Typical Aal cell threshold counts range from 20,000 to 40,000 at threshold 10, therefore, the error caused by the interference in these measurements is from 0.12 to 0.06 percent.

Vero Cell Volume Analysis Control

Control measurements of an inert particle, such as latex, taken with the optical micrometer and with the Coulter Counter are necessary for assurance that major populations of particles can be counted and sized by the Coulter Counter. Yet, because the 6- to 14-micron diameter latex particles were in the lower volume range of the Vero cell, use of the Vero cell sensitivity settings of the Coulter Counter produced greater counting errors than the use of the Aal sensitivity settings. A further control measurement was then proposed. An experiment was designed to measure Vero cells with the optical micrometer and with the Coulter Counter, thus better establishing the

Table 9. Isoton Interference Counts for Coulter Counter Attenuation and Aperture Sensitivity Settings.

Threshold 5 Count	* At 4 Ap 256	At 1 Ap 256	At .500 Ap 512	* At .354 Ap 512	At .250 Ap 512	At .177 Ap 512
	26	88	57	53	111	8413
	26	95	69	61	138	6290
	18	71	104	54	169	8376
	15	86	116	39	156	6774
	13	100	103	50	153	6411
	17	97	97	39	153	8211
	17	112	88	43	181	6374
	20	84	100	56	158	8606
	23	63	93	50	167	6757
	24	57	76	40	181	8652
MEAN	19.9	85.3	90.3	48.5	156.7	7486.4

Threshold 10
Count

	13	40	46	26	27	45
	8	65	46	32	25	43
	5	51	62	32	27	45
	12	46	60	16	26	31
	3	51	55	25	26	46
	8	31	49	27	25	39
	6	35	54	18	36	50
	4	35	61	21	33	39
	11	54	44	27	32	28
	14	47	55	22	27	38
MEAN	8.4	45.5	53.2	24.1	25.8	40.4

* Sensitivity Settings Used for Vero Cell and Aal Cell Coulter Counter Measurements.

acceptability of the Coulter Counter measurements taken at the Vero cell volume range.

Five separate measurements were taken of 1000 Vero cells with the optical micrometer, and five measurements were taken of about 100,000 Vero cells with the Coulter Counter. The results which were obtained from the five measurements of the 200 Vero cells per measurement with the optical micrometer are given in Table 10. This optical measurement shows the average Vero cell volume ranges from 270 to 12,000 cubic microns. Only 0.8 percent of the cells are larger than 12,000 cubic microns, while an average of 93.2 percent of the population is from 500 to 6000 cubic microns, and an average of 81.3 percent of the population is from 500 to 4000 cubic microns in volume.

The percentage relative frequencies of Vero cells at each volume range is given for each of the five optical measurements in Table 11. The percentage relative frequency is computed only from cells found in the 645 to 3664 cubic micron volume range. Also, in this table the average percentage relative frequencies are given. It may be noted that several volume ranges in each of the measurements contain no cells. This occurs because of the resolution of the optical micrometer. Cells which may have been located in these "empty" volume ranges were judged to be slightly larger or smaller and were allocated to other neighboring volume ranges.

After the relative population distributions of Vero cells

Table 10. Optical Micrometer Measurement of Vero Cells.

Total Number of Cells					
Volume Range					
Lower Limit	Trial 1	Trial 2	Trial 3	Trial 4	Trial 5
0	5	3	0	3	1
500	12	0	1	16	7
1000	31	16	26	27	28
1500	41	33	55	40	43
2000	47	52	51	32	50
2500	10	13	8	16	10
3000	22	29	24	25	17
3500	6	6	6	6	7
4000	3	1	2	3	0
4500	13	17	17	9	12
5000	1	9	3	2	3
5500	1	0	3	6	6
6000	0	3	0	0	0
6500	1	5	1	2	0
7000	3	0	1	4	6
7500	0	1	0	1	0
8000	1	0	0	1	1
8500	0	0	0	0	0
9000	0	0	0	2	2
9500	0	1	0	0	0
10000	0	1	0	0	2
10500	0	5	0	1	1
11000	0	1	0	1	1
11500	0	0	0	0	2
12000	0	0	0	0	0
12500	1	0	0	1	0
13000		0	0	1	0
13500		0	0	0	0
14000		0	2	0	0
14500		0		0	0
15000		0		0	1
.					
.					
.					
20000		1			

Table 11. Percent Relative Frequency of Vero Cells Measured with the Optical Micrometer.

Channel No.	Volume (cubic microns)	Trial (%)					Average % Relative Freq.	Cumulative Average % Relative Freq.
		1	2	3	4	5		
7	645.12	4.30	0.00	0.00	4.40	3.21	2.38	2.38
8	737.28	1.23	0.00	0.00	0.00	0.00	0.25	2.63
9	829.44	0.00	0.00	0.00	0.00	0.00	0.00	2.63
10	921.60	1.23	0.00	0.60	4.40	0.64	1.37	4.00
11	1013.76	0.61	0.73	0.60	0.63	0.00	0.51	4.51
12	1105.92	10.43	2.96	10.12	6.29	11.54	8.26	12.77
13	1198.08	1.84	1.45	2.38	5.66	1.94	2.65	15.42
14	1290.24	0.00	0.00	0.00	0.00	0.00	0.00	15.42
15	1382.40	6.14	1.45	2.38	4.40	4.49	3.77	19.19
16	1474.56	0.00	0.00	0.00	0.00	0.00	0.00	19.19
17	1566.72	3.67	1.45	1.79	2.52	4.49	2.66	21.85
18	1658.88	21.47	21.74	26.79	18.24	21.15	21.88	43.73
19	1751.04	0.00	0.00	0.00	0.00	0.00	0.00	43.73
20	1843.20	1.23	1.45	4.17	4.40	1.92	2.63	46.36
21	1935.36	0.00	0.00	0.00	0.00	0.00	0.00	46.36
22	2027.52	6.75	7.97	8.93	7.55	8.33	7.91	54.27
23	2119.68	0.00	0.00	0.00	0.00	0.00	0.00	54.27
24	2211.84	3.68	3.62	4.17	1.26	5.13	3.57	57.84
25	2304.00	0.00	0.00	0.00	0.00	0.00	0.00	57.84
26	2396.16	17.79	26.09	17.26	11.95	18.59	18.37	76.21
27	2488.32	0.00	0.00	0.00	0.00	0.00	0.00	76.21
28	2580.48	0.00	0.00	0.00	0.00	0.00	0.00	76.21
29	2672.64	1.84	0.73	0.60	0.00	3.85	1.40	77.61
30	2764.80	0.00	0.00	0.00	0.00	0.00	0.00	77.61
31	2856.96	4.30	8.70	4.17	9.43	2.56	5.83	83.44
32	2949.12	0.00	0.00	0.00	0.00	0.00	0.00	83.44
33	3041.28	0.00	0.00	0.00	0.00	0.00	0.00	83.44
34	3133.44	2.45	1.45	3.00	3.77	3.21	2.16	85.60
35	3225.60	0.00	0.00	0.00	0.00	0.00	0.00	85.60
36	3317.76	11.66	19.57	11.31	11.95	8.33	12.56	98.16
37	3409.92	0.00	0.00	0.00	0.00	0.00	0.00	98.16
38	3502.08	0.00	0.00	0.00	0.00	0.00	0.00	98.16
39	3594.24	0.00	0.73	1.79	3.45	0.64	1.32	99.48
Total Cells Counted		163	138	158	159	156		

were determined optically, specific Coulter Counter sensitivity settings could be chosen. Tables 5 and 6 list the variety of attenuation and aperture settings desirable for a population of cells such as the Vero cells of which the majority of cells are located between 500 and 4000 cubic microns in volume. The decision of which sensitivity settings to utilize must also be based on the resolution each attenuation and aperture settings will give. Resolution is the extent of the volume range or channel. An attenuation of 4 and an aperture of 256 were the sensitivity settings selected for the Coulter Counter measurements of Vero cells. According to Table 5 and 6, these sensitivity settings will cover a 92 to 9227 cubic micron volume range and allow a resolution or channel width of 92.16 cubic microns. These sensitivity settings were selected because of several rational. First, these sensitivity settings adequately encompass the Vero cell volume range. Second, the necessity of taking an excessive number of threshold counts would arise if the resolution were small. This would cause the sample size to be large (more volumes of fluid would be passed through the Coulter Counter), and more time would be expended. If the resolution were very large, sample size could be reduced, however, the cells would be allocated into more extensive volume ranges, and fine volume differences between cell volume profiles may be lost. Finally, several

trial measurements taken of latex particles with the Coulter Counter resulted in less than 0.23 percent interference or background counts. The Coulter Counter inherent interference could therefore be ignored in further Coulter Counter measurements of Vero cells.

Coulter Counter measurements of Vero cells were then performed as the second part of the control measurement to compare the optical micrometer and Coulter Counter measurements of Vero cells. Figure 21 is an example of one of the five Coulter Counter measurements taken of the Vero cells. Table 12 is a presentation of the percentage relative frequency from each of the five measurements of Vero cells found at the specified volume ranges. The number of total cells counted in each trial is given below the percentage relative frequency column for each trial. From this table the average percentage relative frequency of Vero cells measured with the optical micrometer and with the Coulter Counter can be compared. The optical micrometer average volume profile has four channels where major populations of cells are located. These channels are 12, 18, 26, and 36 which are at the mean volumes of 1106, 1659, 2396, and 3318 cubic microns, respectively. The Coulter Counter average volume profile has no channel where cell population is over 6.4 percent. The cell populations for the Coulter Counter average Vero cell volume profile are more uniformly located.

Figure 21. Example of a Vero Cell Volume Profile.

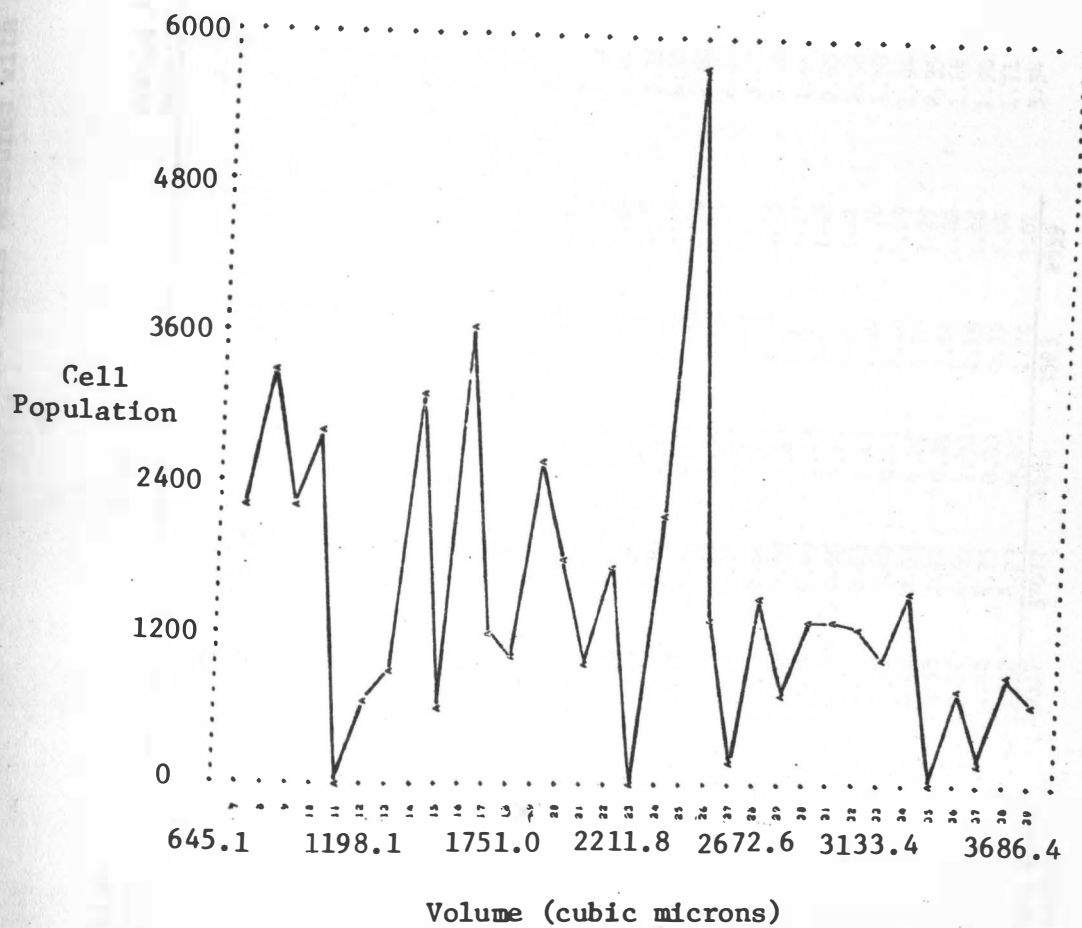


Table 12. Percent Relative Frequency of Vero Cells Measured with the Coulter Counter.

Channel No.	Volume (cubic microns)	Trial (%)					Average % Relative Freq.	Cumulative Average % Relative Freq.
		1	2	3	4	5		
7	645.12	4.45	0.00	1.33	6.05	1.75	2.73	2.73
8	737.28	6.74	2.66	1.67	1.08	4.76	3.38	6.11
9	829.44	4.47	2.86	3.48	1.53	4.34	3.34	9.45
10	921.60	5.72	0.00	3.52	4.68	0.35	2.85	12.30
11	1013.76	0.00	2.90	1.87	2.10	0.45	1.46	13.76
12	1105.92	1.31	3.36	5.75	1.36	0.00	2.32	16.08
13	1198.08	1.82	0.00	3.12	5.39	4.58	2.36	18.44
14	1290.24	6.31	5.35	3.19	2.15	1.47	2.98	21.42
15	1382.40	1.25	4.44	7.51	3.83	1.54	3.71	25.13
16	1474.56	7.44	4.02	2.14	2.19	4.41	4.04	29.17
17	1566.72	2.44	0.00	10.19	4.85	4.44	4.38	33.55
18	1658.88	2.01	5.82	1.83	3.21	5.35	3.64	37.19
19	1751.04	5.28	4.59	6.11	6.02	3.81	5.16	42.35
20	1843.20	3.63	1.80	2.92	0.82	3.43	2.45	44.88
21	1935.36	1.89	6.28	5.15	9.03	4.93	2.52	47.32
22	2027.52	3.52	1.92	3.25	2.13	4.55	5.46	52.78
23	2119.68	0.00	4.97	4.23	5.54	4.34	2.96	58.24
24	2211.84	4.33	4.36	2.12	1.99	3.95	3.35	61.59
25	2304.00	11.72	5.83	4.12	5.39	4.44	6.30	67.89
26	2396.16	2.67	0.65	4.43	2.38	2.80	2.60	70.49
27	2488.32	0.37	3.55	2.36	1.70	3.64	2.32	72.81
28	2580.48	3.03	0.66	3.21	3.09	6.12	3.22	76.03
29	2672.64	1.44	0.00	3.83	3.38	1.75	2.08	78.11
30	2764.80	2.69	0.00	1.87	1.59	1.57	1.54	79.65
31	2856.96	2.65	2.49	1.43	3.24	3.46	2.65	82.30
32	2949.12	2.49	0.90	3.14	2.16	3.11	2.36	84.66
33	3041.28	2.03	2.03	0.13	2.90	1.78	1.78	86.44
34	3133.44	3.19	2.49	0.07	2.13	1.89	1.94	88.38
35	3225.60	0.00	6.03	1.25	1.22	3.25	2.35	90.73
36	3317.76	1.55	2.41	0.89	1.53	1.82	1.64	92.37
37	3409.92	0.36	4.65	1.32	1.19	1.96	1.90	94.27
38	3502.08	1.88	4.75	0.00	0.99	0.94	1.71	95.98
39	3594.24	1.32	8.23	2.45	1.70	3.01	3.34	99.32
Total Cells Counted		49317	37077	4486	3523	2859		

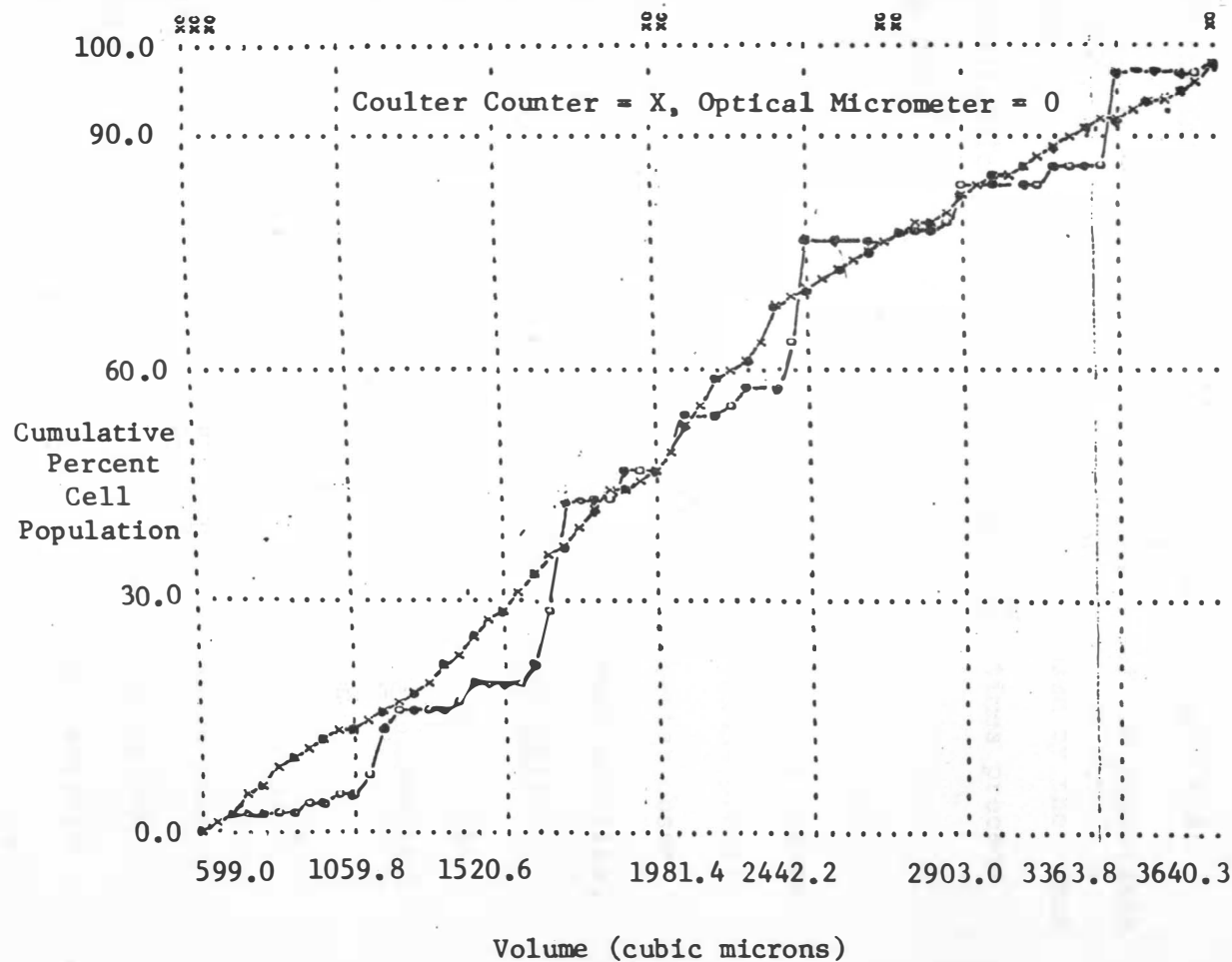
There are major cell populations located at channels 17, 18, 20, 23, and 26 which are at the mean volumes of 1567, 1659, 1843, 2120, and 2396 cubic microns, respectively.

The cumulative average percentage relative frequency is plotted for both the optical micrometer and the Coulter Counter measurements of Vero cells in Figure 22. The optical micrometer curve and the Coulter Counter curve parallel each other closely. Using the format of comparing the volume at which the cumulative percentage equals 50 percent, it can be observed that the optical micrometer cumulative percentage curve reaches 50 percent at a volume of 2010.11 cubic microns, while the Coulter Counter cumulative percentage curve reaches 50 percent at a volume of 1980.60 cubic microns. The optical micrometer and the Coulter Counter cumulative percentage curves differ by only 29.51 cubic microns by using this analysis. From these results the Coulter Counter has demonstrated the reliability and accuracy which makes this instrument useful in volume analysis investigations.

Uninfected and VEE Virus Infected Vero Cell Volume Analysis

Numerous experiments were then conducted to detect volume differences between uninfected Vero cell cultures and VEE virus infected Vero cell cultures. In the following discussion UC will be used to refer to uninfected cell cultures, and IC will be used to refer to VEE virus infected cell cultures at

Figure 22. Cumulative Percent Relative Frequency of a Vero Cell Population Measured with the Optical Micrometer and the Coulter Counter.



various times post-infection. For example, 4UC will refer to 4-hour uninfected Vero cell cultures.

Several independent experiments of uninfected and VEE virus infected cell cultures were performed at 0, 4, 6, 10, 12, and 24 hours post-infection as discussed in the materials and methods section (post-infection is used to designate the time after the infection of some of the group of flasks with virus). These time periods were chosen because of the importance of early detection of the cell volume changes caused by the virus to a rapid detection system. Also most of these times precede observable CPE.

An example of the volume profiles of OUC, 4UC, and 4IC is presented in Figure 23. Much difficulty in comparing volume profiles is encountered. Elimination of the OUC volume profile from the plot as shown in Figure 24 allows for a better observation of the differences between the 4UC and the 4IC profiles, but the significance of these differences is questionable.

Centroid analysis was chosen to overcome the complexity of comparing Coulter Counter volume profiles of the uninfected and of the VEE virus infected Vero cell cultures. It will be recalled that the centroid value of a curve was defined as the center of mass of that curve. Centroids can be calculated for any Coulter Counter volume profile, such as the uninfected Vero cell curve shown in Figure 25. The centroid

Figure 23. Cell Population Volume Profiles of 0 Hour Uninfected, 4 Hour Uninfected, and 4 Hour VEE Virus Infected Vero Cells.

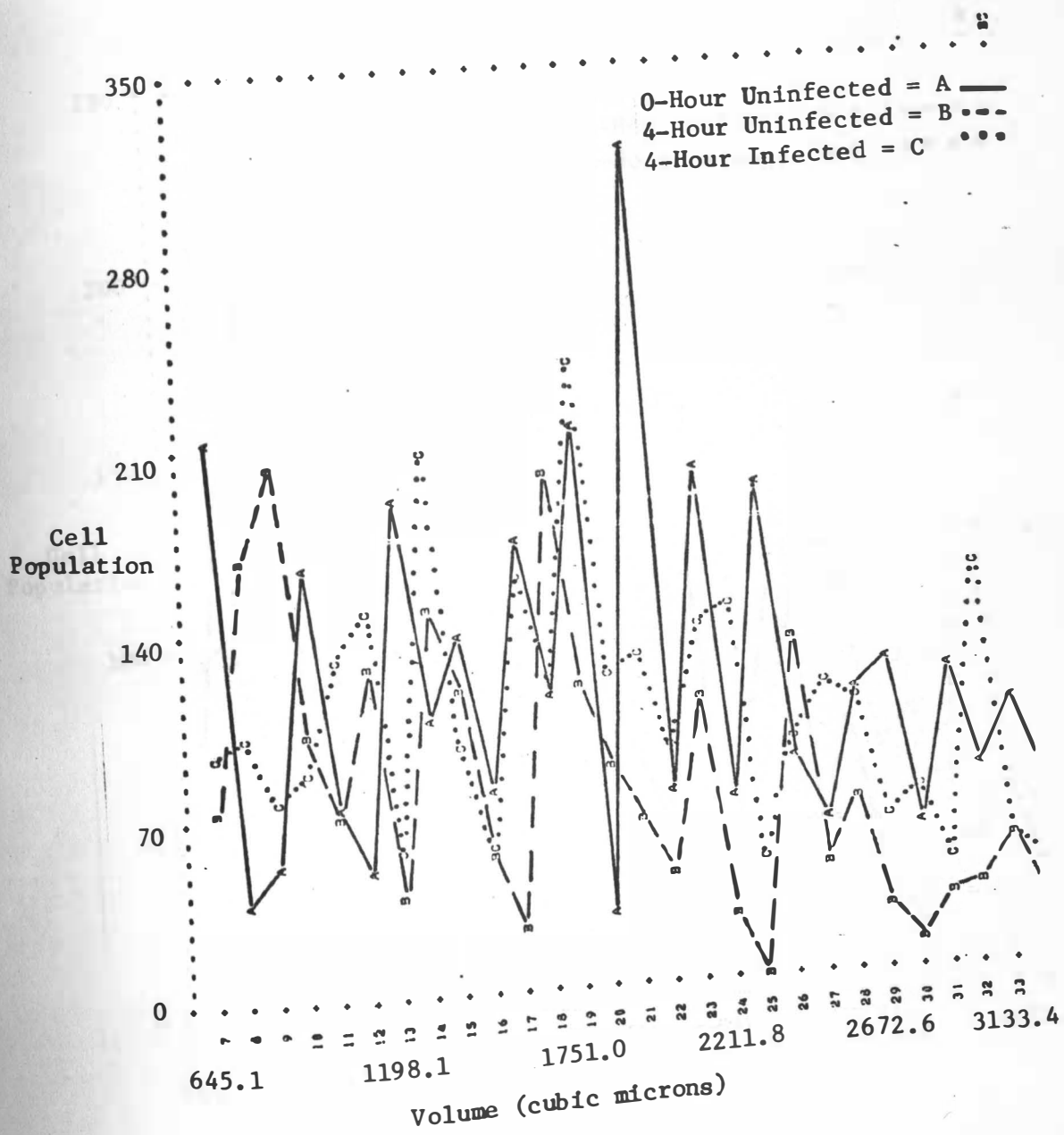


Figure 24. Cell Population Volume Profiles of 4 Hour Uninfected and 4 Hour VEE Virus Infected Vero Cells.

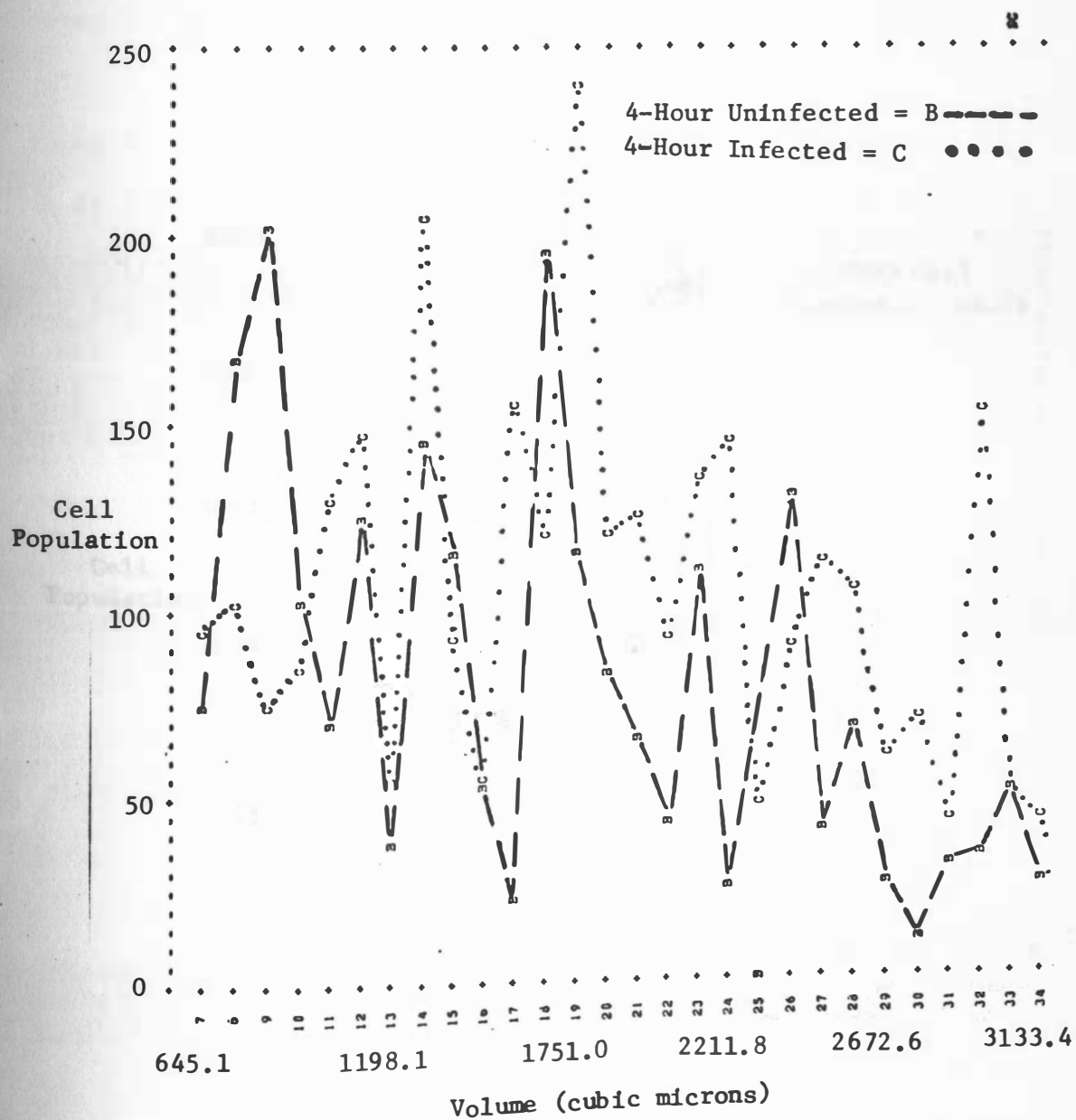
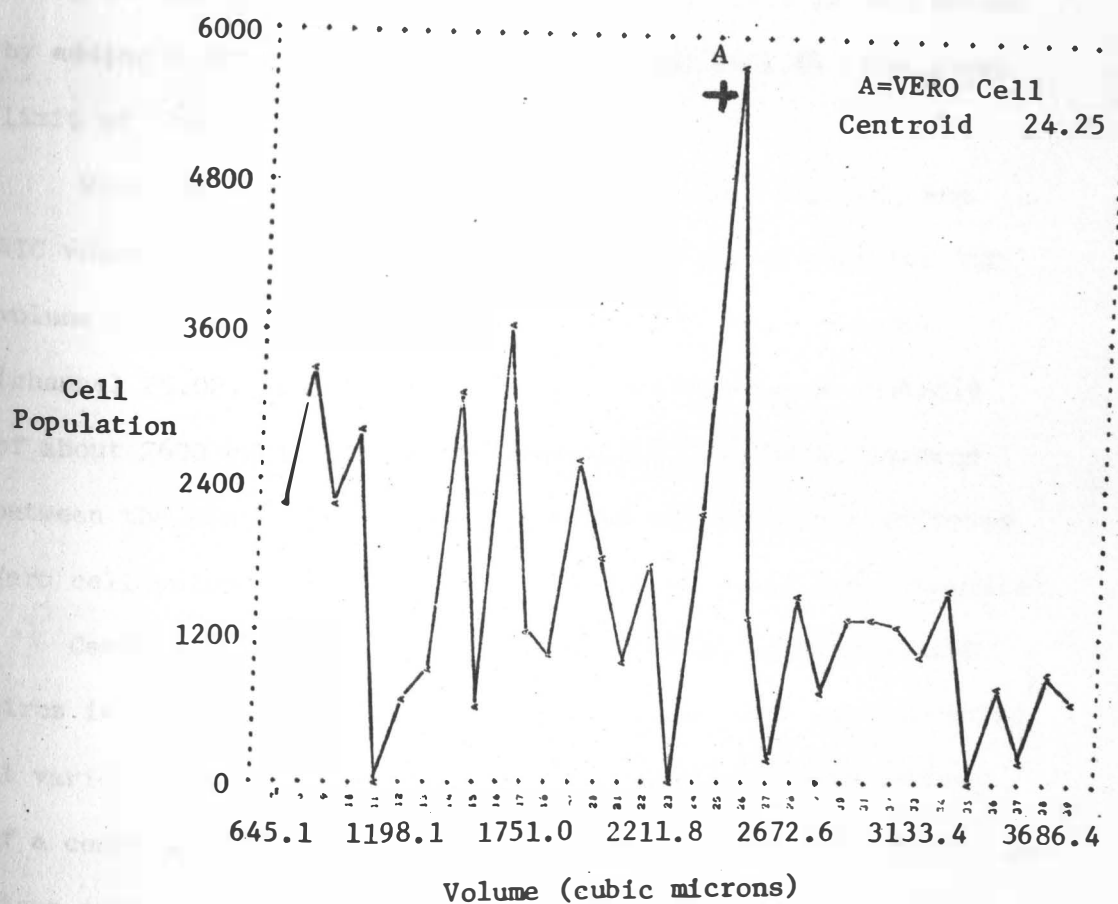


Figure 25. Centroid Analysis of a Vero Cell Volume Profile.

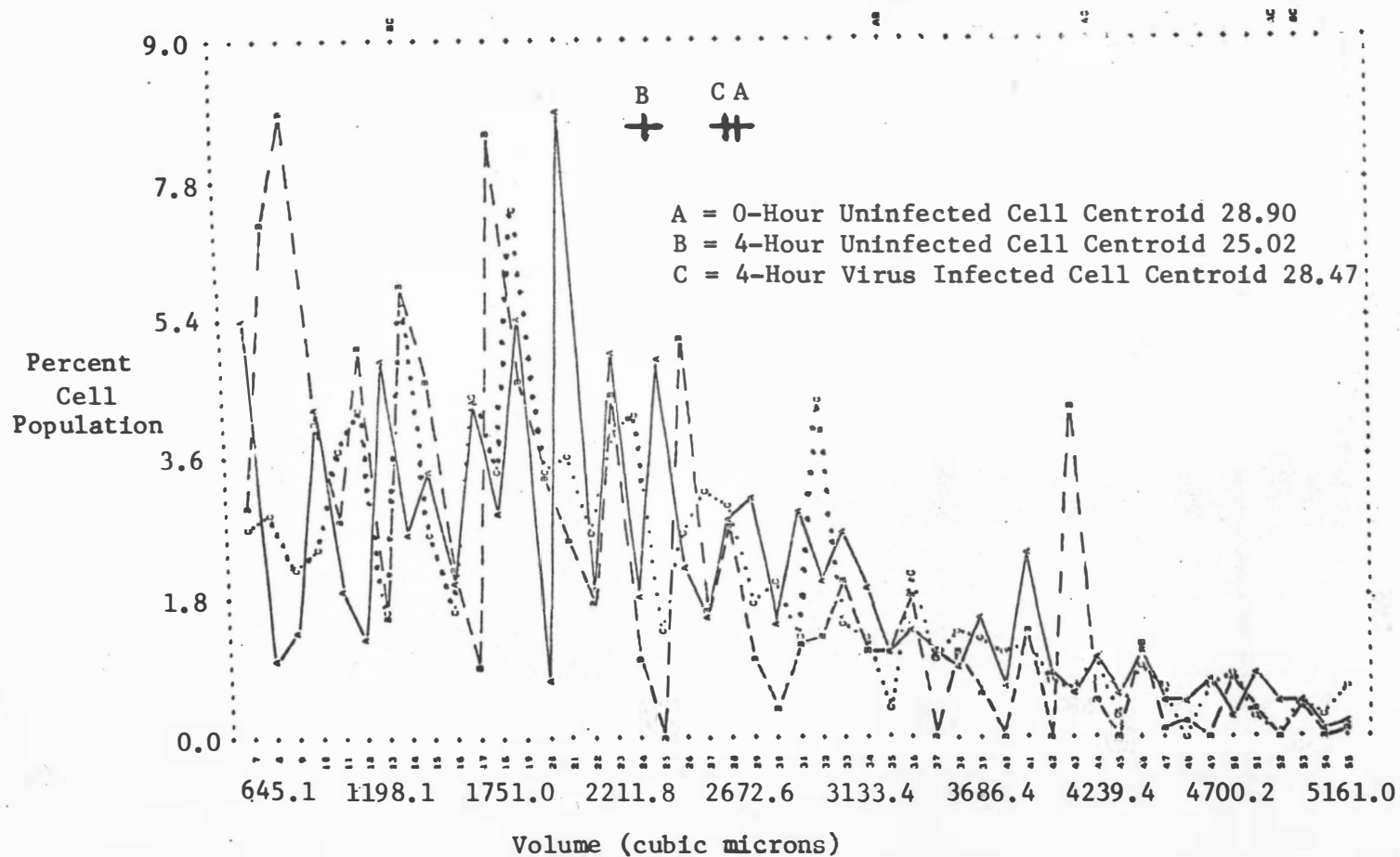


for this curve was determined to be 24.25 using the Coulter Counter program of the Hewlett Packard programmable calculator. This means the center of mass of the curve is located at channel 24.25. Channels are volume ranges which are dependent on the Coulter Counter sensitivity settings, therefore, channels can be easily converted into volume. In the example of the Vero cell volume profile which is given, channel 24 is the volume range extending from 2212 to 2304 cubic microns, and channel 24.25 is the volume 2243.88 cubic microns. This is determined by adding 0.25×92.16 (the resolution) to 2211.84 (the lower limit of channel 24).

When centroid analysis is applied to the OUC, 4UC, and 4IC volume profiles, it can be seen in Figure 26 that the 4UC volume profile has a centroid of about 2300 cubic microns (channel 25.02), while the 4IC volume profile has a centroid of about 2600 cubic microns (channel 28.47). The difference between the centroids of the uninfected and the virus infected Vero cell volume profiles is 317.4 cubic microns (3.45 channels).

Centroid analysis can then be applied to uninfected and virus infected cell volume profiles of which data was collected at various times post-infection. Table 13 is a presentation of a centroid analysis of 0-, 4-, 12-, and 24-hour uninfected and virus infected Vero cell volume profiles which are calculated from channels 7 to 30.

Figure 26. Centroid Analysis of 0-Hour Uninfected, 4-Hour Uninfected, and 4-Hour VEE Virus Infected Vero Cell Volume Profiles.



When the centroids are plotted versus time, significant centroid differences can be observed. Figure 27 is such a plot of centroid versus time from 0-hour through 24-hour post-infection times. In this discussion centroids of the uninfected Vero cell volume profiles are represented by the letters U cent. (uninfected centroid), and the centroids of the VEE virus infected Vero cell volume profiles are represented by the letters I cent. (infected centroid). The U cent. initially decreases while the I cent. remains at a higher centroid value. At about 9 hours post-infection the U cent. and I cent. are equal. From 9 to 20 hours the I cent. is smaller than the U cent., however, this I cent. rapidly surpasses the U cent. after 20 hours.

A possible explanation of Figure 27 is that virus attaches to the cell membrane, penetrates through the cell membrane into the cell, uncoats, and is read by the cellular ribosomes. This causes a 6 hour delay in the normal growth cycle. After 6 hours many cells begin to degenerate, and the centroid value becomes smaller. Soon after 12 hours of infection, masses of virus are being produced, and they contribute to the large cell volumes and a higher centroid. The initial increase in the I cent. may be a nonobservable "cloudy swelling" caused by virus entry. The second centroid increase after 12 hours post-infection may be the initiation of the phase of observable "cloudy swelling" associated with CPE.

Figure 27. Centroids of Uninfected and Virus Infected Vero Cell Volume Profiles Versus Time (Centroids for 0-, 4-, 12-, and 24-Hour Uninfected and VEE Virus Infected Vero Cell Volume Profiles).

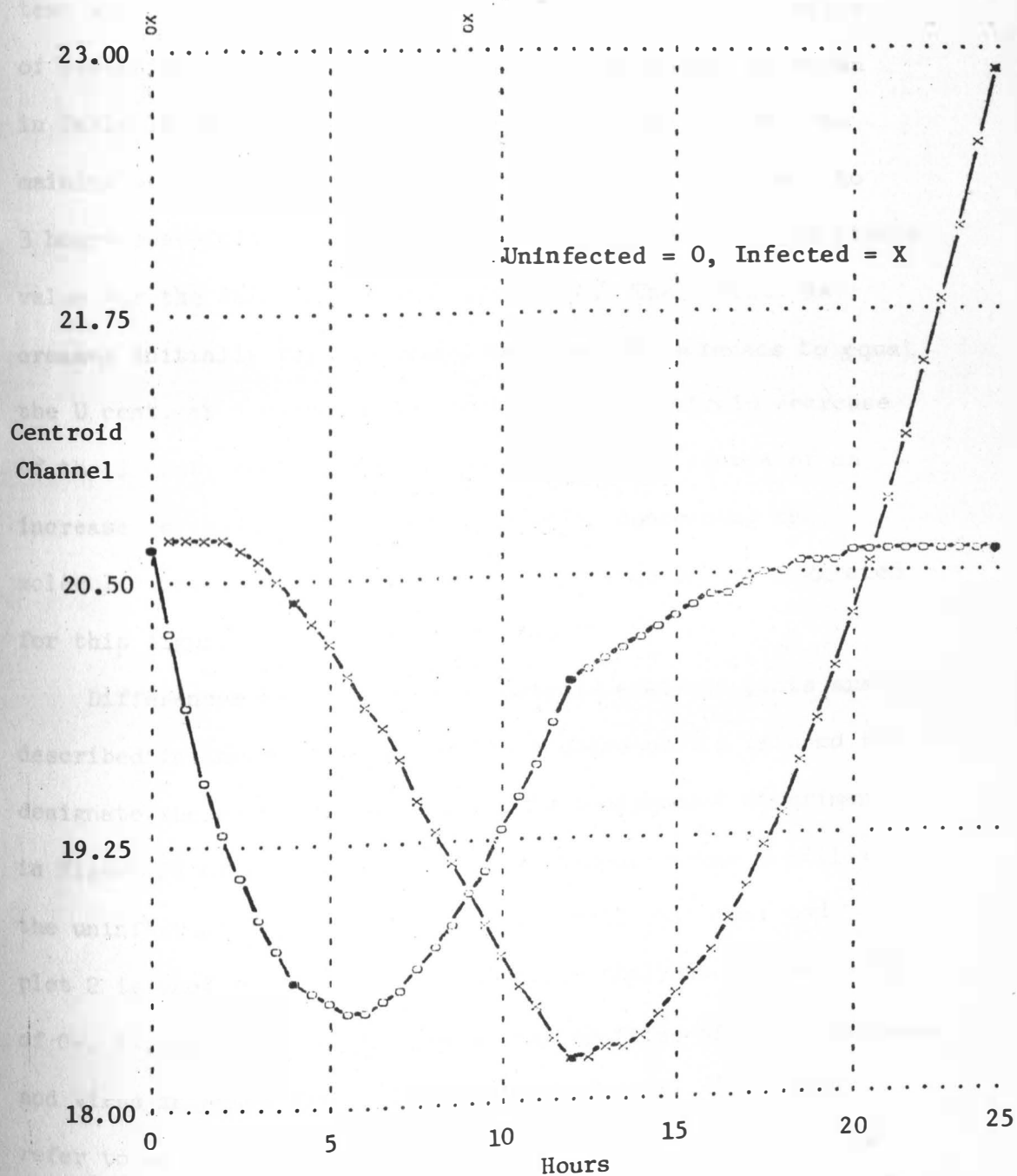


Table 14. *Centroid analysis of VEE virus infected Vero cell volumes at 0, 8, 12, and 16 hours post-infection.*

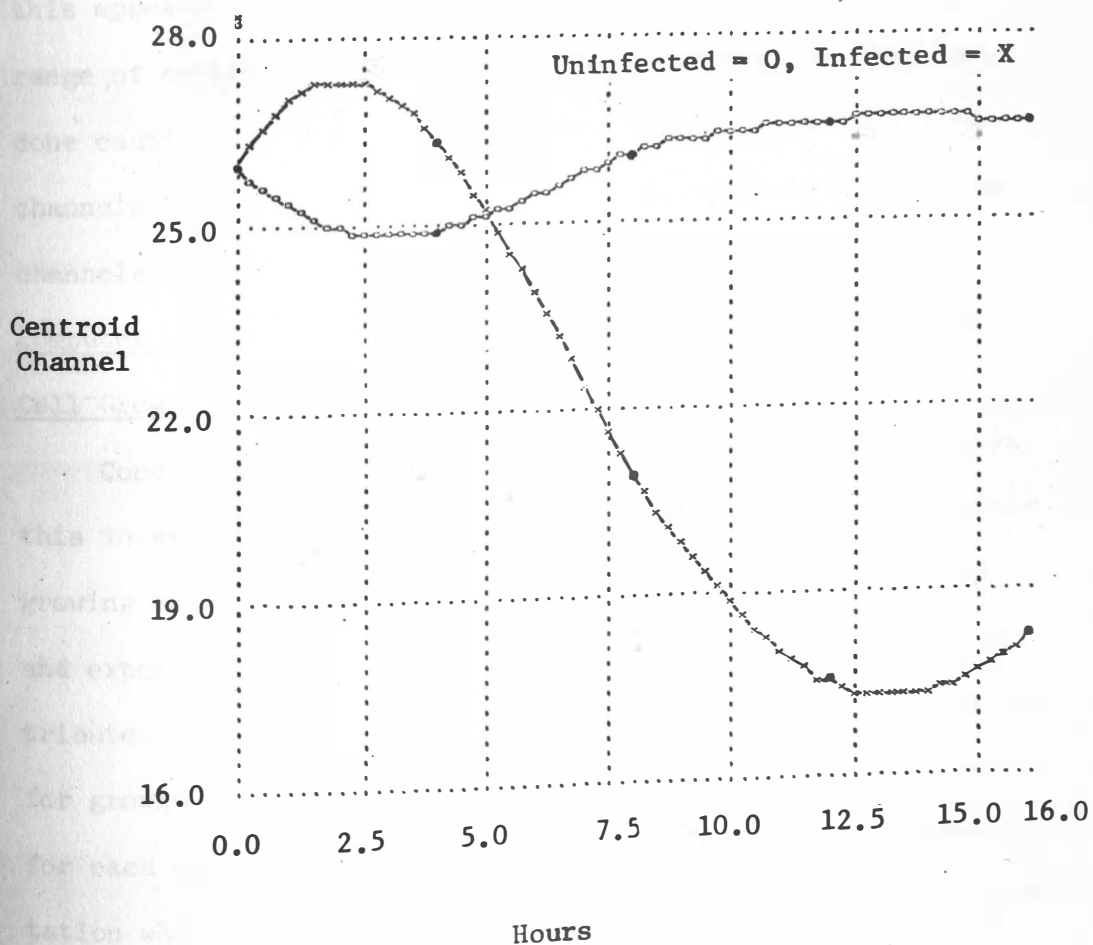
A confirming experiment was also performed which was designed to measure uninfected and VEE virus infected Vero cell volumes at 0, 8, 12, and 16 hours post-infection. This test was done within a 24-hour period of time. Application of centroid analysis to the confirming experiment, as shown in Table 14 and Figure 28, again result in the I cent. remaining at higher values as the U cent. decreases from 0 to 3 hours post-infection. The U cent. then increases to a stable value for the duration of the experiment. The I cent. increases initially for 2.5 hours, and then it decreases to equal the U cent. at 5 hours post-infection. The centroid decrease of the I cent. continues until 14 hours when evidence of an increase is shown. A similar explanation concerning the molecular developments in the virus infection can be suggested for this figure as was made for Figure 27.

Differences between the two centroid analysis plots are described in the following discussion where plot 1 is used to designate the centroid analysis of the independent experiments in Figure 27 of the 0-, 4-, 12-, and 24-hour volume profiles of the uninfected and virus infected Vero cell cultures; and plot 2 is used to designate the centroid analysis in Figure 28 of 0-, 4-, 8-, 12-, and 16-hour volume profiles of the uninfected and virus infected Vero cell cultures. U cent. will again refer to an uninfected centroid, and I cent. will refer to an

Table 14. Channels 7 to 40 Centroid Analysis of 0-, 4-, 8-, 12-, and 16-Hour Uninfected and Virus Infected Vero Cell Volume Profiles.

	Uninfected Centroid Channel	Infected Centroid Channel
0-Hour	25.94	25.94
4-Hour	24.94	26.33
8-Hour	26.13	20.95
12-Hour	26.60	17.50
16-Hour	26.55	18.25

Figure 28. Centroids of Uninfected and Virus Infected Vero Cell Volume Profiles Versus Time (Centroids for 0-, 4-, 8-, 12-, and 16-Hour Uninfected and VEE Virus Infected Vero Cell Volume Profiles).



infected centroid.

The I cent. in plot 1 does not increase in the first 2.5 hours as does the I cent. in plot 2. In plot 1 the U cent. and the I cent. are equal at 8.5 and at 20 hours post-infection, while the U cent. and the I cent. in plot 2 are equal at 5 hours post-infection. It may also be acknowledged that the I cent. of plot 1 covers a range of only 2 channels, while the I cent. of plot 2 covers a range of 10 channels. Though this appears to be a large difference, a comparison of the range of centroid channels between these two plots must be done cautiously; since plot 1 centroids are calculated from channels 7 to 30, while plot 2 centroids are calculated from channels 7 to 40.

Computer Simulation of Uninfected and VEE Virus Infected Vero Cell Growth and Division

Concurrent to the implementation of centroid analysis in this investigation, a computer model was developed to simulate growing and dividing cell populations (31). The difficulty and expense associated with the cell cultures themselves contributed impetus to the cell model development. Time expended for growing and harvesting procedures may require several days for each experiment. For the computer cell model, experimentation which is impractical to perform because of cost or time can be quickly and easily simulated and thus explored. Also,

the often inapparent correlation between such experimental data as shown previously in Figure 23 leads to difficulty in determining the cell cycle dynamics. The development of a working model requires the gathering and organization of a considerable amount of cell cycle information. During this process facts are revealed that may have otherwise escaped attention, and a greater factual understanding of cell volume changes that occur during the cell cycle can be realized. Computer modeling is rapid, reproducible, and makes more aspects of the cell cycle dynamics problem accessible during a given time.

Several simulations were performed as tests of the computer cell model operations. In all tests 2000 cells were initially entered at the half-volume channel 18 (about 1600 cubic microns) with one channel variation and an assigned growth rate of one channel per hour (92.16 cubic microns). The growth rate and the half-volume channel were experimentally determined from Vero cell cultures. These Vero cells were allowed to grow and divide for 10 hours after being transferred, and then Coulter Counter volume measurements were taken at 0, 6, and 10 hours. The rate of cell growth can be determined from the centroid change versus time as shown in Table 15.

In Figure 29 cell population versus volume in channels is plotted for 4, 8, 12, 16, and 20 hours as the first test

Table 15. Rate of Growth Determination of Uninfected and Virus Infected Vero Cells.

$$\text{Slope} = \frac{Y_2 - Y_1}{X_2 - X_1} = \frac{\frac{\Delta C_2}{\Delta t_2} - \frac{\Delta C_1}{\Delta t_1}}{\bar{V}_2 - \bar{V}_1}$$

ΔC =Change in Centroid
 Δt =Change in Time
 $\Delta \bar{V}$ =Change in Mean Volume

Uninfected Cells:

Time (Hours)	Centroid (Channels)	ΔC	Δt	$\frac{\Delta C}{\Delta t}$	\bar{V}
0	22.28				
		-3.02	6	-0.50	20.77
6	19.36				
		7.12	4	1.78	22.82
10	26.38				

Substituting in Rate Formula for Slope:

$$\text{Slope} = \frac{1.78 - (-0.50)}{22.82 - 20.77} = 1.11 \quad 1 \text{ used in Cell Simulations}$$

Infected Cells:

Time (Hours)	Centroid (Channels)	ΔC	Δt	$\frac{\Delta C}{\Delta t}$	\bar{V}
0	25.94				
		0.30	4	0.10	26.14
4	26.33				
		-5.38	4	-1.35	23.64
8	20.95				

Substituting in Rate Formula for Slope:

$$\text{Slope} = \frac{-1.35 - 0.1}{23.64 - 26.14} = 0.58 \quad 0.6 \text{ used in Cell Simulations}$$

Figure 29. Computer Cell Model Test with 2000 Cells in Channel 18.

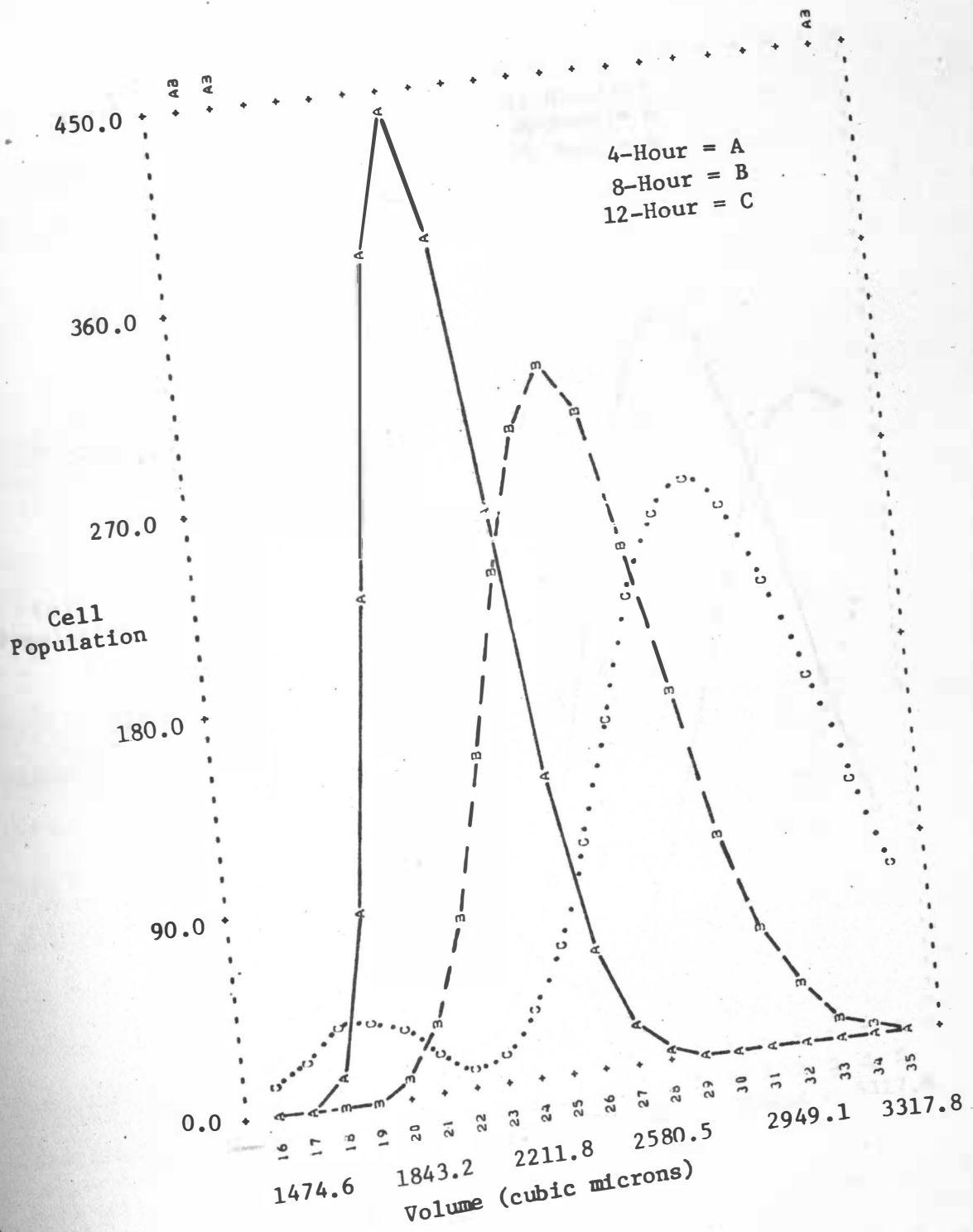
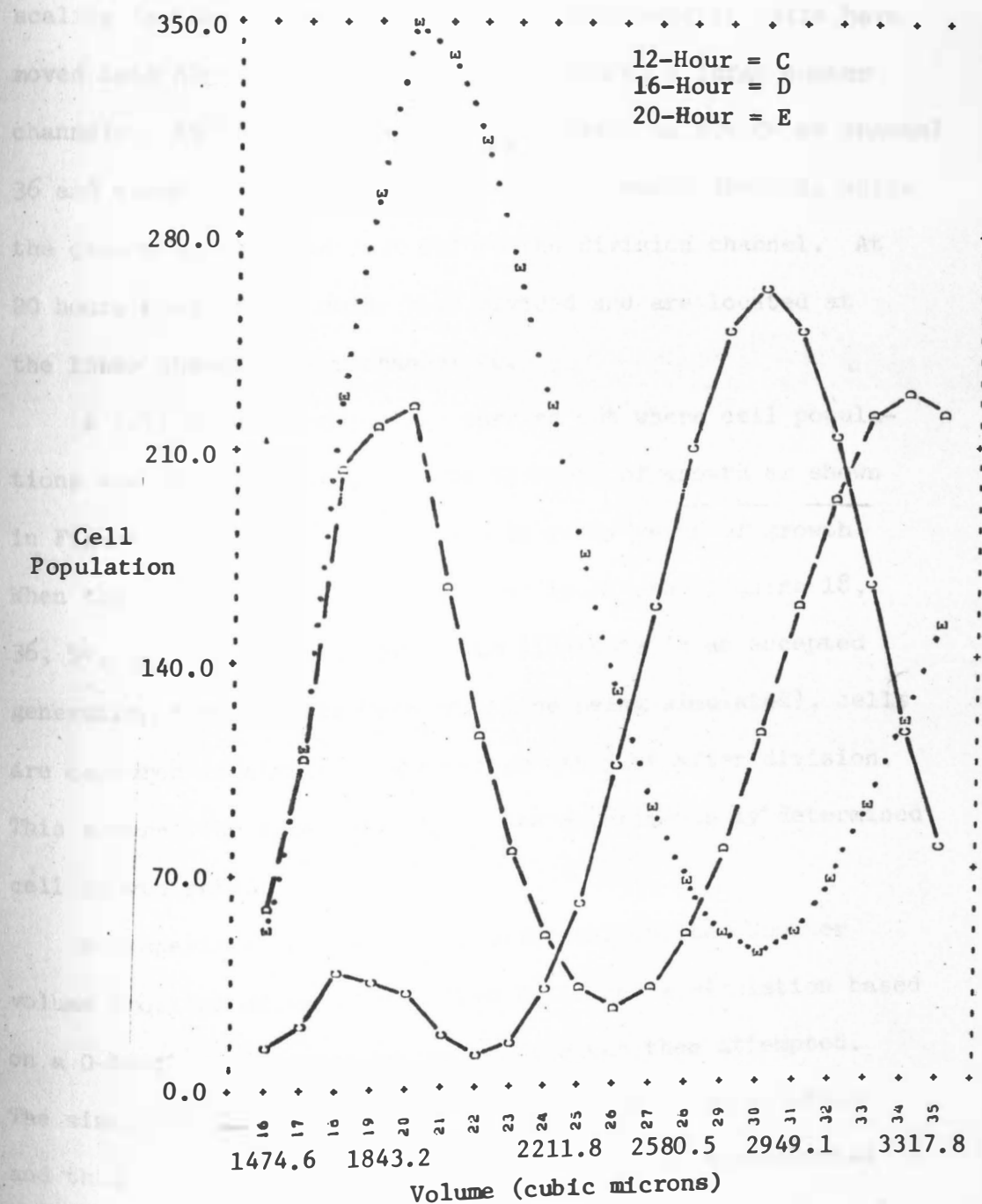


Figure 29. (Con't.)



of the cell model simulation. Figure 29 is presented in two separate plots for ease in viewing. The initial 2000 cells in channel 18 are not shown, due to the need to use a narrow scaling factor. In each successive volume profile cells have moved into higher channels and have occupied a large number channels. At 16 hours the cells have begun to divide at channel 36 and about one-half of the cells have already divided, while the others are located just before the division channel. At 20 hours most of the cells have divided and are located at the lower channels near channel 20.

A cell simulation is also carried out where cell populations are at 10, 20, 30, 40, and 50 hours of growth as shown in Figure 30. Cells are captured in every phase of growth. When the same simulation is repeated in Figure 31 using 18, 36, 54, 72, and 90 hours of growth (18 hours is an accepted generation time for the Vero cell line being simulated), cells are captured in similar stages of growth just after division. This assures the acceptability of the experimentally determined cell growth rate.

A comparison between the experimental Coulter Counter volume profiles of uninfected Vero cells and a simulation based on a 0-hour experimental volume profile was then attempted. The simulated volume profiles, however, tend to be smoothed and this results in difficulty in comparing the experimental

Figure 30. Computer Cell Model Test with 2000 Cells in Channel 18- at 10-Hour Intervals.

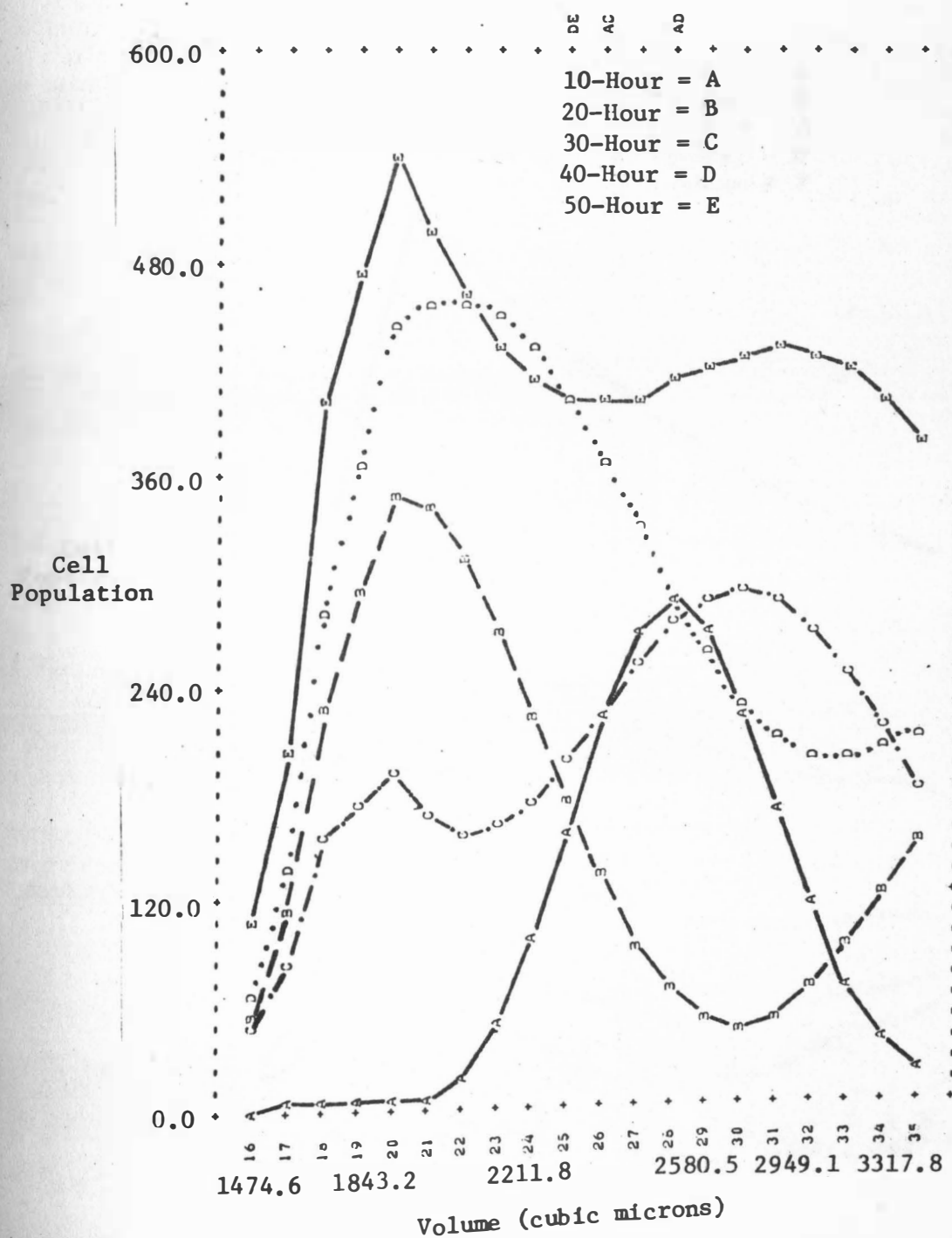
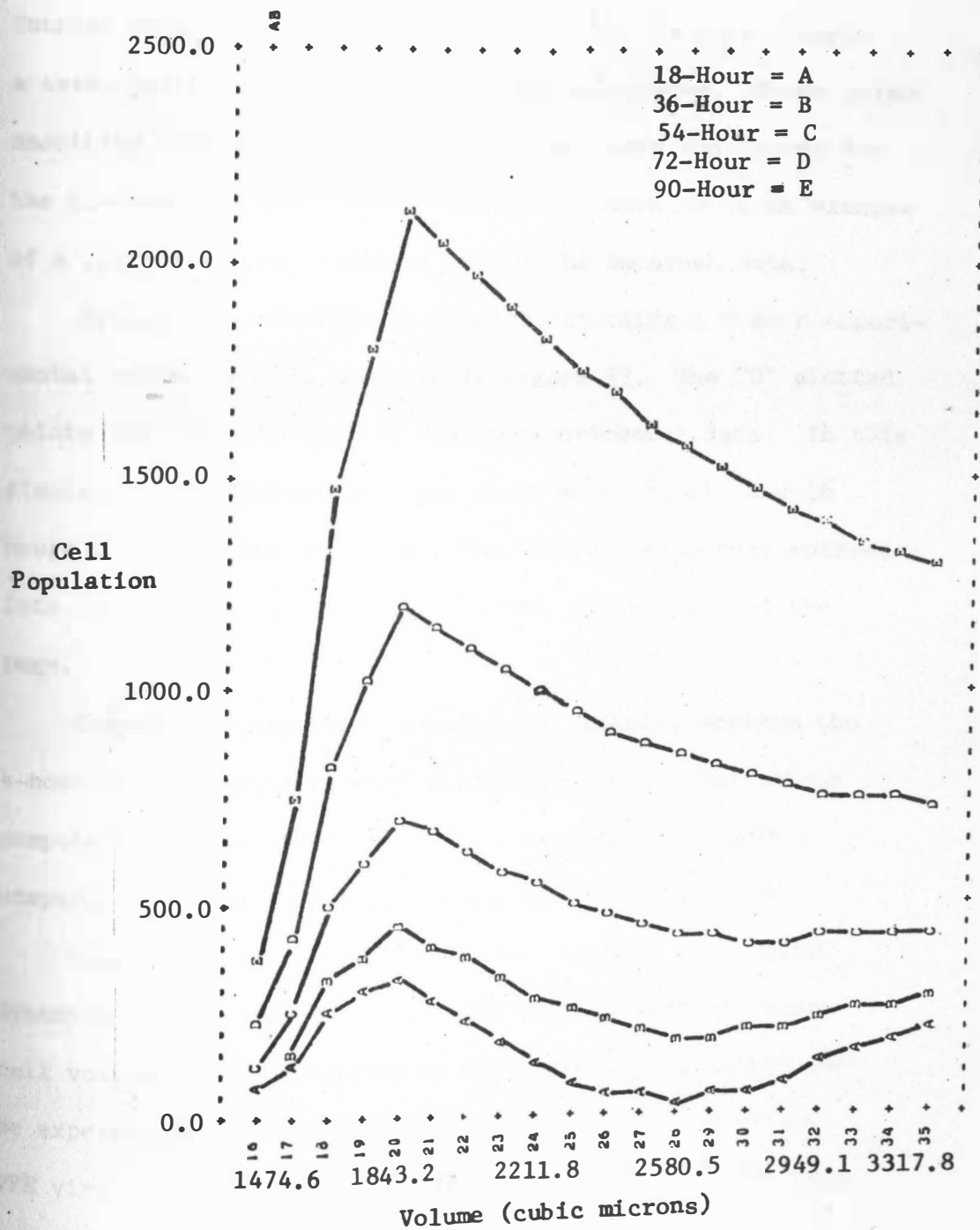


Figure 31. Computer Cell Model Test with 2000 Cells in Channel 18- at 18-Hour Intervals.



and the simulated volume profiles. This comparison was made manageable by the development of a smoothing computer program (Appendix Table IV) which smoothes the experimental Coulter Counter data as demonstrated in Figure 32. In this example a seven point smoothed curve has been calculated. Seven point smoothing denotes that seven points have been considered for the placement of every smoothed point. Table 16 is an example of a list of the experimental and of the smoothed data.

Simulations can then be carried out using a 0-hour experimental volume profile as shown in Figure 33. The "0" plotted points indicate the initial 0-hour experimental data. In this simulation cell populations are shown at 4, 8, 12, and 16 hours of growth and division. The initial parameters entered into the computer cell model are given at the left of the page.

Comparisons may then be made, for example, between the 4-hour smoothed experimental volume profile and the 4-hour computer simulated volume profile. An example of such a comparison of these profiles is presented in Figure 34.

Computer simulation of the virus infected cell cycle dynamics is also accomplished. The rate of infected Vero cell volume change occurring in the infected cell cycle can be experimentally determined from centroid changes in the VEE virus infected Vero cells. The calculation of the rate

Figure 32. Example of 7 Point Smoothing of an Uninfected Vero Cell Volume Profile.

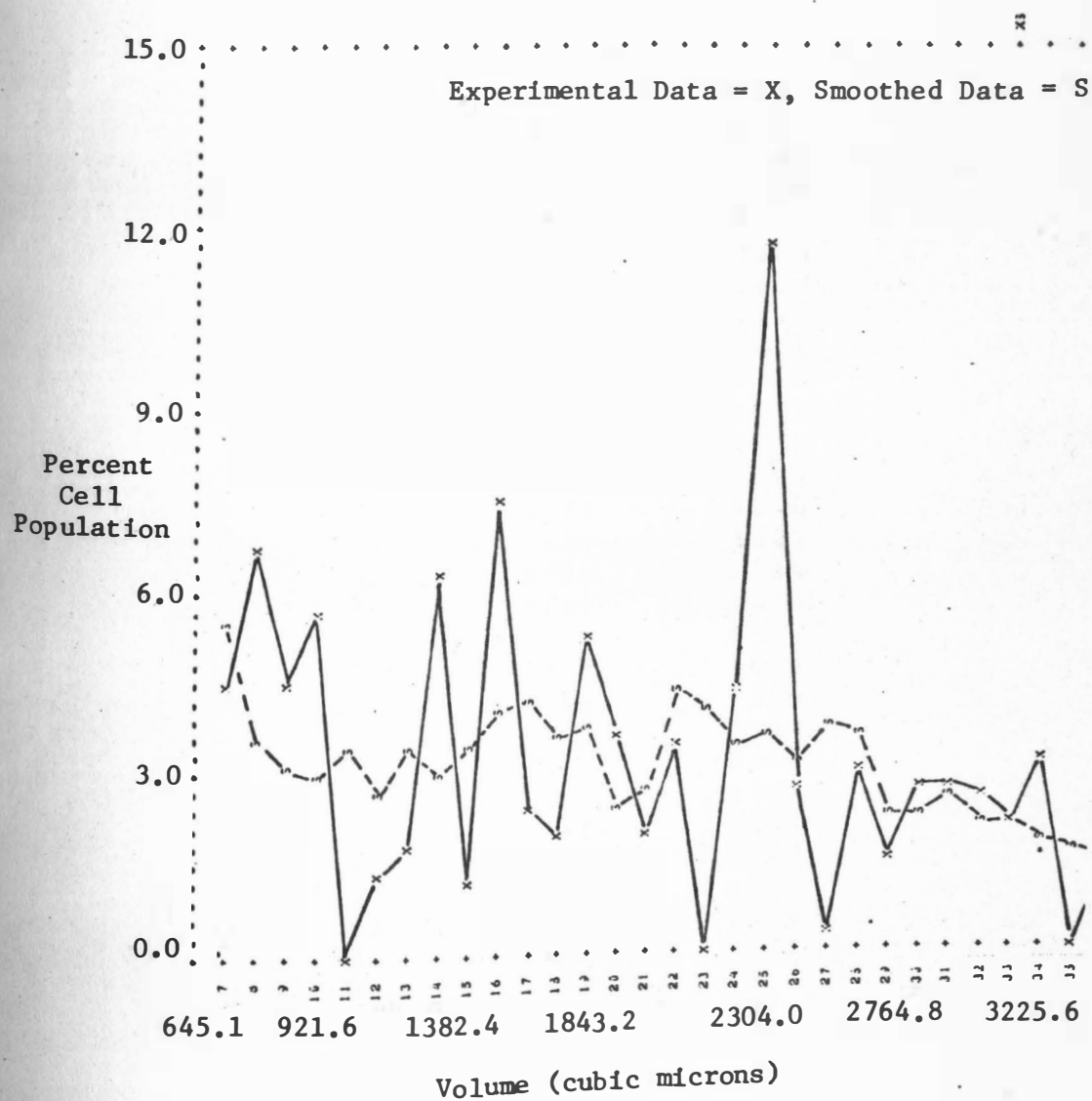


Table 16. Example of Smoothed Data List of an Uninfected Vero Cell Volume Profile.

EXP# 9.1

ATTENUATION= 4
APERTURE= 256

CHANNEL	OLD DATA	SMOOTHED
7	2196	2647
8	3323	1724
9	2204	1497
10	2319	1336
11	-1126	1626
12	645	1234
13	395	1612
14	3112	1413
15	615	1611
16	3670	1384
17	1202	1975
18	991	1675
19	2605	1305
20	1790	1146
21	930	1300
22	1736	2064
23	-911	1379
24	2134	1617
25	5779	1630
26	1313	1519
27	133	1734
28	1492	1666
29	712	1091
30	1329	1043
31	1307	1233
32	1230	1001
33	1000	1000
34	1575	531
35	-79	736
36	765	703
37	177	664
38	923	497
39	650	631

INITIAL-CELL FILE NO. = 28 EXP# 14.1
 OPTION: INITIAL NEGATIVE COUNTS ZEROED
 FIRST CELL VOLUME = 1700 VARIATION = 200
 RATE OF VOLUME INCREASE = 1
 TIME: INTERVAL = 0.25 INITIAL = 0 FINAL = 16

*** CELL COUNT VS. C.C. CHANNEL ***

<2086>TIME(0) = 0, <2337>TIME(4) = A, <2630>TIME(8) = B, <2997>TIME(12) = C, <3440>TIME(16) = D

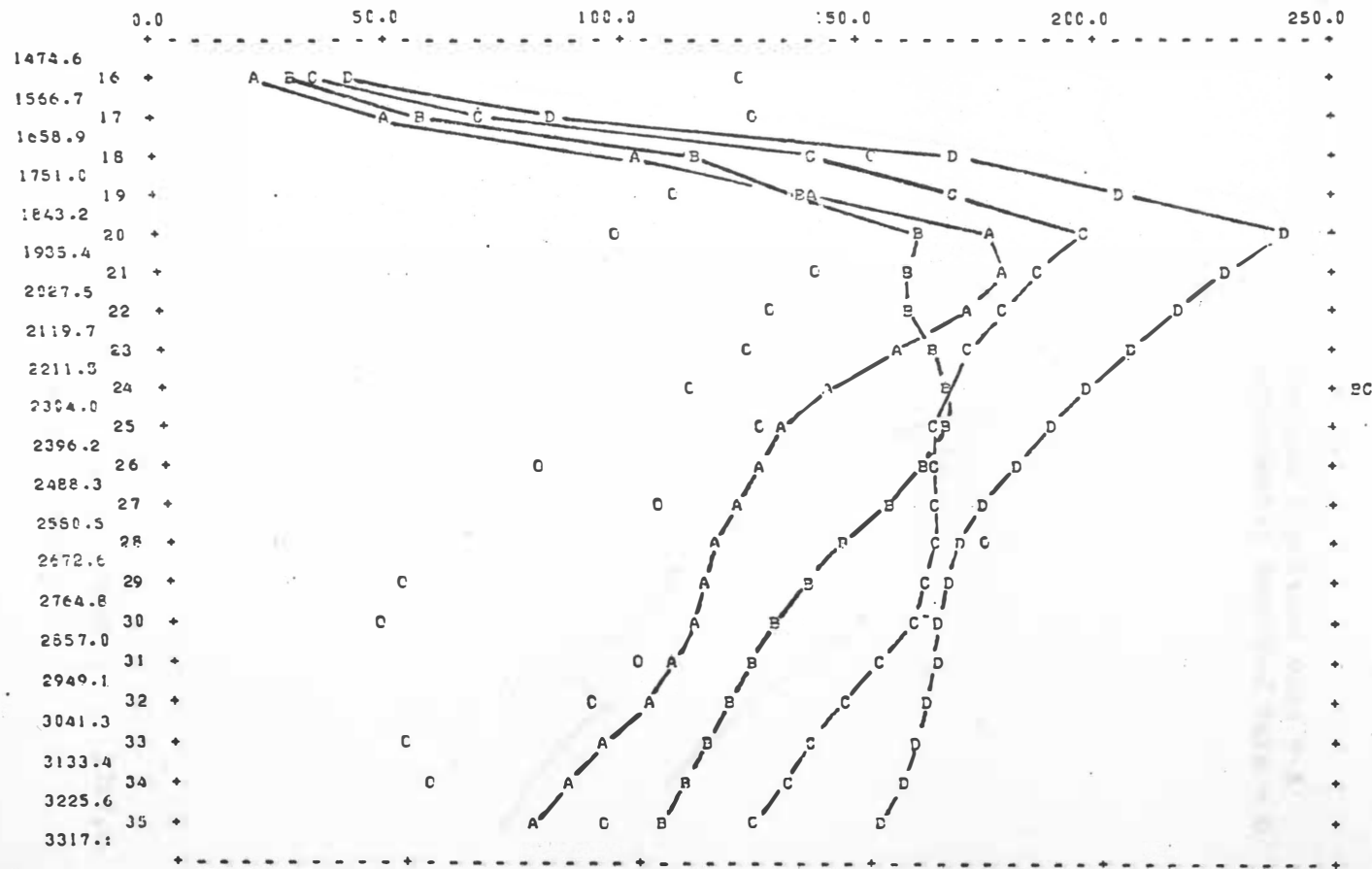
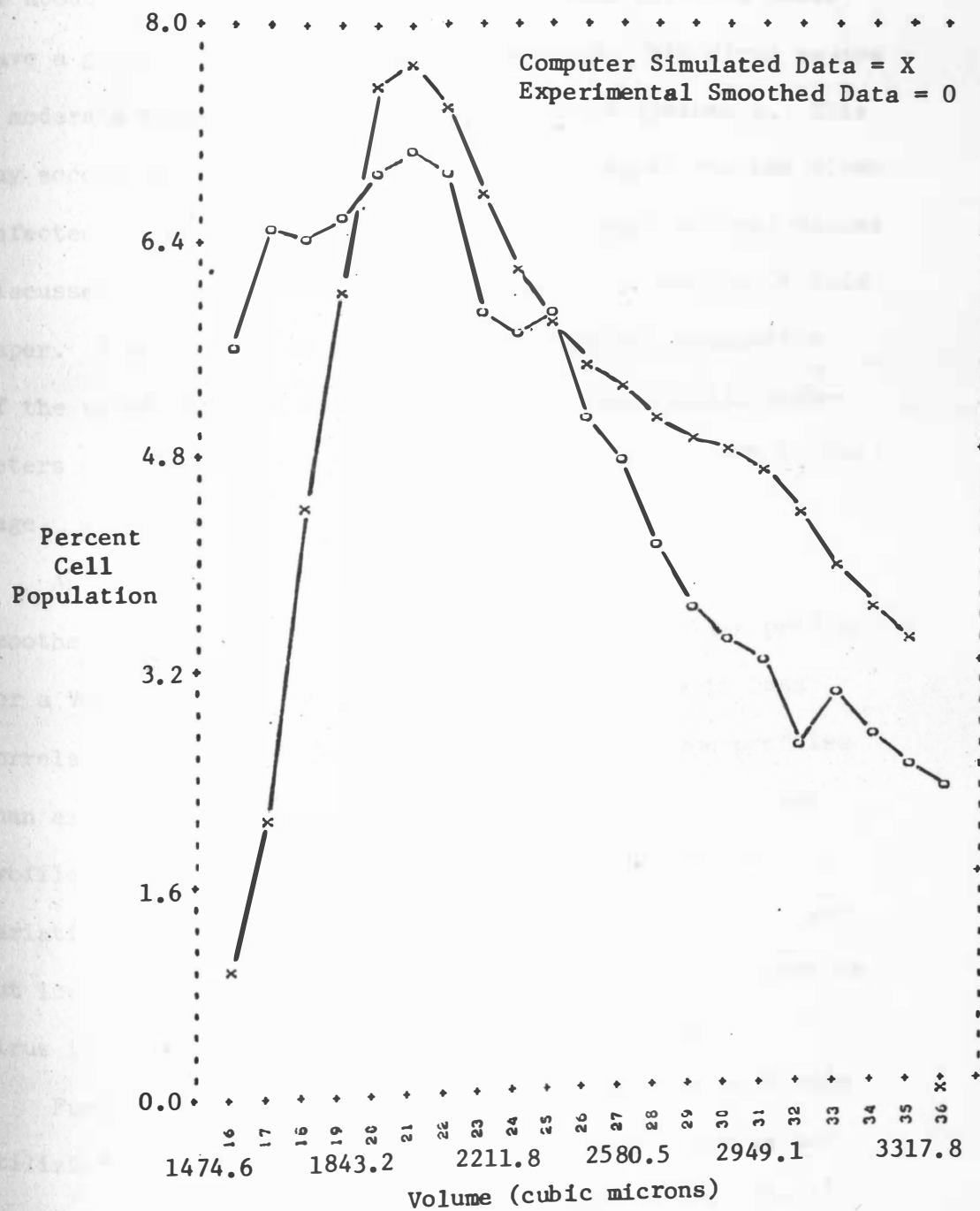


Figure 33. Example of Computer Cell Model Simulation of Uninfected Vero Cell Cycle Dynamics.

Figure 34. Experimental Smoothed and Computer Simulated 4-Hour Uninfected Vero Cell Volume Profiles.



of growth for infected Vero cells measured at 0, 4, and 8 hours post-infection is shown in Table 15. From these calculations it may be seen that the uninfected cells have a growth rate of about 1 channel per hour, while the virus infected cells have a growth rate of 0.6 channels per hour. VEE virus causes a moderate repression of host macromolecular synthesis. This may account for the lower growth rate calculated for the virus infected cells in this table and for the lower centroid values discussed previously in the centroid analysis section of this paper. Figure 35 is an example of the computer simulation of the virus infected cells. Once again, the initial parameters entered into the computer are given on the left of the page.

An example is given in Figure 36 of an experimental smoothed volume profile and computer simulated volume profile for a Vero cell at 4 hours post-infection. There is less correlation between these two virus infected volume profiles than existed between the experimental and simulated volume profile of uninfected Vero cells. Possible extreme rate variations which virus infected cells undergo, but which are not incorporated into the cell model, cause this less precise virus infected cell growth and division simulation.

Further computer cell model simulations which were made utilizing increased volume ranges and different rate values resulted in limited success and are not further described

INITIAL-CELL FILE NO. = 77 EXP# 14.1
 OPTION: INITIAL NEGATIVE COUNTS ZERCED
 FIRST CELL VOLUME = 1700 VARIATION = 200
 RATE OF VOLUME INCREASE = 0.6
 TIME: INTERVAL = 0.25 INITIAL = 0 FINAL = 12

/// CELL COUNT VS. C.C. CHANNEL ///

<2002>TIME(0) = C, <2138>TIME(4) = A, <2287>TIME(8) = B, <2462>TIME(12) = C

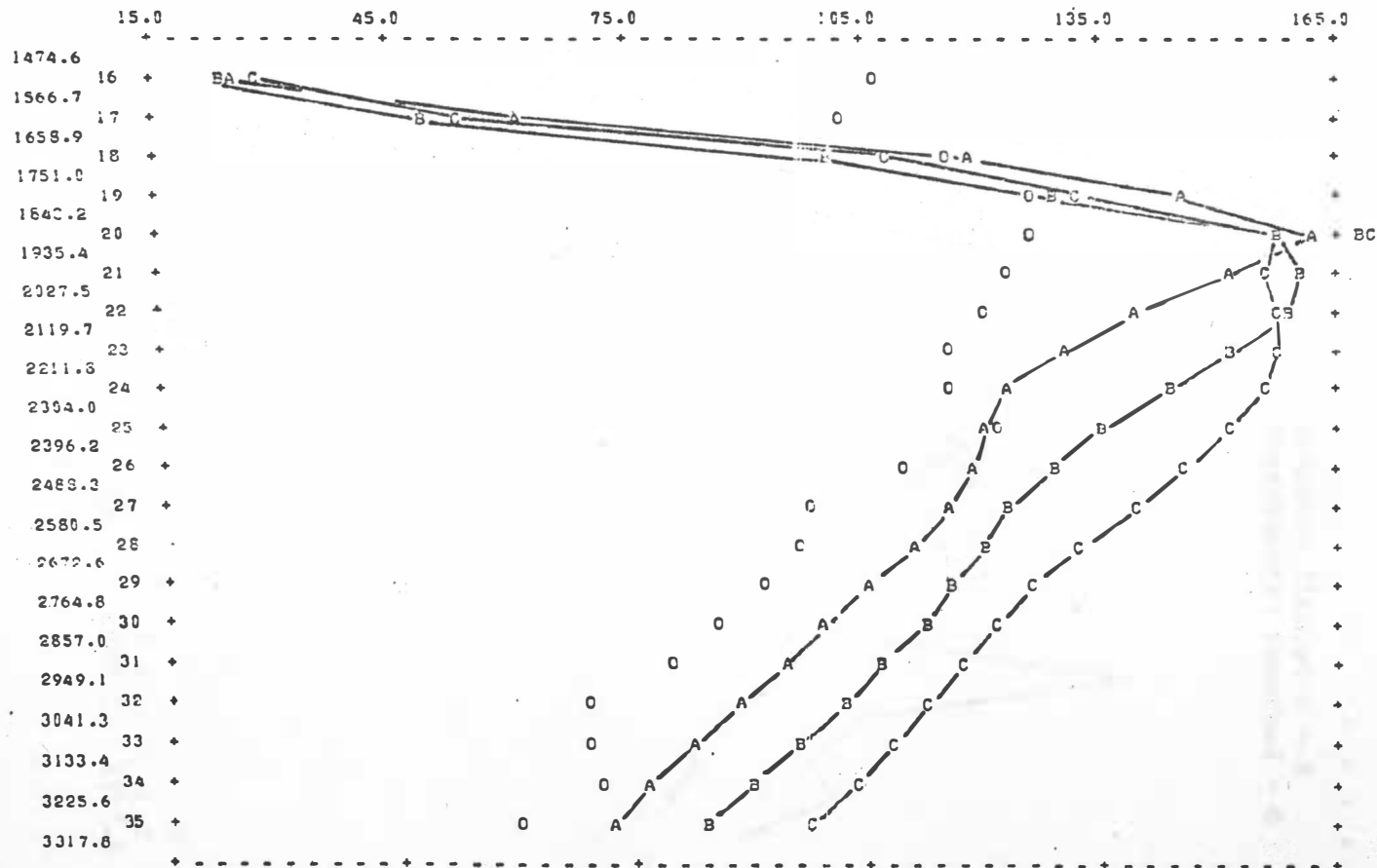


Figure 35. Example of Computer Cell Model Simulation of VEE Virus Infected Vero Cell Cycle Dynamics.

Figure 36. Experimental Smoothed and Computer Simulated 4-Hour VEE Virus Infected Vero Cell Volume Profiles.



in this paper.

Coulter Counter Measurement of Inactivated VEE Virus Treated
Vero Cell Cultures

For the successful clinical application of a rapid virus detection system using the Coulter Counter, more evidence of virus presence is needed than only cellular volume differences when the virus infected cell volumes are compared to uninfected cell volumes. The treatment of some of the virus infected cells with virus-specific antiserum as described in the materials and methods section will allow for the clinical application of the rapid virus detection system.

Coulter Counter volume measurements can be taken of 4-hour uninfected Vero cells, of 4-hour VEE virus infected Vero cells, and of 4-hour VEE virus plus antiserum treated Vero cells. The uninfected and the VEE virus plus antiserum treated Vero cells should display similar volume profiles, while the virus infected cells should display a significantly different volume profile. The use of the VEE virus-specific antiserum (or any other virus-specific antiserum for other viruses) confirms that the volume profile differences are caused by the specific virus.

Figure 37 is a plot of the volume profiles of 4-hour uninfected, 4-hour VEE plus antiserum treated, and 4-hour VEE virus infected Vero cells. Centroid analysis is once again

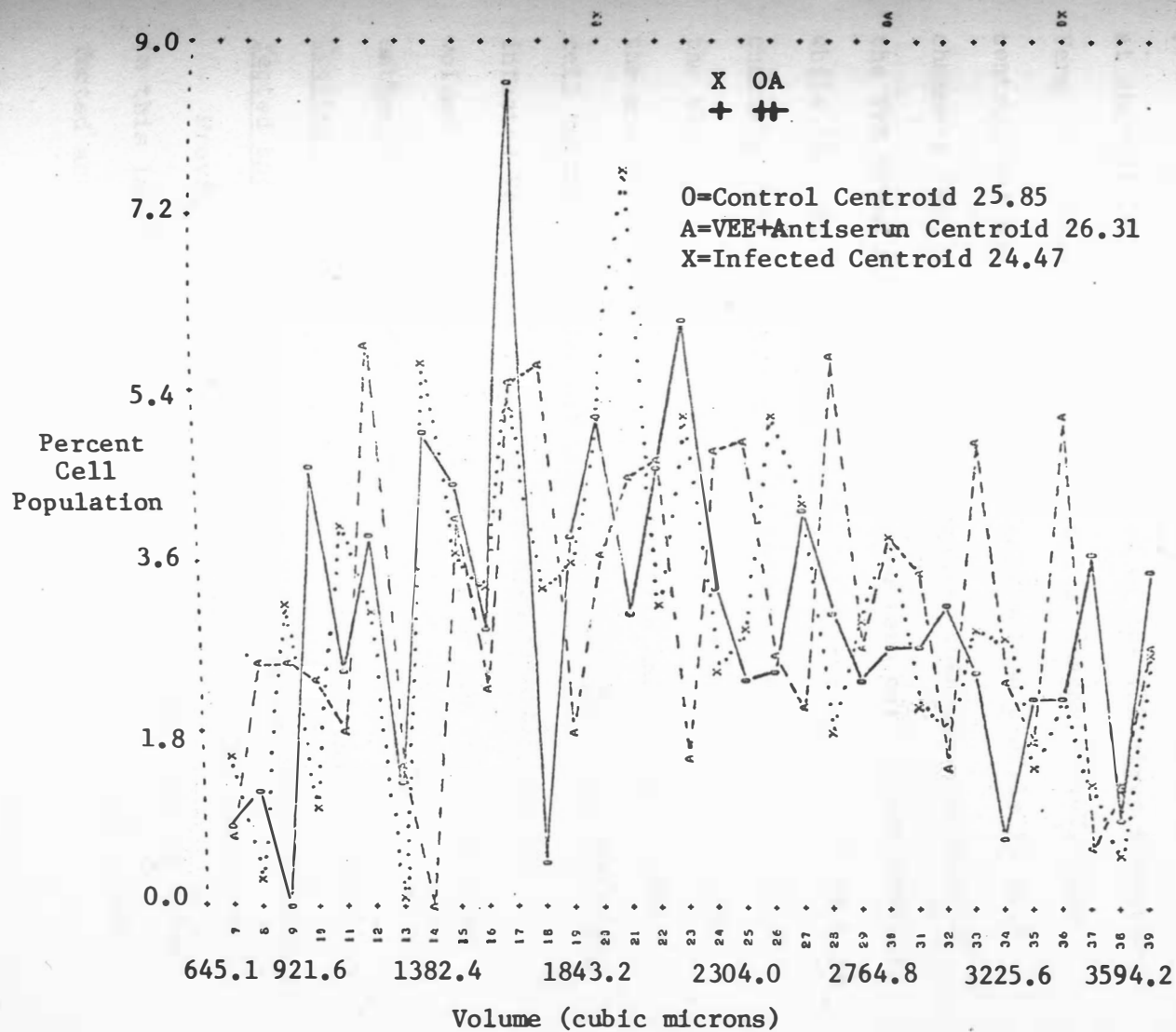


Figure 37. Uninfected, VEE Virus Plus Antiserum Treated, and VEE Virus Infected Vero Cell Volume Profiles.

used to determine the center of mass of each volume profile and to better display the differences between volume profiles. This centroid analysis calculated the centroids from channels 7 to 40. The centroid of the uninfected Vero cell volume profile is located at channel 25.85, the centroid of the VEE plus antiserum treated Vero cell volume profile is located at channel 26.34, and the centroid of the VEE virus infected Vero cell volume profile is located at channel 24.47. The centroid of the uninfected Vero cell volume profile is 0.46 channels (42.39 cubic microns) smaller than the centroid of the VEE virus plus antiserum treated Vero cell volume profile, while the centroid of the uninfected Vero cell profile is 1.38 channels (127.18 cubic microns) larger than the centroid of the VEE virus infected cell volume profile. In other words, the antiserum neutralizes the VEE virus and maintains these cell volumes near the uninfected cell volumes. The VEE virus infected Vero cells are, however, significantly smaller in volume than the uninfected Vero cells or the VEE virus plus antiserum treated Vero cells.

Coulter Counter Measurement of Con A Agglutination of Uninfected and VEE Virus Infected Aedes Albopictus Cell Cultures

Previous Coulter Counter investigations were performed in this laboratory in which measurements were taken of uninfected and VEE virus infected Aal cell cultures (74). Even

though Aal cell cultures demonstrate no CPE when infected with VEE virus, it was hypothesized that expected volume differences could be detected between the uninfected and the virus infected Aal cell cultures using the Coulter Counter. Volume differences indeed may exist between the uninfected and the virus infected Aal cell cultures, however, these differences are probably less dramatic than the early volume differences detected in Vero cell cultures infected with VEE virus.

If volume differences in mosquito cells do not satisfactorily demonstrate application to a rapid virus detection system because of nonreproducibility, then other physical changes in the infected mosquito cell must be sought out and advantageously used. One such property of virus infected cell cultures is their agglutinability when treated with the plant chemical concanavalin A (con A). It has been hypothesized that since VEE virus infected cells produce virus-specific cell membrane components, Aal cell cultures previously infected with VEE virus will be agglutinated to a degree which is detectable with the Coulter Counter when the cells are treated with con A.

Initial optical micrometer measurements were taken of Aal cells, even though volume distributions of Aal cells were previously taken in this laboratory (74). The previous tests in this laboratory utilized Aal cells which were over 20

passages removed from the Aal cells used in this investigation, and the cell size was expected to differ.

The optical micrometer measurement detected that the Aal cells range from 70.32 to 730.35 cubic microns (5.2 to 11.35 microns in diameter). Figure 38 is a presentation of the statistics and histogram of the optical micrometer measurements.

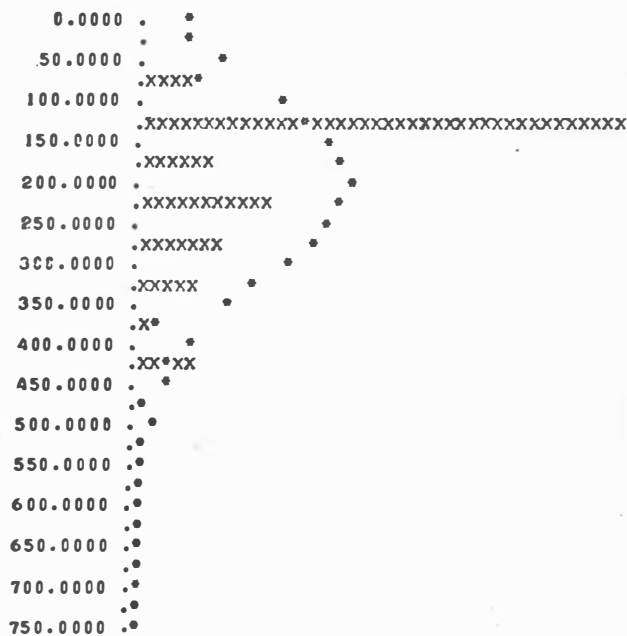
Once the relative size of the Aal cells was determined, acceptable Coulter Counter sensitivity settings could be chosen. An attenuation of 0.354 and an aperture of 512 will measure particles with a range of from 33 to 1625 cubic microns and allow a resolution or channel width of 16.32 cubic microns. These parameters are acceptable for the Coulter Counter measurement of Aal cells in accordance with the optical micrometer data. These sensitivity settings also give an interference error of under 0.12 percent according to Table 9. An example of a Coulter Counter volume profile of Aal cell cultures is given in Figure 39. Measurements are taken from threshold 6 to threshold 40.

Table 17 is a list of the percentage relative frequency and cumulative percentage relative frequency of Aal cells found at the specified volume ranges. From this table it may be observed that the optical micrometer measurement results in five populations of Aal cells located in channels 7, 8, 10, 13, and 15. The largest percentage of Aal cells is found at

Figure 38. Statistics, Histogram, and "Cell" Statistics of Aal Cells Measured with the Optical Micrometer.

N = 200
 MEAN = 205.8463
 STD. DEV = 111.8801
 SKEWNESS = 1.5039
 KURTOSIS = 5.4982
 XMIN = 70.3192
 XMAX = 730.3474
 RANGE = 660.0283

EACH X= 1.08 PERCENT



CELL#	LOWER LIMIT	NO. OF OBS	%RELATIVE FREQ
1	0.0000	0	0.00000
2	50.0000	18	9.00000
3	100.0000	86	43.00000
4	150.0000	15	7.50000
5	200.0000	24	12.00000
6	250.0000	16	8.00000
7	300.0000	12	6.00000
8	350.0000	12	6.00000
9	400.0000	12	6.00000
10	450.0000	1	0.50000
11	500.0000	0	0.00000
12	550.0000	3	1.50000
13	600.0000	0	0.00000
14	650.0000	0	0.00000
15	700.0000	1	0.50000

Figure 39. Uninfected Aal Cell Volume Profile.

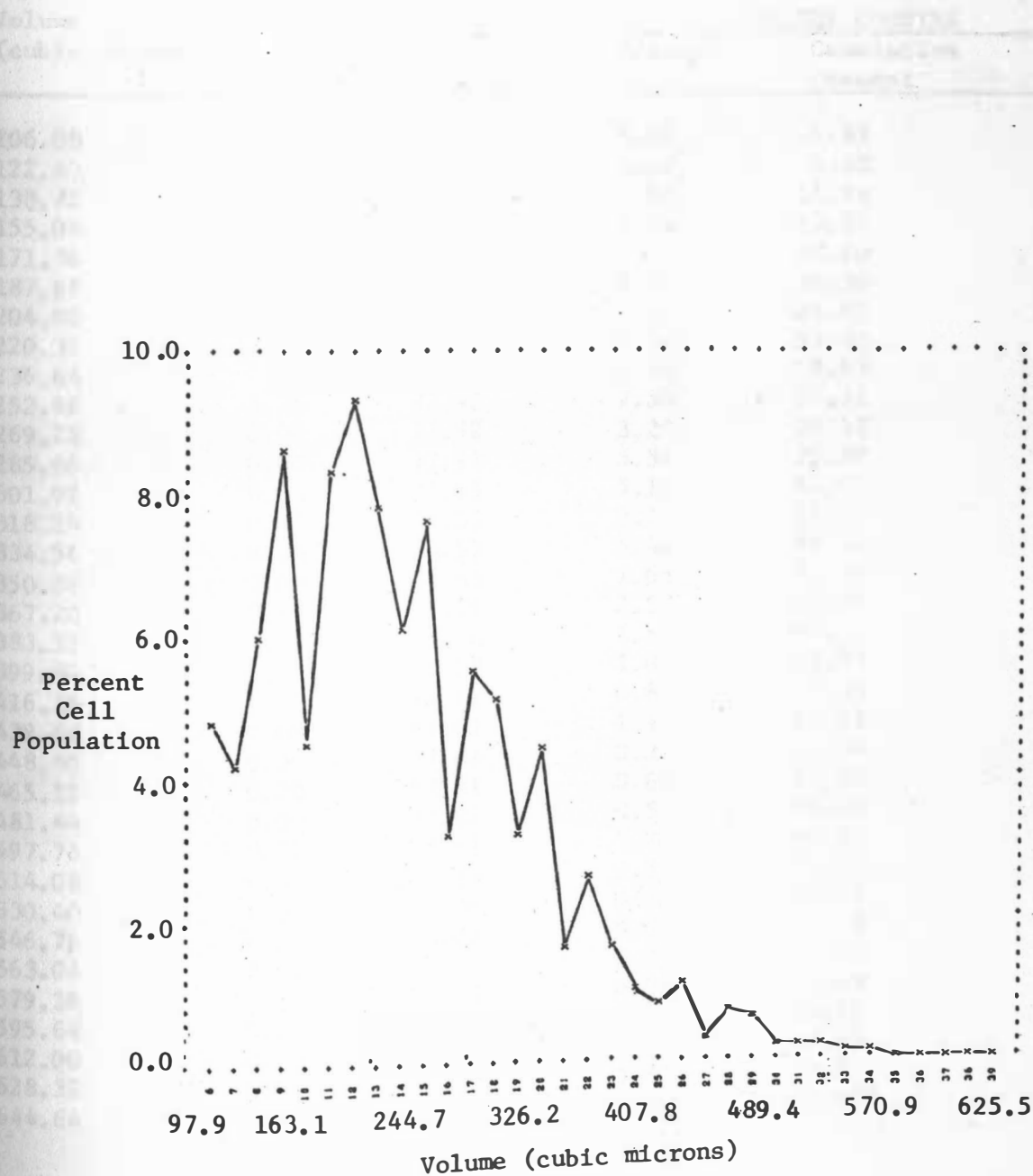


Table 17. Percent and Cumulative Percent of Aal Cells Measured with the Optical Micrometer and the Coulter Counter.

Volume (cubic microns)	OPTICAL MICROMETER		COULTER COUNTER	
	Percent	Cumulative Percent	Percent	Cumulative Percent
106.08	0.00	0.00	4.82	4.82
122.40	17.68	17.68	4.18	9.00
138.72	29.83	47.51	5.98	14.98
155.04	0.00	47.51	8.59	23.57
171.36	8.29	55.80	4.53	28.10
187.68	0.00	55.80	8.36	36.36
204.00	0.00	55.80	9.29	45.65
220.32	13.26	69.06	7.84	53.49
236.64	0.00	69.06	6.14	59.63
252.96	8.86	77.92	7.58	67.21
269.28	0.00	77.92	3.20	70.41
285.60	0.00	77.92	5.51	75.92
301.92	6.63	84.55	5.15	81.07
318.24	0.00	84.55	3.21	84.28
334.56	0.00	84.55	4.42	88.70
350.88	0.00	84.55	1.65	90.35
367.20	6.63	91.18	2.57	92.92
383.52	0.00	91.18	1.61	94.53
399.84	0.00	91.18	1.04	95.57
416.16	6.63	97.81	0.81	96.38
432.48	0.00	97.81	1.14	97.52
448.80	0.00	97.81	0.32	97.84
465.12	0.00	97.81	0.66	98.50
481.44	0.00	97.81	0.57	99.07
497.76	0.00	97.81	0.20	99.27
514.08	0.55	98.36	0.22	99.49
530.40	0.00	98.36	0.20	99.69
546.76	0.00	98.36	0.09	99.78
563.04	0.00	98.36	0.07	99.85
579.36	1.66	100.20	0.03	99.88
595.68	0.00	100.20	0.04	99.92
612.00	0.00	100.20	0.03	99.95
628.32	0.00	100.20	0.02	99.97
644.64	0.00	100.20*	0.02	99.99*

*Error Due To Rounding

a mean volume of 138.72 cubic microns (channel 8). The Coulter Counter measurement shows large Aal cell populations in channels 9, 11, and 12 and has measured more of a uniform distribution of the population. The largest population of Aal cells is located at a mean volume of 204.00 cubic microns (channel 12) in this Coulter Counter measurement.

Figure 40 is a comparison of a single optical micrometer measurement of 200 Aal cells with the Coulter Counter measurement of 47,000 Aal cells. This is a plot of the cumulative percentage relative frequency of Aal cells. Using the format of comparing the volume at which the cumulative percentage equals 50 percent, it can be observed that the optical micrometer cumulative percentage reaches 50 percent at a volume of 167.67 cubic microns. The Coulter Counter cumulative percentage reaches 50 percent at a volume of 212.16 cubic microns. The optical micrometer measurement found more of the smaller Aal cells.

Coulter Counter measurements were then taken of uninfected and VEE virus infected Aal cell cultures to which increasing concentrations of con A were added. Centroid analysis is done for each volume profile as presented in Table 18, and an interpolation plot is made of the centroid versus con A concentration as shown in Figure 41.

At 15 mg. of concanavalin A the 4-hour uninfected

Figure 40. Cumulative Percent Relative Frequency of Uninfected Aal Cells Measured with the Optical Micrometer and the Coulter Counter.

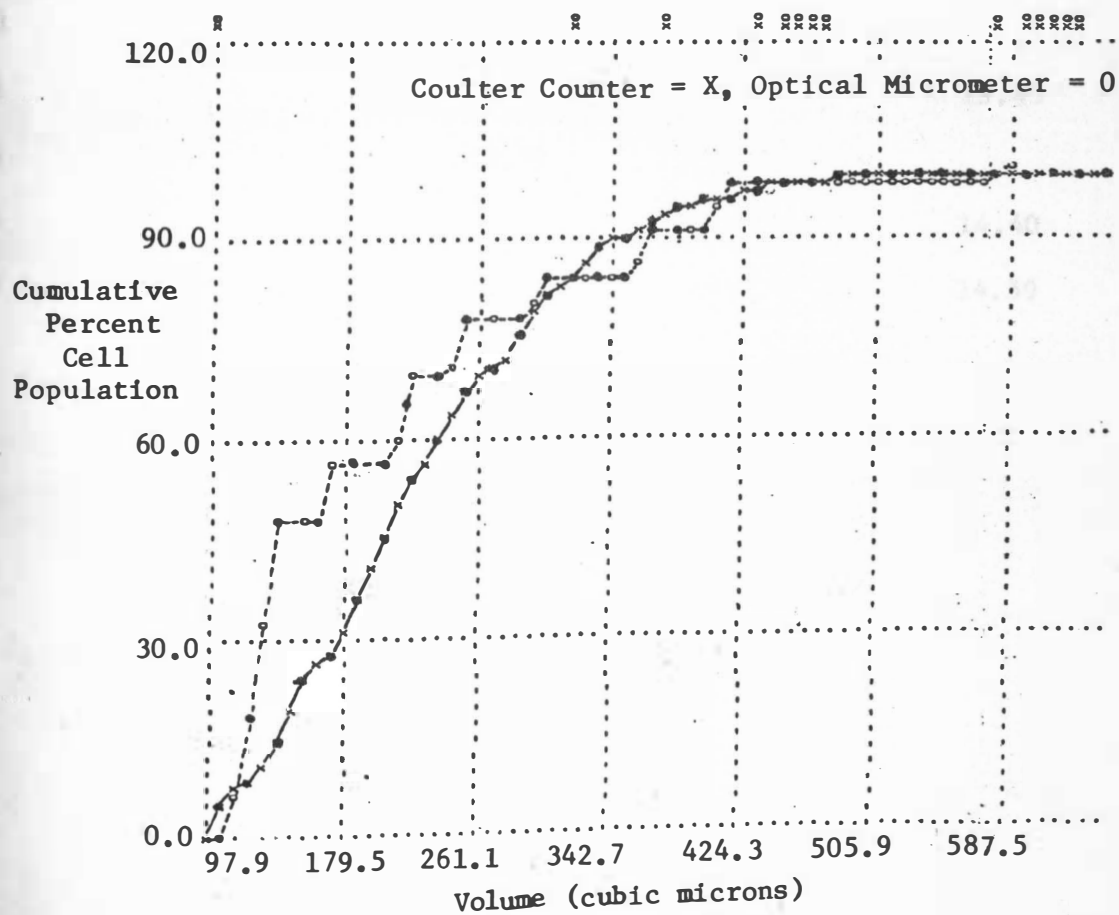
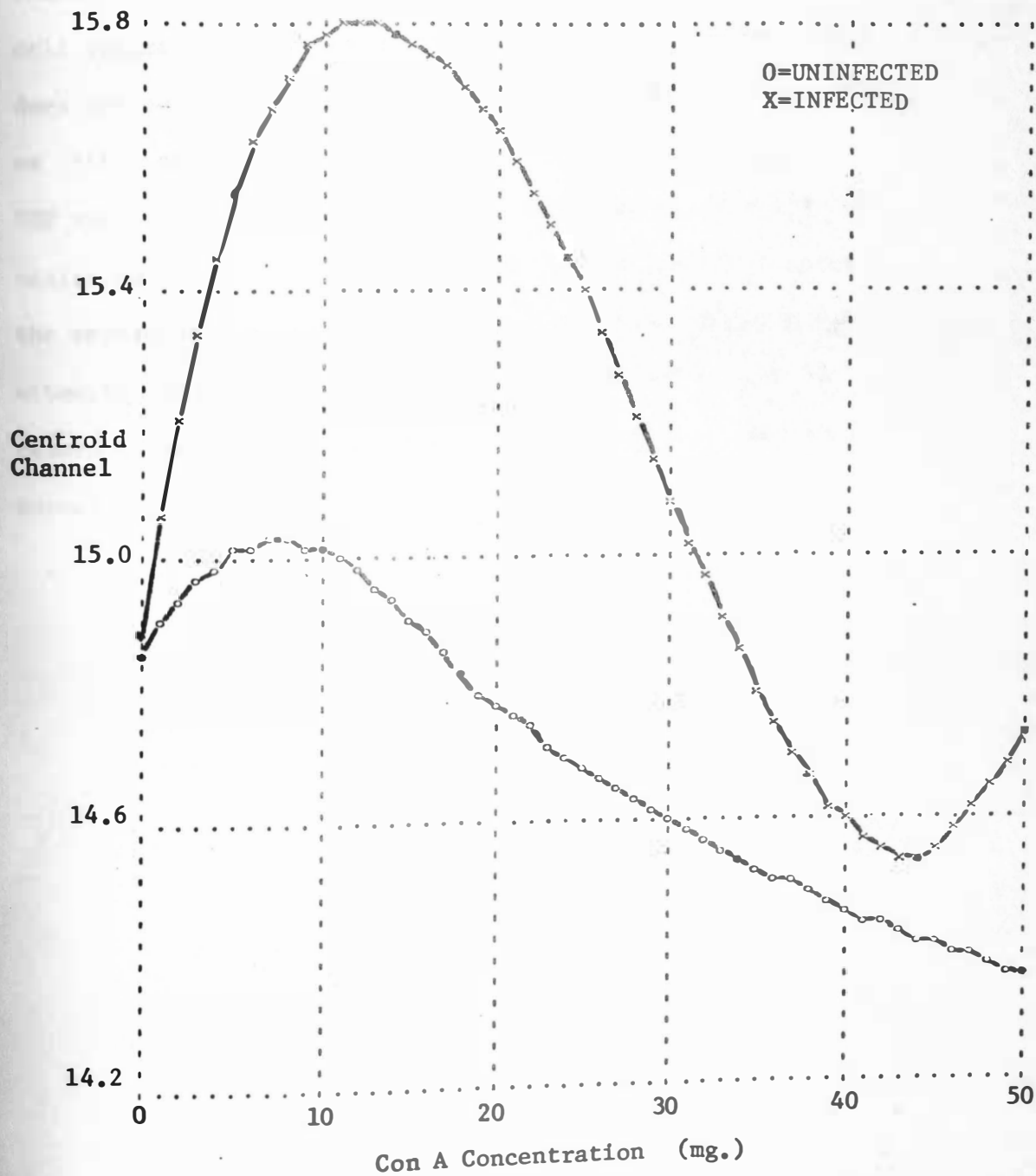


Table 18. Centroid Analysis of Concanavalin A Agglutinated Aedes albopictus Cell Volume Profiles.

Con A Concentration (mg.)	Uninfected Centroid Channel	Infected Centroid Channel
0	14.80	14.90
5		15.58
10	14.92	
14		15.89
18	14.78	
24		15.43
34	14.39	
44		14.40
50	14.21	14.59

Figure 41. Centroid Analysis of Uninfected and VEE Virus Infected Aal Cell Volume Profiles. Centroid Versus Increasing Con A Concentrations.



Aal cell volume profile is located at channel 14.85, while the centroid of the 4-hour infected Aal cell volume profile is located at channel 15.87. This is a difference of 1.02 channels (17.00 cubic microns). The centroid of the infected cell volume profile then decreases at a more rapid rate than does the centroid of the uninfected cell volume profile. With as little as 5 mg. of con A, the Aal cell infected with VEE virus are displaying larger centroids which is a sign of agglutination. Further analysis of the differences between the uninfected and the virus infected Aal cell cultures was attempted by observing single channel shifts which may be caused by agglutination. These analyses showed no immediate success.

CONCLUSIONS

1. Optical micrometer measurements were taken of 200 6 to 14 micron diameter latex particles and were found to extend, from 89.8 to 1797.0 cubic microns and have a mean volume of 363.4 cubic microns.
2. When Coulter Counter measurements were taken of about 45,000 6 to 14 micron diameter latex particles using both Vero cell and Aal cell sensitivity settings, the latex was found to extend from 92 to 9227 cubic microns.
3. When histograms and volume profiles were prepared of the optical micrometer and of the Coulter Counter measurements of 6 to 14 micron diameter latex particles and a comparison was made between the two measurement techniques, the results demonstrated that the Coulter Counter using the Aal cell sensitivity settings compared more closely with the optical micrometer measurements because of the fine resolution.
4. Coulter Counter measurements taken of 2.02 micron diameter latex particles were found to display a distribution of particle populations from 2 to 9.7 cubic microns in volume.
5. Control measurements taken of the Coulter Counter interference counts were found to be in less than 0.3 percent error for the sensitivity settings used in this investigation.
6. When five optical micrometer measurements were done of 1000

Vero cells, it was determined that the Vero cells extend from 270 to 12,000 cubic microns in volume and that 81 percent of the population was from 500 to 4000 cubic microns.

7. Efficient Coulter Counter sensitivity settings chosen for the Vero cell volume measurements were an attenuation of 4 and an aperture of 256.
8. Five Coulter Counter measurements of volume taken of about 100,000 Vero cells showed that the cells extend from 645 to 3594 cubic microns.
9. Histograms and volume profiles were done of the Vero cell volume measurements using the optical micrometer and the Coulter Counter, and comparisons were made between these two measurement techniques. The results demonstrated that the Coulter Counter measurements of the Vero cells compared closely to the optical micrometer measurements of the Vero cells.
10. Coulter Counter measurements were taken of uninfected and VEE virus infected Vero cells at various times post-infection and volume profiles were compared with much difficulty.
11. Centroid analysis was applied to the uninfected and the virus infected cell volume profiles, and it was demonstrated that virus infected Vero cells display significantly different centroids at various times post-infection than the uninfected Vero cells over that same time period.

12. A computer cell model was developed to simulate growing and dividing uninfected and VEE virus infected Vero cells.
13. When a smoothing function was used to compare computer simulated cell growth and division with the experimental volume profiles, the uninfected cell simulations correlated more closely with the experimental smoothed data than did the infected cell simulation.
14. A clinical application of the Coulter Counter rapid virus detection system was studied using antiserum from VEE virus immune horses. The centroid of the virus infected Vero cell profile was significantly smaller than the centroid of the uninfected and the VEE virus plus antiserum treated Vero cell volume profiles.
15. Optical micrometer measurements taken of 200 Aal cells showed that the cells range from 70 to 730 cubic microns in volume and have a mean volume of 206 cubic microns.
16. Efficient Coulter Counter sensitivity settings chosen for the Aal cell volume measurements were an attenuation of 0.356 and an aperture of 512.
17. Coulter Counter measurements of about 45,000 Aal cells resulted in measurements which extend from 106 to 645 cubic microns in volume.
18. Histograms and volume profiles of the Aal cell volume measurements using the optical micrometer and the Coulter Counter

and comparisons were made between the two measurement methods with the results being that the optical micrometer measurement was shown to have found smaller Aal cells.

19. Successive Coulter Counter measurements were taken of uninfected and VEE virus infected Aal cells after increasing concentrations of con A were added.
20. Centroid analysis was applied to the con A agglutination volume profiles of the uninfected and the virus infected Aal cells and significant differences were observed between the uninfected and the virus infected Aal cells.
21. Further application of the Coulter Counter virus detection system may demonstrate the reproducibility of centroid analysis or document a more efficient statistical data analysis system which has been previously overlooked. This virus detection system can be extended for use in detecting cellular volume changes in other virus infections such as the slow degenerative virus diseases of scrapies and kuru. The serum neutralization test presented in this investigation to detect virus presence may be extended to detect virus in test animals, and patients suspected of being infected with a specific virus which is later confirmed by traditional methods. Further rate of volume changes a virus infected cell undergoes must be incorporated into the computer cell model. Finally, the use of concanavalin A can be extended to show higher agglutination in other cell lines with other viruses to be measured with the Coulter Counter.

APPENDIX

Table I. Optical Micrometer Histogram and Statistics Computer Program.

```

110 DISP " PRESS KEY #4, #5, OR #6"
120 END

10 REMARK: INIT, KEY#0
20 DIM CS(200,9),AI(50),PI(32)
30 DISP SPA6"--- DAY OLD CELLS "
40 INPUT D
50 I=PI(D)
60 F=0
70 DISP " PRESS KEY #1 OR #2"
80 END
90 DEF FN(X)
100 IF Y00.25 THEN 120
110 RETURN 1
120 IF Y00.5 THEN 140
130 RETURN 2
140 IF Y01 THEN 160
150 RETURN 3
160 IF Y02 THEN 180
170 RETURN 4
180 IF Y03 THEN 200
190 RETURN 5
200 IF Y04 THEN 220
210 RETURN 6
220 IF Y05 THEN 240
230 RETURN 7
240 IF Y06 THEN 260
250 RETURN 8
260 IF Y07 THEN 280
270 RETURN 9
280 DISP " PE-ENTER: INVALID CELL-AGE. ";
290 INPUT Y
300 GOTO 100

10 REMARK: DATA INIT, KEY#1
20 DISP " DATA INIT PROGRESSING"
30 WAIT 10000
40 MAT C=ZER
50 MAT C=(999)*C
60 DISP " PRESS KEY #3"
70 END

10 REMARK: DATA LOAD, KEY#2
20 DISP SPA5"LOAD DATA-FILE # --- ";
30 INPUT #1
40 IF FI=INT#1 THEN 60
50 IF FI >= 15 AND FI <= 19 THEN 80
60 DISP " ERROR, PE-ENTER: FILE# ="FI,
70 GOTO 30
80 LOAD DATA FI,C
90 DISP " PRESS KEY #3, #5, OR #6"
100 END

10 REMARK: DATA STORE, KEY#4
20 DISP SPA5"STORE DATA-FILE # --- ";
30 INPUT F0
40 IF F0=INT#0 THEN 60
50 IF F0 >= 15 AND F0 <= 19 THEN 80
60 DISP " ERROR, PE-ENTER: FILE# ="F0,
70 GOTO 30
80 STORE DATA F0,C
90 DISP " DATA-STORAGE DONE"
100 END

10 REMARK: DATA LIST, KEY#5
20 JC=1
30 PRINT LIN1,WEYTE12
40 WAIT 1000
50 F=P+1
60 FRINV "PAGE"FI0"- OLD CELLS DATA"
70 PRINT LI#2"PAW CELL DIAMETER"SPA7"CELL"
80 PRINT "DIAMETER (MICRONS) VOLUME"LIN1
90 FOR J=J0 TO 200
100 IF C(J,1)=999 THEN 190
110 M=1.662197393*C(J,1)
120 Y=0.52359877*M^3
130 WRITE (15,170)C(J,1),M,Y
140 IF J/50=INT(J/50) THEN 180
150 JC=J+1
160 GOTO 30
170 FORMAT F6.2,F14.2
180 NEXT J
190 DISP " LIST DONE"
200 END

10 REMARK: BASIC STAT, KEY#6
20 IF C(1,1)=999 THEN 51
30 DISP SPA6"NO ENTERED DATA."
40 GOTO 500
50 DISP SPA10"THE OFFSET ";
60 INPUT C
70 DISP SPA10"CELL WIDTH ";
80 INPUT C
90 P=SC
100 MAT A=ZER
110 P1=PE+Y9
120 R2=-R1
130 S1=S2=S3=S4=R3=R4=R5=T1=M9=V9=0
140 FOR I=1 TO 200
150 IF C(I,1)=999 THEN 370
160 X=3.381238168*C(I,1)^3
170 IF X>P1 THEN 190
180 P1=X
190 IF X<R2 THEN 210
200 P2=X
210 S1=S1+X
220 Y=X*Y
230 S2=S2+Y
240 Y=X*X
250 S3=S3+Y
260 Y=X*X
270 S4=S4+Y
280 Y=INT((Y-C)/C+1.5)
290 IF Y<1 THEN 350

```

```

300 IF Y>B THEN 360
310 A(Y)=A(Y)+1
320 GOTO 360
330 R3=R3+1
340 GOTO 360
350 R4=R4+1
360 NEXT N
370 N=N-1
380 P=P+1
390 PRINT LIN1, WBYTE12
400 WAIT 1000
410 PRKNT "PAGE:P;D"- DAY CLD CELLS  STATISTICS"LIN2
420 M=S1/N
430 S=SQR((S2-M*M*N)/(N-1))
440 M3=S3/N-3*M*S2/N+2*M^3
450 M4=S4/N-4*M*S3/N+6*(M^2)*S2/N
460 M4=M4-3*M^4
470 PRINT "N"="N
480 WRITE (15,490)"MEAN ="M"STD. DEV ="S"SKEWNESS ="M3/S^3"KURTOSIS ="M4/S^4
490 FCPMAT F11.4,/,F11.4,/,F11.4,/,F11.4
500 IF T1=0 THEN 520
510 PRINT "MIN,MAX,RANGE MAY BE INCORRECT"
520 WRITE (15,490)"XMIN ="R1"XMAX ="R2"RANGE ="R2-R1
530 IF R3=0 THEN 550
540 PRINT "NC. TCC SMALL ="R3
550 IF R4=0 THEN 570
560 PRINT "NC. TCC LARGE ="R4
570 DISP " PRESS KEY #7 CR #6"
580 END

```

```

10 REMARK: HISTOGRAM, KEY#7
20 FOR K=1 TO 50
30 IF R5>A(K) THEN 50
40 F5=A(K)
50 NEXT K
60 W=2.5*R5/N
70 U=(N*C/(2.5066*S))*(40/F5)
80 WRITE (15,90)"EACH Y="W" PERCENT"
90 FCPMAT /,2F5.2
100 PRINT LIN1
110 Y=FNC(1)
120 FOR K=1 TO B+1
130 Y=C+(K-1.5)*C
140 WRITE (15,150)Y" .";
150 FCPMAT 2F12.4
160 T=INT(U*EXP(-(Y-M)/S+^2/2)+0.5)
170 PRINT TABT" .";
180 PRINT
190 IF K=B+1 THEN 470
200 Y=Y+0.5*C
210 PRINT TAB13" .";
220 T=INT(U*EXP(-(Y-M)/S+^2/2)+0.5)
230 P=INT((100*A(K)/N)/W)
240 IF T <= P THEN 360
250 IF R=0 THEN 290
260 FOR J=1 TO R
270 PRINT "X";
280 NEXT J
290 IF T=0 THEN 330
300 FOR J=F TO T-2+(R#0)
310 PRINT " .";
320 NEXT J
330 PRINT " .";
340 PRINT
350 GOTO 460

```

```

362 IF T=0 THEN 400
370 FOR J=1 TO T-(T=R)*P+(P=C)
380 PRINT "X";
390 NEXT J
400 PRINT " .";
410 IF T=R THEN 450
420 FOR J=1 TO R-T-1
430 PRINT "X";
440 NEXT J
450 PRINT
460 NEXT K
470 DISP " PRESS KEY #8"
480 END

```

```

10 REMARK: CELL STAT, KEY#6
20 PRINT LIN1"CELL# LOWER LIMIT";
30 PRINT TAB18" NC. OF CES RELATIVE FREQ"
40 Y=FNC(1)
50 FOR K=1 TO B
60 WRITE (15,70)M,C+(K-1.5)*C,A(K),100*A(K)/N
70 FCPMAT F5.0,F12.4,F11.0,F17.5
80 NEXT K
90 DISP " END CELL STATISTICS"
100 END

```

Table II. Coulter Counter Computer Program.

```

10 PEM: INIT
20 DIM DS(100,2),CS(99,6),SS(99,6)
30 DIM J1(6),F1(6),F3(6),G3(112),P3(103),D3(103)
40 DIM ES(6),F3(6)
50 DISP " TODAY'S DATE: MONTH/DAY/YEAR ";
60 INPUT M0,D7,Y3
70 C9=100
80 D5=D9-1
90 FEDI= D(D9,2)
100 MAT C=ZER
110 MAT C=ZER
120 REVIND
130 DISP "FEPCIE C.C. TAPE FROM TRANSPORT."
140 END

```

```

10 PEM: ENTFY
20 DISP SPA7"EXPERIMENT NUMBER ";
30 INPUT D(D9,1)
40 DISP " ATTENUATION,APERTURE SETTING ";
50 INPUT D(D6,1),C(D6,2)
60 PEM: EPPCF CHECK
70 RESTORE
80 FOR J=0 TO 9
90 READ D1
100 IF D(D6,1)≠D1 THEN 140
110 GOTO 160
120 DATA C.125,C.177,0.25,0.354
130 DATA C.5,0.707,1.2,4.8
140 NEXT J
150 DISP D(D6,1)"ERROR: RE-ENTER ATEN."SPA5,
160 INPUT D(D6,1)
170 GOTO 70
180 FOR J=0 TO 9
190 IF D(D6,2)≠J THEN 210
200 GOTO 250
210 NEXT J
220 DISP D(D6,2)"ERROR: RE-ENTER APERTURE.";
230 INPUT D(D6,2)
240 GOTO 160
250 T2=N=0
260 MAT C=ZER
270 N=N+1
280 IF N<D6 THEN 310
290 DISP " ***** DATA LIMIT *****"
300 GOTO 550
310 DISR " THRESHOLD="T2+1" 3 COUNTS ";
320 INPUT T,E(1),E(2),E(3)
330 PEM: CHECK DATA
340 IF T-INTT CP T<1 CP T>100 THEN 390
350 IF T>T2 THEN 410
360 DISP T"CHANNEL NOT " -"T2+1
370 WAIT 10000
380 GOTO 310
390 DISP T"INVALID THRESHOLD"
400 GOTO 370
410 FOR J=1 TO 3
420 IF E(J)-INT(E(J)) THEN 440
430 IF E(J) >= 0 AND E(J) <= 99999 THEN 460
440 DISP E(J)"INVALID COUNT"
450 GOTO 370
460 C(T,J)=E(J)
470 NEXT J

```

```

450 D(N,1)=T
460 D(N,2)=INT((E(1)+E(2)+E(3))/3+.5)
470 V=(E(1)-D(N,2))2+(E(2)-D(N,2))2+(E(3)-D(N,2))2
480 C(N,4)=100*SSRV/D(N,2)
490 T2=T
500 D(D9,2)=N
510 GOTO 270
520 END

```

```

10 REM: CORRECT
20 DISP " CORRECT THRES. NO. TO 3-COUNTS "
30 INPUT T,E(1),E(2),E(3)
40 REM: EFFECT CHECK
50 FOR I=1 TO D(D9,2)
60 IF T=D(I,1) THEN 110
70 NEXT I
80 DISP "THRESHOLD NOT FOUND."
90 WAIT 10000
100 GOTO 20
110 FOR J=1 TO 3
120 IF E(J)-INT(E(J)) THEN 140
130 IF E(J) >= 0 AND E(J) <= 99999 THEN 160
140 DISP E(J)"INVALID COUNT"
150 GOTO 90
160 NEXT J
170 REM: SAVE CORRECT
180 D(1,2)=INT((E(1)+E(2)+E(3))/3+.5)
190 C(1,1)=E(1)
200 C(1,2)=E(2)
210 C(1,3)=E(3)
220 V=(E(1)-C(1,2))2+(E(2)-C(1,2))2+(E(3)-C(1,2))2
230 C(1,4)=100*SSRV/D(1,2)
240 GOTO 20
250 END

```

```

10 REM: LIST
20 DISP SPA7"DATA LIST HEADING "
30 INPUT P3
40 REM: CALC
50 FOR I=1 TO D(D9,2)-1
60 C(I,5)=D(I,2)-D(I+1,2)
70 NEXT I
80 REM: WRITE FILE
90 G4="DATA LIST"
100 J=FNJ0
110 OUTPUT (15,120)"EXP# "D(D9,1)
120 FORMAT F1000.2, /
130 PRINT "ATTENUATION SETTING ="D(D8,1)
140 PRINT "APERTURE SETTING ="D(D9,2);LINE
150 L=8
160 IC=1
170 FOR K=1 TO 3
180 A=C
190 FOR I=10 TO C(D9,2)
200 GOSUB K OF 400,460,500
210 A=A+1
220 IF D(1,1)+1=D(I+1,1) THEN 250
230 IF A/L-INT(A/L)=0 THEN 250
240 NEXT I
250 PRINT
260 WAIT 200
270 NEXT K
280 PRINT
290 IF I >= D(D9,2) THEN 520

```

```

300 10=1+1
310 IF J THEN 170
320 L=L+4
330 IF L<56 THEN 170
340 J=FAJ1
350 PRINT
360 L=4
370 GOTO 170
380 REM: WRITE 1ST LINE
390 FORMAT 2F7.0
400 WRITE (15,390)D(1,1),C(1,1);
410 IF D(1,1)+1#D(1+1,1) THEN 430
420 WRITE (15,390)C(1,5);
430 RETURN
440 REM: WRITE 2ND LINE
450 FORMAT 7X,2F7.0
460 WRITE (15,450)C(1,2),D(1,2);
470 RETURN
480 REM: WRITE 3RD LINE
490 FORMAT 7X,F7.0,F6.1,"X"
500 WRITE (15,490)C(1,3),C(1,4);
510 RETURN
520 END

```

```

10 REM: DATA STORE
20 DISP " STORE DATA CN WHICH FILE # ";
30 INPUT J
40 STORE DATA J,D
50 END

```

```

10 REM: PLCT
20 DISP SFA7"DATA PLCT HEADING ";
30 INPUT P3
40 FOR J=1 TO 6
50 DISP SFA4"FILE# OF DATA SET"J;
60 INPUT J(J)
70 IF J(J)=999 THEN 110
80 DISP J(J)"FILE, PCINT-SYMBOL ";
90 INPUT P3(J,J)
100 NEXT J
110 N=J-1
120 C1=C2=C3=1
130 DISP " ZERC NEGATIVE CCUNTS OPTICN ";
140 INPUT G3
150 IF PCS(G3,"NC") THEN 170
160 C1=0
170 DISP " NORMALIZE CCUNTS TO 3 OPTICN ";
180 INPUT G3
190 IF PCS(G3,"NC") THEN 210
200 C2=0
210 G3="0"
220 DISP " SPECIFY CHANNEL RANGG OPTICN ";
230 INPUT G3(2)
240 IF PCS(G3,"NC") THEN 290
250 C3=0
260 X1=VAL(G4)
270 X2=VAL(G3(PCS(G3,"")+1))
280 REM: DATA LCAD & CALC
290 MAT C=ZER
300 MAT G=ZER
310 Y0=Y0+9E+99
320 X9=Y9=-Y0
330 FOR J=1 TO N
340 LCAD DATA J(J),D

```

```

350 IF J>1 THEN 380
360 T1=D(2,1)
370 T2=D(2,2)
380 IF D(2,1)=T1 AND D(2,2)=T2 THEN 420
390 DISP "FILE"J(J)"APP. (P ATT. NET SCME."
400 STOP
410 REM: DATA TRANSFER & CALC
420 K=0
430 FOR I=1 TO D(9,2)
440 IF D(1,1)+1#D(1+1,1) THEN 580
450 K=K+1
460 REM: Y-MIN.MAY
470 Y=C(K,J)=D(1,1)
480 IF Y >= Y0 THEN 500
490 Y0=Y
500 IF Y <= Y9 THEN 530
510 Y9=Y
520 REM: Y-MIN.MAY
530 Y=C(K,J)=D(1,2)-D(1+1,2)
540 IF Y >= Y0 THEN 560
550 Y0=Y
560 IF Y <= Y9 THEN 580
570 Y9=Y
580 NEXT I
590 C(2,1)=K
600 E(1)=D(9,1)
610 NEXT J
620 REM: OPTICS
630 GOSUB 1690
640 GOSUB NET C1 OF 1620
650 GOSUB NET C2 OF 1720
660 REM: SCALING
670 IF Y0=Y9 THEN 870
680 S=PP(Y9-Y0)
690 IF S<5 THEN 720
700 S=INT(S+0.995)*10^(P0-2)
710 GOTO 730
720 S=INT(2*(S-0.05)+1)/2*10^(P0-2)
730 A1=Y9-100.5*S
740 A9=Y0+0.5*S
750 IC=0
760 IF A1<0 AND A9>0 THEN 900
770 F(1)=10
780 F(2)=5
790 F(3)=2
800 FOR I=1 TO 3
810 FOR P0=1 TO 3
820 K=INT((PP(0.5*(A1+A9))*10^DI/(P(R0)+0.5)
830 IC=Y*F(P0)*10^(P0-DI)
840 IF 10>A1 AND 10<A9 THEN 900
850 NEXT P0
860 NEXT DI
870 DISP " GRAPH SKIPPED: NET SCALEABLE"
880 STOP
890 REM: HEADINGS
900 G3="DATA FLEV"
910 J=FAJ0
920 K=FAJ0
930 FOR I=1 TO N
940 IF C2 THEN 970
950 OUTPUT (15,960)G(2,1);
960 FORMAT "<F1000.0,">
970 OUTPUT (15,960)"EXP#E(1)" = "P3(1,1);
980 FORMAT 2F1000.2
990 IF 1#P THEN 1010
1000 OUTPUT (15,980)"", "

```

```

1010 NEXT I
1020 FCFMAT //,F15.1,5F20.1
1030 WRITE (15,1020)10,20*S+10,40*S+10,60*S+10,100*S+10
1040 REM: GRAPH INIT
1050 A=0.09*TI*T2
1060 FCP K=1 TO 61 STEP 20
1070 B3(K)=-
1080 D3(K)=- + - - - - - +
1090 NEXT K
1100 B3(2,2)=-*-
1110 D3(102,102)=-*-
1120 MAT J=CCN
1130 REM: WORKING GRAPH
1140 WRITE (15,1570) "D3
1150 FCR X=X1 TC Y2
1160 REM: DET GRAPH-PTS
1172 T=0
1180 MAT F=CCN
1190 FCP J=1 TC N
1200 IF G(J(J),J)=X THEN 1230
1210 T=T+1
1220 GOTC 1260
1230 P(J)=(G(J(J),J)-10)/5+2
1240 J(J)=J(J)+1
1250 T=0
1260 NEXT J
1270 IF T=0 THEN 1540
1280 GOTC T=N CF 1560
1290 REM: SET GRAPH-PTS
1300 G3=B3
1310 P9=103
1320 FCR K=1 TC N
1330 IF F(K)=0 THEN 1500
1340 FCP J=K TC N
1350 IF P(J)/F(K) THEN 1460
1360 IF J=K THEN 1470
1370 GOTC D1 CF 1410
1380 P9=P9+1
1390 G3(P9,P9)=F3(K,K)
1400 P9=P9+1
1410 G3(P9,P9)=P3(J,J)
1420 P(J)=0
1430 P9=P9+1
1440 G3(P9,P9)=-,-
1450 D1=1
1460 GOTC 1460
1470 D1=0
1480 NEXT J
1490 G3(P(K),F(K))=P3(K,K)
1500 NEXT K
1510 REM: WRITE GRAPH-PTS
1520 WRITE (15,1530)A*X,Y,G3(1,P9-1)
1530 FCFMAT F6.1,/,F11.0,1X,F1.0
1540 NEXT X
1550 REM: WRITE DIVIDE-LINE
1560 WRITE (15,1570)A*X,D3
1570 FCFMAT F6.1,/,12X,F1.0
1580 T=1
1590 GOTC "X <= Y2 CF 1540
1600 END
1610 REM: ZERO NEG COUNTS
1620 IF Y0 >= 0 THEN 1700
1630 Y0=0
1640 FCP J=1 TC N
1650 FCP I=1 TO C(DE,J)
1660 IF G(I,J) >= 0 THEN 1680

```

```

1670 G(I,J)=L
1680 NEXT I
1690 NEXT J
1700 RETURN
1710 REM: PCFM & COUNTS
1720 Y0=Y0+0
1730 FOR J=1 TO N
1740 T=0
1750 FOR I=1 TO C(D8,J)
1760 T=T+G(I,J)
1770 NEXT I
1780 G(D8,J)=T
1790 FOR I=1 TO C(D8,J)
1800 Y=G(I,J)+100*G(I,J)/T
1810 IF Y >= Y0 THEN 1830
1820 Y0=Y
1830 IF Y <= Y9 THEN 1850
1840 Y9=Y
1850 NEXT I
1860 NEXT J
1870 RETURN
1880 REM: COUNT RANGE
1890 IF ACT (3) THEN 1930
1900 X1=X0
1910 X2=X9
1920 RETURN
1930 Y1=INT(X1+0.5)
1940 X0=INT(X2+0.5)
1950 IF X1>2 THEN 1980
1960 IF Y1>Y0 AND X1<X9 THEN 1980
1970 X1=X0
1980 IF X2>X0 AND X2<X9 THEN 2000
1990 X2=X9
2000 IF X1=X0 AND X2=X9 THEN 2170
2010 Y0=Y0+99
2020 Y9=Y0
2030 FOR J=1 TO N
2040 K=0
2050 FOR I=1 TO C(D8,J)
2060 IF C(I,J)<Y1 OR C(I,J)>X2 THEN 2140
2070 K=K+1
2080 C(K,J)=C(I,J)
2090 Y=G(K,J)+G(I,J)
2100 IF Y >= Y0 THEN 2120
2110 Y0=Y
2120 IF Y <= Y9 THEN 2140
2130 Y9=Y
2140 NEXT I
2150 C(D8,J)=K
2160 NEXT J
2170 RETURN

```

```

10 GA="PLOT LIST"
20 J=1:JC
30 K=1:K0
40 PRINT LINE "CHAN"
50 FOR K=1 TO N
60 WRITE (15,70)E(K)" "
70 FORMAT 2X,2F9.2
80 NEXT K
90 PRINT LINE
100 MAT J=CK
110 FOR N=1 TO N2
120 TC=0
130 FOR K=1 TO N

```

```

140 IF C(J(K),K)≠X AND T0=0 THEN 160
150 T0=T0+1
160 NEXT K
170 GOTO T0=0 CF 290
180 WRITE (15,190)X;
190 FORMAT F4.0
200 FOR K=1 TO T0
210 IF C(J(K),K)=Y THEN 250
220 WRITE (15,232)" ";
230 FORMAT 12X
240 GOTO 280
250 WRITE (15,260)G(J(K),K);
260 FORMAT F12.2
270 J(K)=J(K)+1
280 NEXT K
290 PRINT
300 NEXT Y
310 END

```

```

10 REM: CENTRCID
20 DISP SPA4"CENTRCID CHANNEL RANGE ";
30 INPUT Y1,X2
40 T1=T2=0
50 FOR I=1 TO D(D9,2)
60 IF D(I,1)<X1 OR D(I,1)>X2 THEN 110
70 IF D(I+1,1)≠D(I,1)+1 THEN 110
80 Y=D(K,2)-D(I+1,2)
90 T1=T1+D(I,1)*Y
100 T2=T2+D(I,1)*Y^2
110 NEXT I
120 DISP "CENTRCID ="T2/T1
130 END

```

```

10 PRINT "KEY#"INTK;
20 IF K-INTK=0 THEN 40
30 PRINT "SHIFTED"
40 PRINT
50 END

```

```

10 REM: DATA LCAD
20 DISP " LCAD DATA FROM WHICH FILE # ";
30 INPUT J
40 LCAD DATA J,D
50 END

```



```

1290 INPUT J
1300 IF J THEN 1330
1310 PRINT LINE,WRITE12
1320 WAIT 1000
1330 OUTPUT (15,1340)"P.P. CELL MODEL",M1,D7,Y3,H3
1340 FORMAT F5.0,"/",F1003.0,"/",F1005.0,4X,F1.0
1350 PRINT LINE2"INITIAL-CELL FILE NO. ="F1"EXP#E
1360 GOTO C1 OF 1380
1370 PRINT "OPTION: INITIAL NEGATIVE COUNTS ZERCOED"
1380 PRINT "FIRST CELL VOLUME ="M0"VARIATION ="V
1390 PRINT "RATE OF VOLUME INCREASE ="M
1400 PRINT "TIME: INTERVAL ="D"INITIAL ="T0"FINAL ="T9
1410 IF N <= 12 THEN 1440
1420 PRINT LINE"RAY. NO. CURVGS EXCEEDED BY"N-12
1430 N=12
1440 WRITE (15,1450)""CELL COUNT VS. C.C. CHANNEL ""
1450 FORMAT /,42Y,F1.0
1460 PRINT
1470 FOR I=1 TO N-1
1480 OUTPUT (15,1490)"<"S(51,I)">TIME("S(52,I)") = "P3(1,I)", "I
1490 FORMAT 3F1006.0
1500 IF 100 THEN 1530
1510 PRINT
1520 WAIT 250
1530 NEXT I
1540 OUTPUT (15,1490)"<"S(71,I)">TIME("S(52,I)") = "P3(1,I)
1550 WRITE (15,1500)10,20*S+10,40*S+10,60*S+10,80*S+10,100*S+10
1560 FORMAT /,6X,F9.1,11X,F9.1,11X,F9.1,11X,F9.1,11X,F9.1,11X,F9.1
1570 REM: GRAPH INKT
1580 I=0
1590 FOR Y=1 TO 81 STEP 20
1600 B3(K)=
1610 C3(K)= + - - - - - +
1620 NEXT K
1630 P3(2,21)=
1640 P3(102,102)=
1650 REM: DRAWING GRAPH
1660 WRITE (15,2000)
1670 FOR C=Y0 TO Y9
1680 I=1+I
1690 REM: SET GRAPH-PTS
1700 FOR J=1 TO N
1710 P3(J)=(C3(1,J)-10)/S+2
1720 NEXT J
1730 REM: SET GRAPH-PTS
1740 C3=C3
1750 P3=P3
1760 FOR K=1 TO N
1770 IF P3(K)=0 THEN 1940
1780 FOR J=K TO N
1790 IF P3(J)/P3(K) THEN 1920
1800 IF J=K THEN 1910
1810 GOTO C1 OF 1830
1820 P3=P3+1
1830 C3(C3,P3)=P3(K,K)
1840 P3=P3+1
1850 C3(C3,P3)=P3(J,J)
1860 P3(J)=0
1870 P3=P3+1
1880 C3(C3,P3)=
1890 C1=1
1900 GOTO 1920
1910 C1=0
1920 NEXT J
1930 C3(P3,K)=P3(K,K)
1940 NEXT K

```

```

1950 REM: WRITE GRAPH-PTS
1960 WRITE (15,1960)A°C,C,G$[1,F9-1]
1970 NEXT C
1980 FORMAT F8.1,/,F11.0,1X,F1.0
1990 WRITE (15,2000)A°C,D$
2000 FORMAT F8.1,/,12X,F1.0
2010 REM: TABULAR OUTPUT
2020 DISP SPAS"WRITE THE RESULTS "
2030 INPUT G$
2040 IF PCS(G$,"N") THEN 2290
2050 PRINT LIN1,WPYTE12
2060 WAIT 1000
2070 OUTPUT (15,1340)"R.F. CELL MODEL",PI,D7,Y3,H$
2080 PRINT LIN2"CHANNEL"
2090 FOR I=1 TO N
2100 WRITE (15,2250)" "
2110 IF S(52,1) >= 10 THEN 2132
2120 WRITE (15,2250)" "
2130 OUTPUT (15,1490)"TIME("S(52,1)")"
2140 NEXT I
2150 PRINT LIN1
2160 WAIT 250
2170 C=X0
2180 FOR I=1 TO N0
2190 WRITE (15,2200)C
2200 FORMAT F4.0,2X
2210 FOR J=1 TO N
2220 WRITE (15,2250)S[I,J]
2230 NEXT J
2240 PRINT
2250 FORMAT F10.0
2260 WAIT 250
2270 C=C+1
2280 NEXT I
2290 DISP SPAT"STORE ANY RESULTS "
2300 INPUT G$
2310 IF PCS(G$,"N") THEN 2620
2320 FOR J=1 TO N
2330 P=P(S(G$),P$[J,J])
2340 IF P=0 THEN 2610
2350 P=C+P
2360 IF G$(P,F) >= "0" THEN 2440
2370 DISP "ERRCR: FILE NO. FOR CURVE "P$(1,1)" "
2380 INPUT P$
2390 IF PCS(P$,"N") THEN 2610
2400 IF P$ < "0" THEN 2370
2410 IF P$ > "9" THEN 2370
2420 F1=VAL(P$)
2430 GOTC 2460
2440 IF G$(F,F) > "9" THEN 2370
2450 F1=VAL(G$(P))
2460 C=X0-1
2470 T=INT(S(51,J)+0.5)
2480 MAT C=ZER
2490 FOR I=1 TO N0
2500 D[I,1]=C+C+1
2510 D[I,2]=T
2520 T=T-INT(S(1,J)+0.5)
2530 NEXT I
2540 D[I,1]=C+1
2550 D[I,2]=T
2560 D[D8,1]=A1
2570 D[D8,2]=A2
2580 D[D9,1]=E+1000*S(52,J)
2590 D[F9,2]=1
2600 STORE DATA F1,D
2610 NEXT J
2620 NEXT I
2630 DISP " DO YOU WANT ANOTHER RUN "
2640 INPUT G$
2650 IF PCS(G$,"N")=0 THEN 100
2660 DISP "END"
2660 END

```

Table IV. Data Smoothing Program.

```

10 REM: C.C. DATA SMOOTHING
20 DIM DS(100,2),CS(99,2),SS(99),H$(32),A$(10),B$(10)
30 D9=100
40 REDIM D(D9,2)
50 DISP "LOAD DATA FROM WHICH FILE ?";
60 INPUT J
70 LOAD DATA J,D
80 J=H=0
90 FOR I=1 TO D(D9,2)-1
100 IF D(I+1,1)/D(I,1)+1 THEN 140
110 J=J+1
120 C(J,1)=D(I,1)
130 C(J,2)=D(I,2)-D(I+1,2)
140 NEXT I
150 H=J
160 DISP "SMOOTH (VER -- NUMBERS)";
170 INPUT A
180 IF A=INTN THEN 290
190 IF A<3 THEN 250
200 IF A>D(D9,2) THEN 270
210 IF A/2-INT(A/2)+0 THEN 230
220 GOTO 300
230 DISP "INVALID, RE-ENTER CDD NO.";
240 GOTO 170
250 DISP "INVALID, RE-ENTER A NO.>3";
260 GOTO 170
270 DISP "INVALID, RE-ENTER A NO.<="D(D9,2)";
280 GOTO 170
290 DISP "INVALID, RE-ENTER AN INTEGER";
300 N=J+1=1
310 REM: SMOOTH BEGINNING
320 FOR J2=(N+1)/2 TO N
330 S(1)=FNA0
340 I=1+1
350 NEXT J2
360 IF A=D(D9,2) THEN 480
370 J2=J2-1
380 GOTO 550
390 REM: AVERAGING FUNCTION
400 DEF FNA(X)
410 P=0=0
420 FOR J=J1 TO J2
430 N=N+C(J,1)
440 P=P+D(J,1)*C(J,2)
450 NEXT J
460 RETURN P/N
470 REM: SMOOTH MIDDLE
480 J1=J1+1
490 S(1)=FNA0
500 I=1+1
510 J2=J2+1
520 IF J2<D(D9,2) THEN 480
530 REM: SMOOTH END
540 J2=J2-1
550 J1=J1+1
560 S(1)=FNA0
570 I=1+1
580 IF I <= D(D9,2) THEN 550
590 REM: AFTER SMOOTHING
600 S=0
610 T=D(I,2)
620 FOR I=1 TO D(D9,2)-1
630 D(I,2)=T-S
640 S=S+S(I)
650 IF D(I+1,1)=D(I,1)+1 THEN 680
660 T=D(I+1,2)
670 S=0
680 NEXT I
690 DISP "PRINT RESULTS";
700 INPUT B$
710 IF PCS(B$,"N") THEN 930
720 REM: LIST
730 DISP "READY PRINTER (REPLY 0)";
740 INPUT J
750 I=0
760 IF J THEN 790
770 PRINT LIN1,VBYTE12
780 WAIT 1000
790 J1=1
800 IF I=1 THEN 850
810 PRINT LIN2"EXP"=D(D9,1)
820 PRINT LIN1"ATTENUATION"=D(D9-1,1)
830 PRINT "APERTURE"=D(D9-1,2)
840 J1=J1+5
850 PRINT LIN2"CHANNEL CLD DATA SMOOTHED"
860 J1=J1+2
870 FOR I=1+1 TO H
880 J1=J1+1
890 WRITE (15,900)C(I,1),C(I,2),S(I)
900 FORMAT F4.0,F13.0,F12.0
910 IF J1 >= 55 AND NOT J THEN 770
920 NEXT I
930 DISP "DO YOU WISH TO STORE NEW DATA";
940 INPUT A$
950 IF PCS(A$,"N") THEN 1000
960 DISP "STORE DATA ON WHICH FILE ?";
970 INPUT J
980 DISP "THANK YOU"
990 STORE DATA J,D
1000 END

```

Table V. Interpolation and Graphing Computer Program.

```

10 CCM RS(100,10),GS(200,2),II(10,3),N,10,X0,Y0,X9,Y9,P,SI(10,33),HI(81)
20 DIM JI(10,2),FI(10),PS(10),G3(120),CS(103),Q3(103)
30 DIM MS(10,2),N(4,4),A(4),VS(4),UC(4,4),ES(4)
40 REM: GENERAL INTERPLATION & GRAPHING
50 F=10-0
60 PAT 1=PER
70 PAT 5=PER
80 MAT H=ZER
90 REM >>> EXTERNAL ENTRY <<<<<
100 N=1
110 R0=0
120 N9=10
130 D9=100
140 X0=9E+99
150 Y0=-Y0
160 REDIM R(D9,N9)
170 FOR I=1 TO N9
180 I(1,2)=1
190 NEXT I
200 G3=" 1 0328'()*+,-./0123456789:;<=>? "
210 J3(34)="ABCDEFGHIJKLMNCFORSTUVWVYZ"
220 G3(66)="0123456789:;<=>?ABCDEFGHIJKLMNCFORSTUVWVYZ"
230 IF H(61) THEN 300
240 DISP " DATA DESCRIPTION <60 CHAR> ";
250 INPUT C3
260 H(61)=LEN(C3)
270 FOR I=1 TO H(61)
280 H(I)=POS(G3,C3(I,1))*31
290 NEXT I
300 IF S(N,33) THEN 400
310 DISP " NAME OF CURVE" N <32 CHAR> "I
320 INPUT C3
330 IF POS(C3,"000") THEN 690
340 S(N,33)=LEN(C3)
350 IF S(N,33) <= 32 THEN 370
360 S(N,33)=32
370 FOR I=1 TO S(N,33)
380 S(N,I)=POS(G3,C3(I,1))*31
390 NEXT I
400 I=N
410 GOSUB 3900
420 IF I(N,3) THEN 640
430 I(N,2)=N
440 I(N,3)=R0
450 D1=0
460 D1=D1+1
470 DISP "X,Y DATA PT. -"DIIC3;
480 INPUT N,Y
490 REM: ERROR CHECK
500 IF Y#999 OR Y#999 THEN 540
510 IF D1#4 THEN 620
520 DISP " ENTER 4 POINTS MINIMUM. ";
530 GOTO 480
540 GOTO D1 OF 590
550 IF X>G(I(N,3),1) THEN 590
560 DISP " X="X"NEXT ", PREV.X="G(I(N,3),1),
570 GOTO 480
580 REM: SAVE DATA
590 I(N,3)=I(N,3)+1
600 G(I(N,3),1)=X
610 G(I(N,3),2)=Y
620 GOTO 480
630 REM: CHECK EXTERNAL DATA

```

```

640 IF I(N,3)-R0<4 THEN 670
650 FOR I=R0+1 TO I(N,3)-1
660 IF G(I+1,1)>G(I,1) THEN 800
670 DISP "DELETED CURVE" I(N,2) I(C)
680 WAIT 5000
690 FOR J=N TO N9-1
700 J1=J+1
710 I(J,2)=I(J1,2)
720 I(J,3)=I(J1,3)
730 S(J,33)=S(J1,33)
740 FOR K=1 TO S(J,33)
750 S(J,K)=S(J1,K)
760 NEXT K
770 NEXT J
780 I(J,2)=I(J,3)=0
790 GOTO 300
800 NEXT I
810 REM: MIN, MAX X
820 IF X0 <= G(R0+1,1) THEN 840
830 XC=G(R0+1,1)
840 R0=I(N,3)
850 IF X9 >= G(R0,1) THEN 870
860 X9=G(R0,1)
870 N=N+1
880 IF N <= N9 THEN 300
890 N=N-1
900 DISP SPA7"WRITE THE RESULTS "
910 INPUT Q3
920 DISP SPA7"GRAPH THE RESULTS "
930 INPUT G3
940 IF FCS(G3,"N") THEN 1010
950 FOR I=1 TO N
960 GOSUB 3900
970 DISP "PT-S(MBCL" I(C)
980 INPUT F3(I,1)
990 NEXT I
1000 REM: INTERPOLATION
1010 IF 10 THEN 1040
1020 DISP "INTERVAL OF INTERPOLATION "
1030 INPUT 10
1040 IF 10>0 THEN 1060
1050 10=(X9-X0)/50
1060 Y0=9E+99
1070 Y9=-Y0
1080 J(1,1)=0
1090 J=J(1,2)-R0-1
1100 MAT V=ZER
1110 MAT M=C(N(4,4)
1120 FOR I=1 TO N
1130 D1=1
1140 X=G(R0,1)-10
1150 GOTO 1270
1160 REM: SHIFT MAT RCVS
1170 D1=D1+1
1180 R0=R0+1
1190 FOR K=1 TO 3
1200 J1=K+1
1210 FOR L=2 TO 4
1220 M(K,L)=M(J1,L)
1230 NEXT L
1240 V(K)=V(J1)
1250 NEXT K
1260 REM: BUILD CO-EFF MAT
1270 F0=1
1280 FOR K=2 TO 4
1290 M(4,K)=F0-G(R0,1)*F0
1300 NEXT K
1310 V(4)=G(R0,2)
1320 IF D1<4 THEN 1170
1330 REM: INTERPOLATE!
1340 MAT U=M
1350 CS=0
1360 FOR Q2=1 TO 4
1370 Q3=U(Q2,Q2)
1380 IF (ABS(Q3)-0.00001) <= 0 THEN 1520
1390 FOR Q4=1 TO 4
1400 U(Q2,Q4)=U(Q2,Q4)/Q3
1410 NEXT Q4
1420 U(Q2,Q2)=1/Q3
1430 FOR Q6=1 TO 4
1440 IF Q6=Q2 THEN 1500
1450 G2=U(Q6,Q2)
1460 U(Q6,Q2)=0
1470 FOR Q7=1 TO 4
1480 U(Q6,Q7)=U(Q6,Q7)-G2*U(Q2,Q7)
1490 NEXT Q7
1500 NEXT Q6
1510 GOTO 1540
1520 CS=CS+1
1530 S(CS)=Q2
1540 NEXT Q2
1550 IF CS=0 THEN 1760
1560 FOR W2=1 TO Q5
1570 W1=S(W2)
1580 Q3=U(W1,W1)
1590 IF (ABS(Q3)-0.00001) THEN 1740
1600 FOR W3=1 TO 4
1610 U(W1,W3)=U(W1,W3)/Q3
1620 NEXT W3
1630 U(W1,W1)=1/Q3
1640 FOR Q6=1 TO 4
1650 IF Q6=W1 THEN 1710
1660 G2=U(Q6,W1)
1670 U(Q6,W1)=0
1680 FOR Q7=1 TO 4
1690 U(Q6,Q7)=U(Q6,Q7)-G2*U(W1,Q7)
1700 NEXT Q7
1710 NEXT W2
1720 NEXT W3
1730 GOTO 1760
1740 DISP "INVERSE IMPOSSIBLE"
1750 GOTO 1760
1760 MAT A=U
1770 GOTO 1810
1780 WAIT 1000
1790 DISP "CHANGE X VALUE" M(W1,2) "AND RERUN"
1800 STOP
1810 MAT A=N*U
1820 IF X <= M(3,2) THEN 1860
1830 IF 50<I(1,3) THEN 1170
1840 IF X >= G(R0,1) THEN 1050
1850 REM: Y, MIN, MAX
1860 GOSUB 3840
1870 Y=X+10
1880 Y9=J(1,1), J(1,2)=A(1)+X*(A(2)+X*(A(3)+X*A(4)))
1890 IF Y0 <= Y THEN 1910
1900 Y0=Y
1910 IF X0 >= Y THEN 1820
1920 Y9=Y
1930 GOTO 1820
1940 REM: SAVE S-NDX
1950 I(1,1)=J(1,1)

```

```

1960 I(1,2)=J(1,2)
1970 R0=I(1,3)+1
1980 NEXT I
1990 IF PCS(G3,"N") AND PCS(G3,"N") THEN 3730
2000 DISP SPA5"READY PRINTER, REPLY 0. ",
2010 INPUT J0
2020 IF PCS(G3,"N") THEN 2670
2030 REM >>> WRITE DATA <<<<<<<
2040 REM: INIT
2050 J1=-1
2060 MAT M=ZEN(10,2)
2070 M(1,1)=G(1,1)
2080 M(1,2)=1
2090 FOR J=2 TO N
2100 M(J,2)=I(J-1,3)+1
2110 M(J,1)=G(M(J,2),1)
2120 NEXT J
2130 GCSUB 3700
2140 J1=J1+2
2150 J2=J1+1
2160 IF J2 <= N THEN 2190
2170 J2=N
2180 REM: HEADINGS
2190 C3="DATA"
2200 GCSUB 3900
2210 FOR I=J1 TO J2
2220 S724=INT(S(1,33)/2)
2230 PRINT SPA5
2240 GCSUB 3900
2250 WRITE (15,3720)(S)
2260 IF I=J2 THEN 2260
2270 PRINT SP7(46-S-S(1,33))
2280 NEXT I
2290 PRINT
2300 FOR J=J1 TO J2
2310 WRITE (15,2320)" ***** GIVEN ***** "
2320 FORMAT " === INTERPLATED === ",F1.0
2330 NEXT J
2340 PRINT
2350 FOR J=J1 TO J2
2362 WRITE (15,2370)" X Y ",F1.0
2370 FORMAT " X Y ",F1.0
2380 NEXT J
2390 PRINT
2400 L=6
2410 REM: WRITE LINE
2420 FOR J=J1 TO J2
2430 IF M(J,2) <= I(J,3) THEN 2500
2440 IF J=J2 THEN 2590
2450 WRITE (15,2460)" "
2460 WRITE (15,2460)" "
2470 GOTO 2590
2480 FORMAT 22X,F1.0
2490 FORMAT F10.3,1X,F11.4,1X
2500 WRITE (15,2490)M(J,1),R(J(J,1),J(J,2))
2510 IF G(M(J,2),1)>M(J,1) THEN 2550
2520 WRITE (15,2490)G(M(J,2),1),G(M(J,2),2)
2530 M(J,2)=M(J,2)+1
2540 GOTO 2570
2550 IF J=J2 (R M(J,2)>I(J,3) THEN 2570
2560 WRITE (15,2460)" "
2570 M(J,1)=M(J,1)+10
2580 GCSUB 3640
2590 NEXT J
2600 PRINT
2610 L=L+1

```

```

2620 PEM: WRITE ANOTHER LINE?
2630 IF P(J1,2)>I(J1,3) AND P(J2,2)>I(J2,3) THEN 2660
2640 IF L<57 OR J0 THEN 2420
2650 GOTO 2190
2660 IF J2<N THEN 2140
2670 IF P(S(G), "N") THEN 3730
2680 PEM >>> GRAPHING <<<<<<<<<
2690 REM: SCALING
2700 IF Y0=Y9 THEN 2900
2710 S=FRF(Y9-Y0)
2720 IF S<4 THEN 2750
2730 S=INT(S*0.995)*10-2(P0-2)
2740 GOTO 2760
2750 S=INT(2.5*(S-0.005)+1)/2.5*10-2(P0-2)
2760 A1=Y9-100.5*S
2770 A9=Y0+0.5*S
2780 A=L
2790 IF A1<0 AND A9>0 THEN 2990
2800 P(1)=10
2810 P(2)=5
2820 P(3)=2
2830 FOR D1=1 TO 3
2840 K=PIF(0.5*(A1+A9))*10-D1
2850 FOR P0=1 TO 3
2860 A=PCP0*INT(K/P(R0)+0.5)*10-2(P0-D1)
2870 IF A>A1 AND A<A9 THEN 2990
2880 NEXT P0
2890 NEXT D1
2900 DISP " GRAPH SKIPPED: NOT SCALEABLE."
2910 STOP
2920 PEM: "POWER FUNCTION"
2930 DEF FPF(X)
2940 F0=0
2950 IF X=0 THEN 2970
2960 F0=INTLGTA95X
2970 RETURN X*10-2(-P0)
2980 PEM: HEADINGS
2990 CS="GRAPH"
3000 J0=J0 AND P(S(CS, "N"))
3010 GOSUB 3960
3020 K=0
3030 FOR I=1 TO N
3040 GOSUB 3900
3050 WRITE (15,3720)CS" = "P3(1,1)
3060 IF I=1 THEN 3110
3070 WRITE (15,3740)", "I
3080 K=P+S(1,33)+6
3090 IF K<95 THEN 3130
3100 K=0
3110 PRINT
3120 WAIT 250
3130 NEXT I
3140 WRITE (15,3150)A,25*S+A,50*S+A,75*S+A,100*S+A
3150 FORPAT /,6X,F10.3,15X,F10.3,15X,F10.3,15X,F10.3,15X,F10.3
3160 PEM: INIT
3170 FOR K=1 TO 76 STEP 25
3180 C(K)=" "
3190 NEXT K
3200 FOR K71 TO 81 STEP 20
3210 C(K)="- - - - -"
3220 NEXT K
3230 K=0
3240 D1=0.5*10
3250 PEDIM M(10,2)
3260 FOR J=1 TO N
3270 M(J,1)=GCK+1,1)

```



```

3280 K=I(J,3)
3290 M(J,2)=10*INT((G(K,1)-M(J,1))/10+1)+M(J,1)+D
3300 M(J,1)=M(J,1)-D1
3310 NEXT J
3320 GCSUB 3760
3330 L=9
3340 REM: WCRK SECTION
3350 FOR X=X0 TO X9 STEP 10
3360 L=L+1
3372 GOTO L=10 CF 3400
3380 G3=C3
3390 GOTO 3430
3400 L=0
3410 G3=Q3
3420 REM: "DET GRAPH-PTS
3430 FOR J=1 TO N
3440 F(J)=1
3450 IF X<M(J,1) OR X >= M(J,2) THEN 3480
3460 P(J)=(R(J(J,1),J(J,2))-A)/S+2
3470 GCSUB 3640
3480 NEXT J
3490 REM: FIX GRAPH-PTS
3500 P9=103
3510 FOR K=1 TO N
3520 IF P(K)=0 THEN 3690
3530 FOR J=K TO N
3540 IF P(J)/P(K) THEN 3670
3550 IF J=K THEN 3660
3560 GOTO D1 CF 3600
3570 P9=P9+1
3580 G3(P9,P9)=P3(K,K)
3590 P9=P9+1
3600 G3(P9,P9)=P3(J,J)
3610 P(J)=0
3620 P9=P9+3
3630 G4(P9,P9)=","
3640 D1=1
3650 GOTO 3670
3660 D1=0
3670 NEXT J
3680 G4(P(K),P(K))=P3(K)
3690 NEXT K
3700 WRITE (15,3720)X,G3(1,P9-1)
3710 NEXT X
3720 FORMAT F10.3,I1X,F1.0
3730 DISP " END"
3740 END
3750 REM: R-NDX PCINTER INIT
3760 J(1,1)=J(1,2)=1
3770 FOR J=2 TO N
3780 J(J,1)=J(J-1,1)+1
3790 J(J,2)=J(J-1,2)
3800 GCSUB 3850
3810 NEXT J
3820 RETURN
3830 REM: R-NDX PCINTER
3840 J(J,1)=J(J,1)+1
3850 IF J(J,1) <= D9 THEN 3880
3860 J(J,1)=1
3870 J(J,2)=J(J,2)+1
3880 RETURN
3890 REM: MAT S->C3 TRANS
3900 FOR J=1 TO S(1,33)
3910 OUTPUT (C3(J),3940)S(1,J)
3920 NEXT J
3930 RETURN

```

```

3940 FORMAT B
3950 REM: WHITE HEADING
3960 IF J0 THEN 3990
3970 PRINT LIN1,WEYTE12
3980 WAIT 1000
3990 P=P+1
4000 WRITE (15,4010)P108
4010 FORCAT "PAGE",F3.0,47,"GENERAL INTERPOLATION",J
4020 FOR I=1 TO P(21)
4030 WRITE (15,3940)M(1)
4040 NEXT I
4050 PRINT LIN2
4060 RETURN
4070 END

```

LITERATURE CITED

1. Allan, D., J. Auger and M. J. Crumpton. 1972. Purification of concanavalin A receptor from pig lymphocyte plasma membrane. *Biochem. J.* 126:6P.
2. Anderson, E. C. and D. F. Petersen. 1967. Cell growth and division II. Experimental studies of cell volume distributions in mammalian suspension cultures. *Biophys. J.* 7:353-364.
3. Arrameas, S. and B. Guilbert. 1971. Biologically active water-insoluble protein polymers. Their use for the isolation of specifically interacting proteins. *Biochem.* 53:604-614.
4. Barber, B. H. and J. P. Carver. 1973. The proton relaxation enhancement properties of concanavalin A. *J. Biol. Chem.* 248:3353.
5. Beck, C. E. and R. W. G. Wyckoff. 1938. Venezuelan equine encephalomyelitis. *Science* 88:530.
6. Bell, G. I. and E. C. Anderson. 1967. Cell growth and division I. A mathematical model with applications to cell volume distributions in mammalian suspension cultures. *Biophys. J.* 7:329-351.
7. Bell, G. I. 1968. Cell growth and division III. Conditions for balanced exponential growth in a mathematical model. *Biophys. J.* 8:431-444.
8. Brecher, G., M. Schneiderman and G. Z. Williams. 1956. Evaluation of electronic red blood cell counter. *Am. J. Clin. Path.* 26:1439-1449.
9. Brecher, G., E. F. Jakobek, M. A. Schneiderman, G. Z. Williams and P. J. Schmidt. 1962. Size distribution of erythrocytes. *An. N.Y. Acad. Sci.* 99:242-261.
10. Brewer, C. F., D. M. Maraus and A. P. Grollman. 1974. Interaction of saccharides with concanavalin A: Relation between calcium ions and the binding of saccharides to concanavalin A. *J. Biol. Chem.* 249:4614-4616.
11. Buckley, S. M. 1969. Susceptibility of the *Aedes albopictus* and *A. aegypti* cell lines to infection with arboviruses. *Proc. Soc. Exp. Biol. Med.* 131:625-630.

12. Bykovsky, A. F., F. I. Yershov and Y. M. Zhdanov. 1969. Morphogenesis of Venezuelan equine encephalomyelitis virus. *J. Virol.* 4:496-504.
13. Casals, J. and L. V. Brown. 1954. Hemagglutination with arthropod-borne viruses. *J. Exp. Med.* 99:429-449.
14. Casals, J. 1957. The arthropod-borne group of animal viruses. *Trans. N.Y. Acad. Sci.* 19:219-235.
15. Casals, J. and D. H. Clarke. 1965. Arboviruses: Group A, p. 583. *In* F. L. Horsfall and I. Tamm (eds.). *Viral and rickettsial infections of man*. J. B. Lippincott Company, Philadelphia.
16. Chamberlain, R. W., W. D. Sudia, P. H. Coleman and T. H. Work. 1964. Venezuelan equine encephalitis virus from Southern Florida. *Science* 145:272-274.
17. Chappell, W. A., C. H. Calisher, R. F. Toole, K. C. Maness, D. R. Sasso and B. E. Henderson. 1971. Comparison of three methods used to isolate Dengue virus type 2. *Appl. Microbiol.* 22:1100-1103.
18. Chen, T. T., I. Wantanabe, W. Zeaman and J. Mealy. 1969. Propagation of measles in brain biopsy. *Science* 163:1193-1194.
19. Cline, M. J. and D. C. Livingston. 1971. Binding of ³H-concanavalin A by normal and transformed cells. *Nat. New Biol.* 232:155-156.
20. Converse, J. L. and S. C. Nagle. 1967. Multiplication of yellow fever virus in insect tissue cultures. *J. Virol.* 1:1096-1097.
21. Cook, J. S. 1967. Size determination of human erythrocytes with an electronic counter. *J. Lab. and Clin. Med.* 70:849-856.
22. Coulter, W. H. 1953. U.S. Patent No. 2,656,508.
23. Cunningham, C. H., M. P. Spring and K. Nazerian. 1972. Replication of avian infectious bronchitis virus in African green monkey kidney cell line. Vero. *J. Gen. Virol.* 16:423-427.

24. Davey, M. W., D. P. Donnet and L. Dalgarno. 1973. The growth of two togaviruses in cultured mosquito and vertebrate cells. *J. Gen. Virol.* 20:225-232.
25. Donnelly, E. H. and I. J. Goldstein. 1970. Gluteraldehyde - insoluable concanavalin A: An absorbent for specific isolation of polysaccharides and glycoproteins. *Biochem. J.* 118:679-680.
26. Drake, J. F. and H. M. Tsuchiya. 1973. Differential counting in mixed cultures with Coulter Counters. *Appl. Microbiol.* 26:9-13.
27. Dwyer, D. M. 1974. Lectin binding saccharides on a parasitic protozoan. *Science* 184:471-472.
28. Edwards, J. G. and J. A. Campbell. 1971. The aggregation of trypsinized BHK21 cells. *J. Cell Sci.* 8:53-71.
29. Ehrenkranz, N. J., E. M. Sinclair, E. Buff and D. Lyman. 1970. The natural occurrence of Venezuelan equine encephalitis infection in the United States - First case and epidemiological investigations. *New Eng. J. Med.* 282:298-302.
30. Fried, J. 1967. Estimating the median generation time of proliferating cell systems in steady state. *Biophys. J.* 8:710-729.
31. Fulker, R. H., G. C. Parikh and L. G. Nusz. 1976. VEE virus induced cell volume changes as detected with the Coulter Counter. I. Computer simulation of cell cycle volume changes. To be published in *Proc. 7th Ann. Pittsburgh Modelling and Simulation Conf. Pittsburgh, Penn.*
32. Gillette, R. 1971. VEE vaccine: Fortuitous spin-off from B W research. *Science* 173:405.
33. Goldstein, I. J. and L. L. So. 1965. Protein-carbohydrate interaction III. Agar gel-diffusion studies on the interaction of concanavalin A, a lectin isolated from Jack Bean, with polysaccharides. *Arch. Biochem. Biophys.* 111:407-414.
34. Goldstein, I. J., C. M. Reichert and A. Misaki. 1974. Interaction of concanavalin A with model substrates. *Ann. N.Y. Acad. Sci.* 234:283-295.
35. Grace, T. D. C. 1966. Establishment of a line of mosquito (*Aedes aegypti*) cells grown in vitro. *Nature* 211:366-367.

36. Grant, J. L., M. C. Britton and T. E. Kurtz. 1960. Measurement of red blood cell volume with the electronic cell counter. *Am. J. Clin. Path.* 33:138-143.
37. Gregg, E. C. and K. D. Steidley. 1965. Electrical counting and sizing of mammalian cells in suspension. *Biophys. J.* 5:393-405.
38. Hardy, F. M. 1959. The growth of Venezuelan equine encephalomyelitis virus in various tissue cultures. *Am. J. Hyg.* 70:21-27.
39. Hardy, F. M. and A. Brown. 1961. Growth of Venezuelan equine encephalomyelitis virus in L cells I. Growth in monolayer cultures. *J. Bact.* 81:20-27.
40. Hardy, F. M. and A. Brown. 1961. Growth of Venezuelan equine encephalomyelitis virus in L cells II. Growth in submerged culture. *J. Bact.* 82:449-457.
41. Haughton, G. J. Hoat, L. Révész, and G. Kline. 1965. Lymphoma growth in vivo: Electronic discrimination between tumors and stroma cells. *Science* 150:769-771.
42. Henderson, B. E., W. A. Chappel, J. G. Johnston, Jr. and W. A. Sudia. 1971. Experimental infection of horses with three strains of Venezuelan equine encephalomyelitis virus. *Am J. Epid.* 93:194-211.
43. Heydrick, F. P., J. E. Comer and R. E. Wachter. 1971. Phospholipid composition of Venezuelan equine encephalitis virus. *J. Virol.* 7:642-645.
44. Hirsch, H. R. and H. J. Curtis. 1973. Dynamics of growth in mammalian diploid tissue cultures. *J. Theor. Biol.* 42:227-244.
45. Horzinek, M. 1969. A simple method for concentration of arboviruses propagated in tissue culture. *Am. J. Trop. Med.* 18:588-591.
46. Inbar, M. and L. Sachs. 1969. Structural differences in sites on the surface membrane of normal and transformed cells. *Nature* 223:710.
47. Inoue, M. 1974. Cell agglutination mediated by concanavalin A and the dynamic state of the cell surface. *J. Cell Sci.* 14:197-202.

48. Ito, M. and A. L. Barron. 1974. Inactivation of herpes simplex virus by concanavalin A. *J. Virol.* 13:1312-1318.
49. Itoh, H., Y. Morimoto, Y. Doi, T. Sanpe and H. Tsunoda. 1968. Susceptibility of an African green monkey kidney cell line-Vero. *Virus* 18:214-228.
50. Itoh, H., T. Sanpe, Y. Doi and Y. Morimoto. 1968. Studies on rubella virus: Cytopathic effect (CPE) in Vero cells - cercopithecus kidney line. *Virus* 18:482-484.
51. Itoh, H., Y. Morimoto, Y. Doi and T. Sanpe. 1970. Studies on simian viruses: Some properties of SV41 grown in Vero cell cultures and search for serum neutralization antibodies in humans and various animals. *Virus* 18:495-503.
52. Johnson, J. W. 1969. Growth of Venezuelan and eastern equine encephalomyelitis viruses in tissue cultures of minced *Aedes aegypti* larvae. *Am. J. Trop. Med. Hyg.* 18:103-114.
53. Kass, L., O. D. Ratnoff and M. A. Leon. 1969. Studies on the purification of antihemophilic factor (factor VIII) I. Precipitation of antihemophilic factor by concanavalin A. *J. Clin. Invest.* 48:351.
54. Kiley, M. P., R. H. Gray and F. E. Payne. 1974. Replication of measles virus: Distinct species of short nucleocapsids in cytoplasmic extracts of infected cells. *J. Virol.* 13:721-728.
55. Kiley, M. P. and F. E. Payne. 1974. Replication of measles virus: Continued synthesis of nucleocapsid RNA and increased synthesis of mRNA in the presence of cycloheximide. *J. Virol.* 14:758-764.
56. Kim, M., K. Bahrami and K. B. Woo. 1975. Mathematical description and analysis of cell cycle kinetics and the application to Ehrlich ascites tumor. *J. Theor. Biol.* 50:437-459.
57. Kissling, R. E., R. W. Chamberlain, D. B. Nelson and D. D. Stamm. 1956. Venezuelan equine encephalomyelitis in horses. *Am. J. Hyg.* 63:274-287.
58. Klenk, H., H. Becht and R. Rott. 1974. Reactions of viruses and virus-infected cells with heterophile agglutinins. *An. N.Y. Acad. Sci.* 234:355-368.

59. Klimenko, S. M., F. I. Yershov, Y. P. Gofman, A. P. Nabatinicov and V. M. Zhdanov. 1965. Architecture of Venezuelan equine encephalomyelitis virus. *Virology* 27:125-128.
60. Koch, A. L. and M. Schaechter. 1962. A model for statistics of the cell division process. *J. Gen. Microbiol.* 29: 435-454.
61. Kubas, V. and E. A. Rios. 1939. The causative agent of infectious equine encephalomyelitis in Venezuela. *Science* 90:20-21.
62. Kubitschek, H. E. 1958. Electronic counting and sizing of bacteria. *Nature* 182:234-235.
63. Kubitschek, H. E. 1960. Electronic measurement of particle size. *Research* 13:128-135.
64. Lackie, J. M. 1974. The aggregation of rabbit polymorpho-nuclear leucocytes: Effects of antimitotic agents, cyclic nucleotides, and methyl xanthines. *J. Cell Sci.* 16:167-180.
65. Landinsky, J. L., G. E. Sarto and B. M. Peckham. 1964. Cell size distribution patterns as a means of uterine cancer detection. *J. Lab. and Clin. Med.* 64:970-976.
66. Levitt, N. H., H. V. Miller, C. E. Pedersen, Jr. and G. A. Eddy. 1975. A microprecipitation test for rapid selection and identification of Venezuelan, eastern and western equine encephalomyelitis viruses. *Am. J. Trop. Med. Hyg.* 24:127-130.
67. Limrigar, M. D. and S. S. Kadam. 1974. Comparative sensitivity of suckling mice and vero cells for primary isolation of chickungunya virus. *Indiana J. Med. Res.* 62:1893-1896.
68. Lite, S. W. and R. C. Wallis. 1970. Growth of primary monolayer cell cultures from the mosquito *Culex salinarius* (Diptera, Culicidae). *Mosquito News* 30:539-542.
69. Lloyd, C. W. and G. M. W. Cook. 1974. On the mechanism of the increased aggregation by neuramidase of 16C malignant rat dermal fibroblasts in vitro. *J. Cell Sci.* 15:575-590.

70. Mattern, F. T., F. S. Brackett and B. J. Olson. 1957. Determination of number and size of particles by electrical gating: Blood Cells. *J. Appl. Physiol.* 10:56.
71. Mitsuhashi, J. and K. Maramorosch. 1964. Leaf hopper tissue culture: Embryonic, nymphal and imaginal tissues from aseptic insects. *Contrib. Boyce Thompson Inst.* 22:435-460.
72. Morrison, G. A. and A. L. Tomkins. 1973. Determination of mean cell size of tetrahymena in growing cultures. *J. Gen. Microbiol.* 77:383-392.
73. Mussgay, M. and J. Weibel. 1962. Electron microscopic and biological studies on the growth of Venezuelan equine encephalitis virus in KB cells. *Virology* 16:52-62.
74. Naeve, C. W. 1974. RNA and cell volume distribution analysis of VEE virus infected mosquito cell cultures. M. S. Thesis. South Dakota State University.
75. Oram, J. D., D. C. Ellwood, G. A. Appleyard and J. L. Stanley. 1971. Agglutination of an arbovirus by concanavalin A. *Nature New Biology* 233:50-51.
76. Ou, J. T. 1973. Inhibition of formation of *Escherichia coli* mating pairs by f1 and MS2 bacteriophages as determined with the Coulter Counter. *J. Bact.* 114:1108-1115.
77. Ozanne, B. and A. Vogel. 1974. Selection of revertants of Kirsten sarcoma virus transformed nonproducer BALB/3T3 cells. *J. Virol.* 14:239-248.
78. Parikh, G. C., T. C. Sorensen and C. S. Duvall. 1973. Identification and quantification of viruses and virus-specific antibodies utilizing latex particles and ¹²⁵I isotope. Presented at Symposium on Rapid Methods and Automation in Microbiology, Stockholm, Sweden and to be published in *Bio-Technology and Engineering*.
79. Parikh, G. C., T. C. Sorensen and G. C. K. Ho. 1975. Universal virus absorption on inert particles utilizing coated latex absorption method (CLAM). Report A001AE prepared for Office of Naval Research 800 N. Quincy Street, Arlington, VA. 22217 and Office of Naval Research Elliot Hall Minneapolis, Minn. 55455.

80. Paul, S. D. and K. R. P. Singh. 1969. Comparative sensitivity of mosquito cell lines, Vero cell and infant mice to infection with arboviruses. *Curr. Sci.* 38:241-242.
81. Pedersen, C. E., Jr. and G. A. Eddy. 1974. Separation, isolation, and immunological studies of the structural proteins of Venezuelan equine encephalomyelitis virus. *J. Virol.* 14:740-744.
82. Peleg, J. 1968. Growth of arboviruses in monolayers from subcultured mosquito embryo cells. *Virology* 35:617-619.
83. Peleg, J. 1969. Inapparent persistent virus infection in continuously grown *Aedes aegypti* mosquito cells. *J. Gen. Virol.* 5:463-471.
84. Petrucci, J. V., P. A. Dunne and C. C. Chapman. 1971. Spurious erythrocyte indices as measured by the model S Coulter Counter due to cold agglutinins. *Amer. J. Clin. Path.* 56:500-503.
85. Powell, E. O. 1964. A note on Koch and Schaechter's hypothesis about growth and fission of bacteria. *J. Gen. Microbiol.* 37:231-249.
86. Princen, L. H. and W. F. Kaolek. 1965. Coincidence correction for particle size determinations with the Coulter Counter. *Rev. Scient. Instrum.* 36:646-653.
87. Quastler, H. 1960. Cell population kinetics. *An. N.Y. Acad. Sci.* 90:580-591.
88. Reeke, G. N., J. W. Becker, B. A. Cunningham, G. R. Gunther, J. L. Wang and G. M. Edelman. 1974. Relationships between the structure and activities of concanavalin A. *An. N.Y. Acad. Sci.* 234:369-382.
89. Rhim, J. S. and K. Schell. 1967. Cytopathic effects of the parainfluenza virus SV5 in Vero cells (African green monkey). *Nature* 216:271-272.
90. Rhim, J. S., K. Schell, B. Creasy and W. Case. 1969. Biological characteristics and viral susceptibility of an African green monkey kidney cell line (Vero). *Proc. Soc. Exp. Biol. Med.* 132:670-678.

91. Richards, J. D. and D. S. Thompson. 1973. Quality control and automated blood counting equipment with a special reference to the Coulter Counter model S. Lab. Practice 22:623-625.
92. Rigas, D. A. 1962. Theoretical considerations of cellular proliferation as studied by cell-labelling process. An. N. Y. Acad. Sci. 96:1008-1028.
93. Ross, D. W. and H. C. Mel. 1972. Growth dynamics of mitochondria in synchronized Chinese hamster cells. Biophys. J. 12:1562-1572.
94. Sanmartin-Barberi, C., H. Groat and E. Osborn-Mese. 1954. Human epidemic in Columbia caused by the Venezuelan equine encephalomyelitis virus. Am. J. Trop. Med. Hyg. 3:283-293.
95. Santen, R. J. 1965. Automated estimation of diploid and tetraploid nuclei with an electronic particle counter. Ex. Cell Res. 40:413-420.
96. Sawyer, W. H., G. H. Mckemie and L. W. Nichol. 1974. A conformational transition in concanavalin A: Conformational differences between intact and fragmented units. Aust. J. Bio. Sci. 27:1-6.
97. Schneider, I. 1967. Insect tissue culture. p. 543-554. In F. Wilt and N. Wessells (eds.). Methods in developmental biology. Crowell, New York.
98. Schneider, I. 1969. Establishment of three diploid cell lines of Anopheles stephensis (Diptera: Culicidae). J. Cell. Biol. 42:603-606.
99. Sellers, R. F., G. H. Bergold, O. M. Suarez and A. Morales. 1965. Investigations during Venezuelan equine encephalitis outbreaks in Venezuela 1962-1964. Am. J. Trop. Med. Hyg. 14:460-469.
100. Sharon, N. and H. Lis. 1972. Lectins: Cell-agglutinating and sugar-specific proteins. Science 177:949-959.
101. Simons, J. W. 1970. Characterization of somatic cells by determination of the volumes with Coulter Counter. J. Cell. Biol. 46:610-2.

102. Sinarachatanant, P. and L. C. Olson. 1973. Replication of Dengue virus type 2 in Aedes albopictus cell culture. J. Virol. 12:275-283.
103. Sinclair, W. K. and D. W. Ross. 1969. Modes of growth in mammalian cells. Biophys. J. 9:1056-1070.
104. Singh, K. R. P. 1967. Cell cultures derived from larvae of Aedes albopictus (Skuse) and Aedes aegypti (L.). Curr. Sci. 36:506-508.
105. Singh, K. R. P. and S. D. Paul. 1968. Multiplication of arboviruses in cell lines from Aedes albopictus and Aedes aegypti. Curr. Sci. 37:65-67.
106. Singh, K. R. P. and S. D. Paul. 1968. Susceptibility of Aedes albopictus and Aedes aegypti cell lines to infection by arbo and other viruses. Indian J. Med. Res. 56:815-820.
107. So., L. L. and I. J. Goldstein. 1968. Protein carbohydrate interaction XIII The interaction of concanavalin A with α -mannans from a variety of microorganisms. J. Biol. Chem. 243:2003-2007.
108. Sorensen, T. C. 1972. Detection and assay of viruses using latex particles. M. S. Thesis. South Dakota State University.
109. Springer, G. F., P. R. Desal and B. Kolecki. 1964. Synthesis and immunochemistry of fucose methyl ethers and their methyloglycosides. Biochem. 3:1076-85.
110. Stim, T. B. 1969. Arbovirus plaquing in two simian kidney cell lines. J. Gen. Virol. 5:329-338.
111. Stockert, R. J., A. G. Morell and I. H. Scheinberg. 1974. Mammalian hepatic lectin. Science 186:365-366.
112. Sweet, B. H. and J. S. McHale. 1970. Characterization of cell lines derived from Culiseta inornata and Aedes uexans mosquitoes. Exp. Cell Res. 61:51-63.
113. Taylor, W. P. and I. D. Marshall. 1975. Adaptation studies with Ross river virus: Laboratory mice and cell cultures. J. Gen. Virol. 28:59-72.

114. Tiggertt, W. D. and W. G. Downs. 1962. Studies on the virus of Venezuelan equine encephalomyelitis in Trinidad, W.I.I. The 1943-1944 epizootic. *Am. J. Trop. Med. Hyg.* 11:822-834.
115. Toivanen, P. and A. Toivanen. 1973. Selective activation of chicken T lymphocytes by concanavalin A. *J. Immunology* 111:1602-3.
116. Trager, W. 1938. Multiplication of equine encephalomyelitis in surviving mosquito tissues. *Am. J. Trop. Med.* 18: 387-393.
117. Varma, M. G. R. and M. Pudney. 1969. The growth and serial passage of cell lines from *Aedes aegypti* (L.) larvae in different media. *J. Med. Entomol.* 6:432-439.
118. Wachter, R. R. and E. W. Johnson. 1962. Lipid content of the equine encephalitis viruses. *Fed. Proc.* 21:461.
119. Walder, R. and C. J. Bradish. 1975. Venezuelan equine encephalomyelitis virus (VEEV): Strain differentiation and specification of virulence markers. *J. Gen. Virol.* 26:265-275.
120. Wales, M. and J. N. Wilson. 1961. Theory of coincidence in Coulter particle counters. *Rev. Sci. Inst.* 32:1132-1136.
121. Willingham, C. and I. Pastan. 1974. Cyclic AMP mediates the concanavalin A agglutinability of mouse fibroblasts. *J. Cell Biol.* 63:288-294.
122. Work, T. H. 1964. Serological evidence of arbovirus infection in Seminole Indians of Southern Florida. *Science* 145:270-272.
123. Yasumura, Y. and Y. Kawakita. 1963. Study on SV40 virus in tissue culture. *Nippon Rinsho* 21:1201.
124. Yoshinaka, Y. and T. Shiomi. 1975. Agglutination of Japanese encephalitis virus with concanavalin A. *J. Virol.* 15:671-674.
125. Yunker, C. E. and J. Cory. 1968. Growth of some group B arboviruses in two established insect cell lines. *Proc. 23rd. Ann. Int. Northwest Conf. on Diseases in Nature Communicable to man* (19-21 Aug.). p. 79-82.